

TECHNISCHE UNIVERSITÄT DRESDEN

Game Theory and Microeconomic Theory for Beamforming Design in Multiple-Input Single-Output Interference Channels

Rami Mochaourab
geboren am 16. März 1982

von der Fakultät Elektrotechnik und Informationstechnik der Technischen
Universität Dresden

zur Erlangung des akademischen Grades eines

Doktoringenieurs
(Dr.-Ing.)

genehmigte Dissertation

Vorsitzender: Prof. Dr. rer. nat. habil. Hans Georg Krauthäuser

Gutachter: Prof. Dr.-Ing. Eduard A. Jorswieck

Gutachter: Prof. Dr. Erik G. Larsson

Tag der Einreichung: 5. März 2012

Tag der Verteidigung: 11. Mai 2012

© Rami Mochaourab 2012

To my parents and Ulrike

When things get complicated enough, you're forced to change your level of description.

*Douglas R. Hofstadter, *Metamagical Themas*.*

Abstract

In interference-limited wireless networks, interference management techniques are important in order to improve the performance of the systems. Given that spectrum and energy are scarce resources in these networks, techniques that exploit the resources efficiently are desired. We consider a set of base stations operating concurrently in the same spectral band. Each base station is equipped with multiple antennas and transmits data to a single-antenna mobile user. This setting corresponds to the multiple-input single-output (MISO) interference channel (IFC). The receivers are assumed to treat interference signals as noise. Moreover, each transmitter is assumed to know the channels between itself and all receivers perfectly. We study the conflict between the transmitter-receiver pairs (links) using models from game theory and microeconomic theory. These models provide solutions to resource allocation problems which in our case correspond to the joint beamforming design at the transmitters. Our interest lies in solutions that are Pareto optimal. Pareto optimality ensures that it is not further possible to improve the performance of any link without reducing the performance of another link.

Strategic games in game theory determine the noncooperative choice of strategies of the players. The outcome of a strategic game is a Nash equilibrium. While the Nash equilibrium in the MISO IFC is generally not efficient, we characterize the necessary null-shaping constraints on the strategy space of each transmitter such that the Nash equilibrium outcome is Pareto optimal. An arbitrator is involved in this setting which dictates the constraints at each transmitter. In contrast to strategic games, coalitional games provide cooperative solutions between the players. We study cooperation between the links via coalitional games without transferable utility. Cooperative beamforming schemes considered are either zero forcing transmission or Wiener filter precoding. We characterize the necessary and sufficient conditions under which the core of the coalitional game with zero forcing transmission is not empty. The core solution concept specifies the strategies with which all players have the incentive to cooperate jointly in a grand coalition. While the core only considers the formation of the grand coalition, coalition formation games study coalition dynamics. We utilize a coalition formation algorithm, called merge-and-split, to determine stable link grouping. Numerical results

show that while in the low signal-to-noise ratio (SNR) regime noncooperation between the links is efficient, at high SNR all links benefit in forming a grand coalition. Coalition formation shows its significance in the mid SNR regime where subset link cooperation provides joint performance gains.

We use the models of exchange and competitive market from microeconomic theory to determine Pareto optimal equilibria in the two-user MISO IFC. In the exchange model, the links are represented as consumers that can trade goods within themselves. The goods in our setting correspond to the parameters of the beamforming vectors necessary to achieve all Pareto optimal points in the utility region. We utilize the conflict representation of the consumers in the Edgeworth box, a graphical tool that depicts the allocation of the goods for the two consumers, to provide closed-form solution to all Pareto optimal outcomes. The exchange equilibria are a subset of the points on the Pareto boundary at which both consumers achieve larger utility than at the Nash equilibrium. We propose a decentralized bargaining process between the consumers which starts at the Nash equilibrium and ends at an outcome arbitrarily close to an exchange equilibrium. The design of the bargaining process relies on a systematic study of the allocations in the Edgeworth box. In comparison to the exchange model, a competitive market additionally defines prices for the goods. The equilibrium in this economy is called Walrasian and corresponds to the prices that equate the demand to the supply of goods. We calculate the unique Walrasian equilibrium and propose a coordination process that is realized by the arbitrator which distributes the Walrasian prices to the consumers. The consumers then calculate in a decentralized manner their optimal demand corresponding to beamforming vectors that achieve the Walrasian equilibrium. This outcome is Pareto optimal and lies in the set of exchange equilibria.

In this thesis, based on the game theoretic and microeconomic models, efficient beamforming strategies are proposed that jointly improve the performance of the systems. The gained results are applicable in interference-limited wireless networks requiring either coordination from the arbitrator or direct cooperation between the transmitters.

Acknowledgements

I want to express my gratitude to Professor Eduard Jorswieck for giving me the opportunity to do research under his supervision. I thank him for suggesting interesting and challenging research problems and also introducing me to game theory. He has always found time for discussions and has always been supportive of new ideas and theoretical models. I am grateful for being his student. He has inspired me in many ways.

I want to thank Professor Erik Larsson for reading and refereeing this thesis. I also thank him along with Johannes Lindblom and Dr. Eleftherios Karipidis for welcoming me at CommSys, Linköping during my visit in March 2010. The discussions and sharing of ideas with Johannes and Eleftherios has been both stimulating and motivating. Moreover, I would like to thank Dr. Nizar Zorba for the interesting discussions we had during his one month visit at our lab.

I also want to thank all my current colleagues for their unbounded support. Special thanks to Martin Mittelbach and Christian Scheunert for discussions on mathematical problems and providing literature. Moreover, I want to thank Zhijiat Chong for sharing the office with me which has lead to discussions on different problems and exchange of interesting ideas. Many thanks to Sybille Siegel for taking care of administrative work.

Finally, I want to thank my parents and brother and sister for their continuous support and also Ulrike for her love and care.

Rami Mochaourab
Dresden, May 2012

Contents

List of Figures	xi
List of Tables	xv
Nomenclatur	xvii
1. Introduction	1
1.1. Motivation	1
1.2. Interference Channels	3
1.3. Transmit Beamforming	4
1.4. Conflict Analysis and Resource Allocation	6
1.4.1. Microeconomic Theory	8
1.4.2. Game Theory	12
2. System Model and Problem Formulation	19
2.1. System and Channel Model	19
2.2. Problem Formulation and Contributions	23
2.3. Related Work	26
2.3.1. Beamforming in Interference Channels	26
2.3.2. Game Theoretic and Microeconomic Theory Applications	31
3. Game Theoretic Applications	35
3.1. Noncooperative Games	35
3.1.1. Game in Strategic Form	35
3.1.2. Constraints for Efficient Nash Equilibrium	39
3.2. Cooperative Games	42
3.2.1. Game in Coalitional Form	42
3.2.2. Coalition Formation	46
3.2.3. Merge-and-Split Algorithm	47
3.3. Proofs	51

4. Microeconomic Theory Applications	55
4.1. Exchange Economy	55
4.1.1. Model of Exchange	56
4.1.2. Exchange Equilibria	62
4.1.3. Bargaining	63
4.2. Competitive Markets	72
4.2.1. Competitive Market Model	72
4.2.2. Walrasian Equilibrium	75
4.2.3. Coordination Mechanism	78
4.3. Proofs	84
5. Conclusions	93
5.1. Open Problems	95
A. Further Contributions	97
Bibliography	103

List of Figures

1.1.	The transmitters are connected to the arbitrator which coordinates their choice of beamforming vectors.	2
1.2.	The transmitters are directly connected to each other for signaling regarding the joint choice of beamforming vector.	3
1.3.	Two-user interference channel.	4
1.4.	An illustration of a transmitter with N antennas and two receivers with single antennas.	5
1.5.	Array pattern for a two-element linear array. The solid and dashed lines correspond to the maximum ratio transmission and cooperative beamforming, respectively.	6
1.6.	Illustration of an economic model with J producers of n goods. The goods are sold at markets which determine their prices. The K consumers buy goods from the markets.	7
1.7.	Distinction in equilibrium concepts in microeconomic theory.	8
1.8.	Distinctions in game theory.	12
1.9.	Illustration of a Nash equilibrium.	14
2.1.	Illustration of a K -user MISO IFC. The transmitters use multiple antennas while each receiver uses a single antenna. The solid arrows represent the links' intended channel vectors. The dashed arrows represent the interference channel vectors.	20
2.2.	Illustration of a two-user rate region.	21
2.3.	Illustration of a power gain region.	22
3.1.	Two-user rate region at -10 dB SNR.	38
3.2.	Two-user rate region at 5 dB SNR.	38
3.3.	Two-user rate region at 20 dB SNR.	39
3.4.	Plot of the Price of Anarchy in the MISO IFC for increasing SNR.	39
3.5.	In the γ -core, no coalition \mathcal{S} has the incentive to deviate from the grand coalition.	43

List of Figures

3.6. Illustration of the conditions for full cooperation (nonempty core) and conditions for no cooperation (single-player coalitions) for ZF coalitional game.	45
3.7. Illustration of a coalition structure $\mathcal{C} = \{\mathcal{S}_1, \mathcal{S}_2, \mathcal{S}_3\}$	46
3.8. An illustration of the merge operation.	47
3.9. An illustration of the split operation.	47
3.10. Distribution of the links in the plane.	48
3.11. Link rates at 15 dB SNR.	49
3.12. Average rate of the 8 links. The number under (above) the curve is the number of coalitions with ZF (WF).	50
4.1. Illustration of the initial distribution of the two goods.	56
4.2. Illustration of the distribution of the two goods during exchange.	57
4.3. Preference representation of the consumers. I_1 and I_2 are indifference curves of consumer 1 and 2, respectively.	58
4.4. An illustration of an Edgeworth box.	60
4.5. Course of the contract curve in the Edgeworth box for different SNR values.	61
4.6. An illustration of the exchange equilibria in the Edgeworth box.	62
4.7. An illustration of the exchange equilibria in the SINR region.	63
4.8. An illustration of the bargaining steps and stages during the bargaining process.	65
4.9. Six Edgeworth boxes which illustrate the possible positions of the allocation $\mathbf{x}^{(t)}$ of a bargaining-step.	66
4.10. SINR region of a two-user MISO IFC with SNR = 0 dB. The bargaining outcomes are marked with squares for three different initial step-lengths $(\delta_1^{(0)}, \delta_2^{(0)})$. $BO_1 : (0.02, 0.01)$, $BO_2 : (0.015, 0.01)$, $BO_3 : (0.01, 0.01)$	69
4.11. Edgeworth box representation of the bargaining process for $(\delta_1^{(0)}, \delta_2^{(0)}) = (0.1, 0.1)$. Two antennas are used at each transmitter and SNR = 0 dB.	70
4.12. SINR values over the bargaining-steps for $(\delta_1^{(0)}, \delta_2^{(0)}) = (0.1, 0.1)$. Two antennas are used at each transmitter and SNR = 0 dB.	70
4.13. Flowchart for consumer 1 (analogously consumer 2) for a new proposal.	71
4.14. An illustration of the budget set of consumer 1.	73
4.15. An illustration of an Edgeworth box. I_1 and I_2 are indifference curves of consumer 1 and 2 respectively. The line with slope $-p_1^*/p_2^*$ separates the budget sets of the consumers in Walrasian equilibrium.	75

4.16. An illustration of the Kalai-Smorodinsky and Nash bargaining solutions in the SINR region.	77
4.17. Convergence of the price ratio in the price adjustment process to the Walrasian price ratio.	81
4.18. Edgeworth box which depicts the allocation for the Walrasian prices. . .	81
4.19. SINR region of a two-user MISO IFC with SNR = 0 dB and two antennas at the transmitters.	82

List of Figures

List of Tables

4.1. Required information at the arbitrator and transmitters to implement the Walrassian equilibrium in one-shot.	79
4.2. Required information at the arbitrator and transmitters for the price adjustment process.	79

List of Tables

Nomenclatur

List of Notations

\mathbf{a}	Column vectors are written in boldface lowercase letters
\mathbf{A}	Matrices are written in boldface uppercase letters
\mathcal{S}	Sets are written in calligraphic font
$(a_i)_{i \in \mathcal{S}}$	A profile with the elements corresponding to the set \mathcal{S}
\mathbb{R}	Set of all real numbers
\mathbb{R}_+	Set of all nonnegative real numbers
\mathbb{C}	Set of all complex numbers
$\ \mathbf{a}\ $	Euclidean norm of $\mathbf{a} \in \mathbb{C}^N$
$ b $	Absolute value of $b \in \mathbb{C}$
$\text{sign}(a)$	The sign of $a \in \mathbb{R}$
$ \mathcal{S} $	The cardinality of a set \mathcal{S}
$(\cdot)^T$	Transpose
$(\cdot)^H$	Hermitian transpose
$\mathcal{CN}(\mathbf{0}, \mathbf{A})$	Circularly-symmetric Gaussian complex random vector with zero mean and covariance matrix \mathbf{A}
\mathbf{I}	An identity matrix
$\mathbf{\Pi}_Z$	The orthogonal projector onto the column space of \mathbf{Z} is $\mathbf{\Pi}_Z := \mathbf{Z}(\mathbf{Z}^H \mathbf{Z})^{-1} \mathbf{Z}^H$
$\mathbf{\Pi}_Z^\perp$	The orthogonal projector onto the orthogonal complement of the column space of \mathbf{Z} is $\mathbf{\Pi}_Z^\perp := \mathbf{I} - \mathbf{\Pi}_Z$
$\mathbf{v}_{max}(\mathbf{Z})$	Eigenvector which corresponds to the largest eigenvalue of \mathbf{Z}
$\mu_{max}(\mathbf{Z})$	Largest eigenvalue of \mathbf{Z}
$\mathbf{v}_i(\mathbf{Z})$	Eigenvector which corresponds to the i th largest eigenvalue of \mathbf{Z}
$\mu_i(\mathbf{Z})$	i th largest eigenvalue of \mathbf{Z}

List of Symbols

IFC	Interference Channel
MAC	Multiple Access Channel
BC	Broadcast Channel
SISO	Single-Input Single-Output
MISO	Multiple-Input Single-Output
MIMO	Multiple-Input Multiple-Output
CSI	Channel State Information
SINR	Signal-to-Interference-and-Noise Ratio
SNR	Signal-to-Noise Ratio
SUD	Single-User Decoding
MUD	Multi-User Decoding
MRT	Maximum Ratio Transmission
ZF	Zero Forcing Transmission
WF	Wiener Filter
NE	Nash Equilibrium
NBS	Nash Bargaining Solution
KS	Kalai-Smorodinsky Solution
UP	Utopia Point
TDD	Time-Division Duplex
TDMA	Time-Division Multiple-Access
FDMA	Frequency-Division Multiple-Access
OFDMA	Orthogonal Frequency-Division Multiple-Access
CDMA	Code-Division Multiple-Access
SDMA	Space-Division Multiple-Access
SOCP	Second Order Cone Programming
SDP	Semidefinite Programming
QCQP	Quadratically Constrained Quadratic Program

Chapter 1.

Introduction

1.1. Motivation

Wireless broadband networks¹ provide mobile users with high data rate services. In these networks, base stations are associated with coverage areas called cells. Mobile users located in these cells are granted access to high-speed data services from the corresponding base stations. The wireless connections between the base stations and the users enable user mobility.

Due to spectrum scarcity, universal frequency reuse is a prerequisite in wireless broadband networks [BPG⁺09]. The transmissions from all base stations are at the same frequencies and at the same time. Nevertheless, in order to support the increasing number of users, small cells (femto cells) are to be deployed [DMC⁺12, LMF⁺11] to increase the network coverage and reduce the load on existing base stations (macro cells). The base stations are to be equipped with multiple antennas in order to increase the cell spectral efficiency through multiplexing and spacial diversity techniques [KFV06, ACH07, LLL⁺10].

Having universal frequency reuse as well as dense deployment of base stations, interference becomes the main source of performance degradation in the network. The interference at a mobile user can be distinguished between intra-cell interference and inter-cell interference. Intra-cell interference at a user originates from the transmission of the associated base station to other users in the same cell. Intra-cell interference is usually managed through orthogonal multiple access methods [ACH07]. These methods divide the available resources (frequency, time, code, space) into orthogonal resource blocks. A set of resource blocks is then allocated to a single user for transmission. Inter-cell interference, on the other hand, is caused by transmissions in other

¹Such as IEEE 802.16 systems and Third Generation Partnership Project (3GPP) Long Term Evolution (LTE).

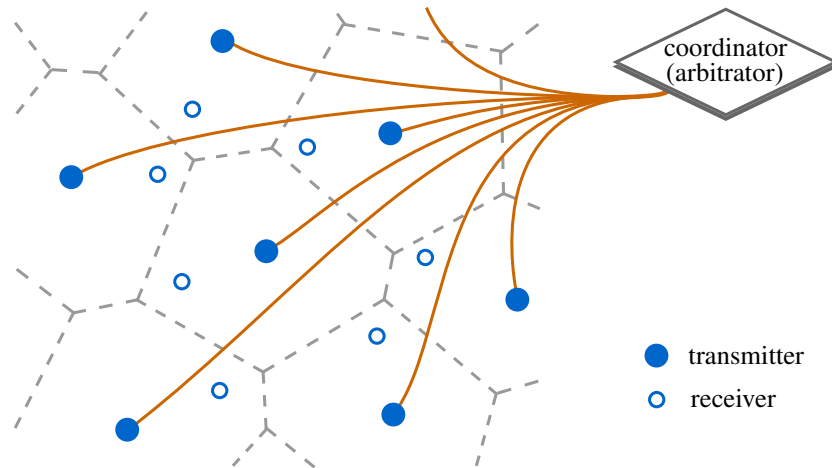


Figure 1.1.: The transmitters are connected to the arbitrator which coordinates their choice of beamforming vectors.

cells. Inter-cell interference is to be mitigated by interference management techniques [KFV06, ACH07, BPG⁺09, LLL⁺10].

Interference management techniques aim at coordinating the transmissions between the cells. The processing complexity for this purpose is desired to be at the base stations. In general, the base stations are larger in size and are capable to carry out larger computational overhead than the mobile users. Accordingly, the number of antennas at the base stations will be much larger than at the mobile users [ACH07]. Moreover, complex processing such as beamforming is to be performed at the base stations. Beamforming is a technique for transmitting (or receiving) the desired signal from multiple antennas to maximize the signal power in desired spacial directions. If the base station knows the channels between itself and all receivers, then beamforming can reduce or even null the interference at unintended receivers while maintaining acceptable signal power at the intended receiver [ACH07, GHH⁺10].

We distinguish between two models for interference management between the cells:

1. The first model requires a central controller which coordinates the transmissions of the base stations. This setting is illustrated in Figure 1.1. We refer to the central controller as the arbitrator. The arbitrator can acquire any necessary information from all transmitters.
2. The second model relies on direct communication between the base stations. This setting is illustrated in Figure 1.2. The base stations in this setting can exchange necessary information for cooperative transmissions.

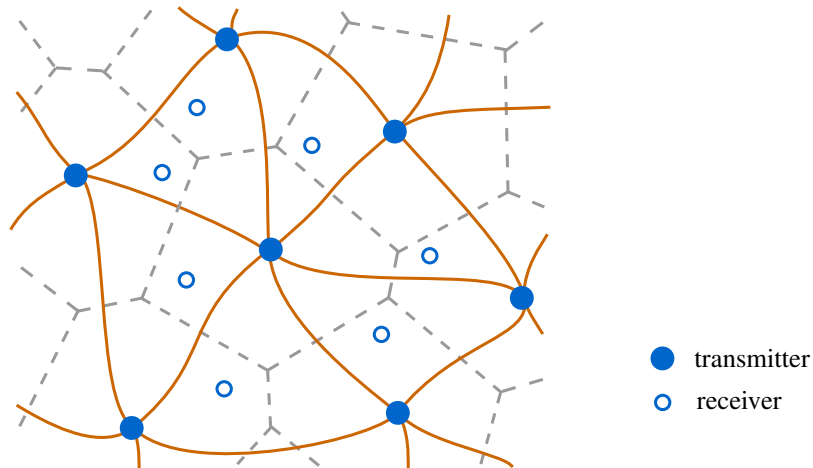


Figure 1.2.: The transmitters are directly connected to each other for signaling regarding the joint choice of beamforming vector.

Both mentioned models rely on the existence of backhaul connections which already exist in wireless broadband network standards [Raz11]. In the context of coordination or cooperation between the base stations, the base stations are to be regarded as intelligent systems [KfV06, AKG11]. With this respect, game theoretic models are appropriate to describe the interaction between the base stations.

1.2. Interference Channels

The interference channel (IFC) [CT91] is a mathematical model which describes a setting in which multiple transmitter-receiver pairs operate in the same spectral band. In Figure 1.3, a two-user IFC is illustrated. Transmitter 1 sends useful information to receiver 1, and transmitter 2 sends useful information to receiver 2. Each receiver receives a superposition of the signals sent from both transmitters. At receiver 1 (analogously receiver 2) the signal from transmitter 2 interferes on the intended signal from transmitter 1.

The standard form in Figure 1.3 is a representation of the IFC after specific normalization [Car78]. The direct channel coefficients are unity. The interference channel gain from transmitter 1 to receiver 2 is a . The channel gain from transmitter 2 to receiver 1 is b . Transmitter 1 and transmitter 2 have a total transmission power of P_1 and P_2 , respectively. The signals at receiver 1 and 2 are

$$y_1 = s_1 + bs_2 + n_1, \quad y_2 = as_1 + s_2 + n_2, \quad (1.1)$$

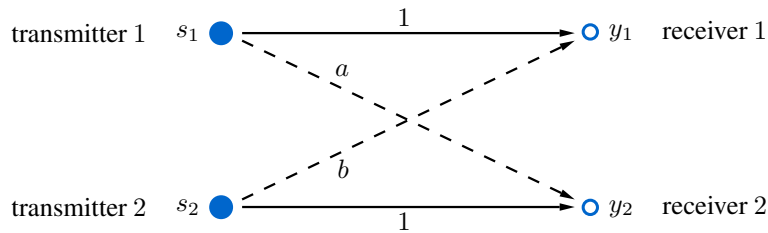


Figure 1.3.: Two-user interference channel.

respectively, where s_i is the message transmitted from transmitter $i \in \{1, 2\}$. The noise terms are $n_i \sim \mathcal{CN}(0, 1)$, $i \in \{1, 2\}$. If both receivers treat interference signals as noise, then achievable rates at receiver 1 and 2 with single user decoding (SUD) are

$$R_1 = \log_2 \left(1 + \frac{P_1}{1 + bP_2} \right), \quad R_2 = \log_2 \left(1 + \frac{P_2}{1 + aP_1} \right), \quad (1.2)$$

respectively.

The capacity region of an interference channel is composed of all jointly achievable data rates. Finding the capacity region of the IFC in general is still an open problem. In [Cos85], an overview of the results on the capacity region of the interference channel is provided. In [Car78], it is shown that if interference is very high ($a \geq 1 + P_2$ and $b \geq 1 + P_1$), then it can be decoded and subtracted from the intended signal. In this case, the capacity region has a rectangular shape. In [HK81] and [Sat81], it is shown that in the strong interference regime ($a \geq 1$ and $b \geq 1$), an achievable rate region is the intersection of two multiple access channel capacity regions. The largest known rate region for the interference channel is according to the Han-Kobayashi scheme [HK81]. Recently, it has been proven that the Han-Kobayashi scheme is within one bit from the capacity region of the IFC [ETW08].

In this thesis, we consider the multiple-input single-output (MISO) IFC [VJ04]. All transmitters are equipped with multiple antennas while all receivers use single antennas.

1.3. Transmit Beamforming

In this section, we briefly discuss how transmit beamforming techniques can be applied for interference management in interference networks. In Figure 1.4, a transmitter and two receivers are illustrated. The transmitter uses N antennas. The channel vectors from the transmitter to receiver 1 and 2 are $\mathbf{h}_1 \in \mathbb{C}^N$ and $\mathbf{h}_2 \in \mathbb{C}^N$, respectively. At each transmit antenna i the transmitted symbol s is multiplied by the complex weight $w_i \in \mathbb{C}$. The beamforming vector used at the transmitter is $\mathbf{w} = [w_1, \dots, w_N]^T$. A total

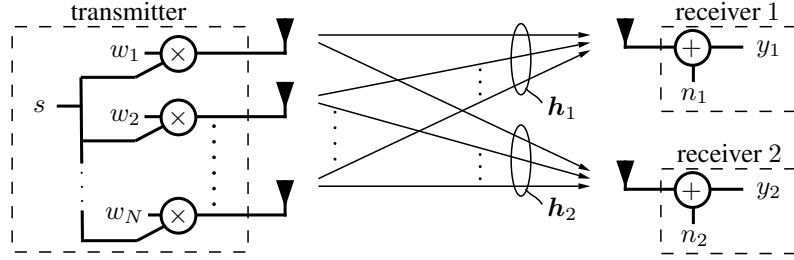


Figure 1.4.: An illustration of a transmitter with N antennas and two receivers with single antennas.

power constraint P at the transmitter is a constraint on the sum of powers used at the antennas:

$$\sum_{k=1}^N |w_k|^2 = \|\mathbf{w}\|^2 \leq P. \quad (1.3)$$

Beamforming is a signal processing technique which enables the possibility to increase the radiation power in desired directions while reducing the radiation power in undesired directions [BO01, GSS⁺10]. Transmit beamforming exploits the knowledge of the downlink channels. In order to acquire channel knowledge at the transmitter several techniques are discussed in [BO01]. In time-division duplex (TDD) systems, reciprocity between the uplink and downlink channels can be used to estimate the channel at the transmitter using training data from the receivers. Another method of obtaining channel knowledge at the transmitter is by estimating the channel at the receiver and forwarding the channel information to the transmitter via a feedback link.

In Figure 1.4, assume receiver 1 is the intended receiver of the transmitter and receiver 2 is the unintended receiver. The transmitter can maximize the power gain at receiver 1 by matching the beamforming vector \mathbf{w} to the channel \mathbf{h}_1 . The beamforming design for this purpose is called maximum ratio transmission (MRT). Moreover, it is possible to null the received signal power at receiver 2 when the beamforming vector \mathbf{w} is chosen orthogonal to the channel vector \mathbf{h}_2 . The beamforming design which maximizes the power at receiver 1 and nulls the interference power at receiver 2 corresponds to zero forcing (ZF) transmission.

We illustrate the effect of transmit beamforming by an example. Assume the transmitter uses a linear antenna array [Hay96] and the single-antenna receivers are located in the far field of the array. Moreover, the intended receiver is located at 0 degrees while the unintended receiver is at an angle of 30 degrees from the normal of the array. The channels are assumed to be quasi-static block flat fading. In Figure 1.5, MRT array

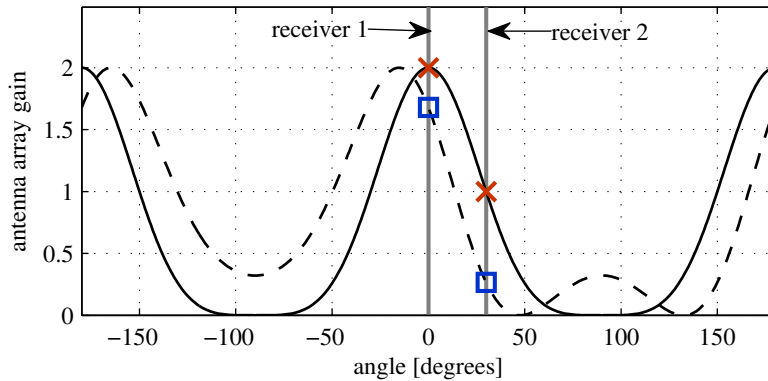


Figure 1.5.: Array pattern for a two-element linear array. The solid and dashed lines correspond to the maximum ratio transmission and cooperative beamforming, respectively.

pattern, plotted in solid line, achieves highest power gain at the intended receiver and also high interference gain at the unintended receiver. The array pattern for a choice of beamforming vector desired to mitigate interference at receiver 2 is plotted with the dashed line. It can be observed that the power gain at the intended receiver is less than the gain achieved with MRT. However, the interference gain is reduced significantly.

1.4. Conflict Analysis and Resource Allocation

Economic theory is concerned with efficient allocation of limited resources to economic agents. The economic agents represent individuals that have the desire to possess the valuable resources. The scarcity of the resources brings up a conflict between the individuals on how to distribute the resources among them.

Microeconomic theory [JR03, MCWG95] is a field in economics which studies economic agent behavior in markets. The economic agents represent both consumers and producers of goods. While generally the goods in a market can be said to flow directly between the consumers, prices are usually considered as means of trade for the goods. Producers sell their goods at the markets which make them accessible to the consumers at specified prices as is illustrated in Figure 1.6. Consumers on the other hand, are endowed with monetary budget which enables them to buy the goods. The consumers naturally have preferences over the available goods. Each consumer determines his demand of the goods according to his budget and preferences. The prices of the goods are adapted depending on the overall amount of goods demanded by the consumers as well as their supply by the producers. This interaction between the producers and consumers

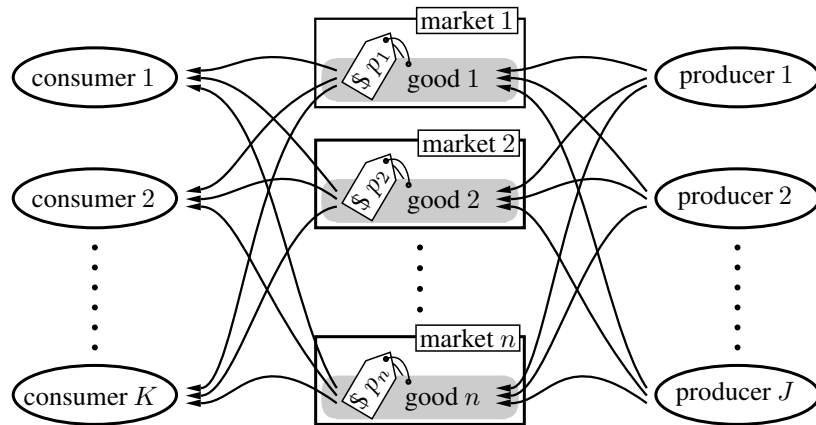


Figure 1.6.: Illustration of an economic model with J producers of n goods. The goods are sold at markets which determine their prices. The K consumers buy goods from the markets.

at markets can be studied using tools from microeconomic theory.

The behavior of economic agents plays a major role in determining the state of an economic system [Mye08]. Each economic agent is a decision-maker which seeks choices between different alternatives with the attempt to increase his wealth. His preference over the available goods is usually represented by a utility function. The behavior of the economic agent must conform with the maximization of his utility function. That is, after observing the market prices, quantities of goods are bought by the consumers in such a way that their utilities are maximized. Important in this behavior is that an economic agent is not aware of the structure of the market and the factors that lead to the prices of the goods. In other word, each economic agent takes prices as given and is incapable of altering them. Different market structures as well as their equilibria are discussed in Section 1.4.1.

Game theory is created by von Neumann and Morgenstern in *The Theory of Games and Economic Behavior* [vNM44] to provide tools for studying economic behavior. The reason for creating game theory is due to the fact that the mathematical methods used in economic analysis have not been adequate to analyze complex economic dynamics [Leo95]. With this respect, game theory is concerned with modeling conflict situations and providing solutions that range between competitive and cooperative individuals. The individuals in game theory are considered to be more intelligent than in microeconomic theory [Mye99]. Each individual maximizes his utility function having the

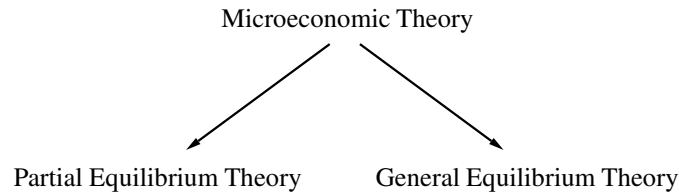


Figure 1.7.: Distinction in equilibrium concepts in microeconomic theory.

awareness of the entire market structure. As in microeconomic theory, the solutions of conflict situations in game theory rely on notions of stability. We discuss game theoretic models in Section 1.4.2.

Resource allocation problems arise in multiuser wireless scenarios [HL08]. There, multiple users can share the wireless channel for communication. Multiple-access schemes are concerned with efficient allocation of the channel resources to the users. The resources may be time-slots in time-division multiple access (TDMA), frequency bands in frequency-division multiple access (FDMA), code in code-division multiple access (CDMA) or space in space-division multiple access (SDMA). These resources can be regarded as valuable goods which the base station (producer) has to allocate to the users (consumers).

1.4.1. Microeconomic Theory

Two main building blocks of microeconomic theory is consumer theory and the theory of the firm [JR03]. Consumer theory deals with the decisions made by a consumer to maximize his preference. The theory of the firm studies production plans of a firm aimed at maximizing its profit. The solution concepts in microeconomic theory are distinguished between partial equilibrium theory and general equilibrium theory [JR03]. This distinction is illustrated in Figure 1.7. In partial equilibrium theory, the changes in one market are assumed not to affect the prices in other markets. In general equilibrium theory, the prices in different markets are connected. That is, a change in the price of one good leads to a change in the prices of other goods. The study in microeconomic theory is also classified according to market structures. Market structures can be distinguished between the least competitive (pure monopoly) to the most competitive (perfect competitive markets).

Partial Equilibrium Theory

We discuss the partial equilibrium in three market structures corresponding to pure monopoly, Cournot oligopoly and Bertrand oligopoly. The equilibrium in Cournot oligopoly and Bertrand oligopoly is related to the Nash equilibrium in game theory which is discussed in Section 1.4.2.

In a pure monopoly, there exists a single firm which produces quantities of the same good. There exists a set of consumers which buy quantities of this good. In this setting, the monopolist does not need to consider any actions or competition from other firms. The monopolist maximizes his profit by determining the amount of the good to be produced as well as the good's price. An oligopoly is a more competitive market model in comparison to pure monopoly. In a Cournot oligopoly, there exists a set of firms which sell quantities of the same good on a common market. The market determines the price of the good depending on its total supply. The profit of a firm is the gain from selling its goods minus the cost for producing these goods. In a Cournot oligopoly, each firm has to determine independently the amount of the good to produce. The Cournot equilibrium, proposed by Cournot in 1838, corresponds to a Nash equilibrium of a strategic game between the firms. The formulation of a strategic game as well as its solution are presented in Section 1.4.2. In contrast to a Cournot oligopoly, in a Bertrand oligopoly each firm can determine the price of its produced good independently. The consumers buy the goods only from the firm that provides the lowest prices. Therefore, the firm which sets the lowest price is the only firm that sells its good. The equilibrium in this setting corresponds to the prices set by the firms such that each firm's profit is zero.

General Equilibrium Theory

In perfect competitive markets, there exists a set of K consumers $\mathcal{K} = \{1, \dots, K\}$ and a number n of divisible goods. The total amount of good $i \in \{1, \dots, n\}$ is c_i and has a unit price of p_i . Define the vector of prices for the goods as $\mathbf{p} = [p_1, \dots, p_n]$. Each consumer is initially endowed with a budget b_k which he uses to buy goods. The *budget set* of consumer k is defined as

$$\mathcal{B}_k = \{\mathbf{x} \in \mathbb{R}_+^n : \mathbf{p}^T \mathbf{x} \leq b_k\}. \quad (1.4)$$

In the Arrow-Debreu market model, it is assumed that each consumer is initially endowed with amount of goods instead of a fixed monetary budget. Define the endowment vector of consumer k as $\mathbf{e}^k = (e_1^k, \dots, e_n^k)$. The budget of consumer k is the revenue

gained from selling his bundle of goods \mathbf{e}^k at the given prices. Hence, in the Arrow-Debreu market model, the budget of consumer k is $b_k = \mathbf{p}^T \mathbf{e}^k$.

Each consumer chooses the amount of goods to buy without taking into account the decisions of the other consumers. This leads to a distributed decision-making of the consumers. Each consumer k has a utility function $u_k : [0, c_1] \times \cdots \times [0, c_n] \rightarrow \mathbb{R}_+$ which reveals his preference over the goods. A consumer k *demands* quantities of goods to maximize his utility function. Thus, the demand function $\mathbf{d}^k = [d_1^k, \dots, d_n^k]$ of consumer k , depending on the prices of the goods, is defined as:

$$\mathbf{d}^k(\mathbf{p}) = \arg \max_{\mathbf{x} \in \mathcal{B}_k} u_k(\mathbf{x}). \quad (1.5)$$

The general equilibrium in competitive markets is due to Walras [Wal74] and describes the state at which the prices of the goods are chosen such that the demand of each good equals its supply, i.e.

$$\sum_{k=1}^K d_i^k(\mathbf{p}^*) = c_i, \quad \text{for all } i \in \{1, \dots, n\}. \quad (1.6)$$

The existence of a Walrasian equilibrium² is guaranteed if the following conditions are satisfied [JR03, Theorem 5.5]:

- the consumer utility function $u_k(\mathbf{x})$ is continuous, strongly increasing³, and strictly quasiconcave⁴ on \mathbb{R}_+^n ,
- the endowment of each good is strictly positive, i.e., $\sum_{k=1}^K e_i^k > 0$ for all $i \in \{1, \dots, n\}$.

In a competitive market, the properties of the aggregate excess demand of the goods plays an important role in the analysis of the Walrasian equilibrium. The *aggregate excess demand* of good i is defined as [JR03, Definition 5.4]:

$$z_i(\mathbf{p}) = \sum_{k=1}^K d_i^k(\mathbf{p}) - c_i, \quad (1.7)$$

where $d_i^k(\mathbf{p})$ is consumer k 's demand of good i in (1.5). Let $\mathbf{z}(\mathbf{p}) = [z_1(\mathbf{p}), \dots, z_n(\mathbf{p})]$. Walras' law is formulated as [JR03, Section 5.2]:

$$\mathbf{p}^T \mathbf{z}(\mathbf{p}) = 0. \quad (1.8)$$

²We will use the term Walrasian equilibrium to refer to the distribution of the goods according to the Walrasian prices and also to the corresponding utilities of the consumers.

³A function $f : D \rightarrow \mathbb{R}$ with $D \subset \mathbb{R}^n$ is strongly increasing if $f(\mathbf{x}') > f(\mathbf{x})$ whenever $\mathbf{x}' \geq \mathbf{x}$ (the inequality is componentwise) and $\mathbf{x}' \neq \mathbf{x}$ [JR03, Definition A1.17].

⁴A function $f : D \rightarrow \mathbb{R}$ with $D \subset \mathbb{R}^n$ is strictly quasiconcave if and only if, for all $\mathbf{x}' \neq \mathbf{x}$ in D , $f(t\mathbf{x}' + (1-t)\mathbf{x}) > \min\{f(\mathbf{x}'), f(\mathbf{x})\}$ for all $t \in (0, 1)$ [JR03, Definition A1.25].

Walras' law implies that if the excess demand is larger than zero in one market, then the excess demand in another market must be negative.

The existence of a unique Walrasian equilibrium depends on the properties of the aggregate excess demand function. The aggregate excess demand $\mathbf{z}(\mathbf{p})$ in (1.7) has the *gross substitute property* if when the price of one good i is increased from p_i to p'_i , and the prices of the other goods stay the same, then $z_j([p_1, \dots, p_{i-1}, p'_i, p_{i+1}, \dots, p_n]) > z_j(\mathbf{p})$ for $j \neq i$ [MCWG95, Definition 17.F.2]. If the aggregate excess demand satisfies the gross substitute property, then there exists at most one Walrasian equilibrium [MCWG95, Proposition 17.F.3]. In order to reach the Walrasian equilibrium, a price adjustment process (tâtonnement process) is required. Specifically, if the demand of one good is larger than its supply, the price of this good is increased. On the other hand, if a good is supplied in quantities larger than its demand then its price is reduced. If the aggregate excess demand has the gross substitute property, then the tâtonnement process is globally convergent [ABH59]. In Section 4.2, we use the competitive market model to characterize the Walrasian equilibrium in the two-user MISO IFC.

Pareto demonstrated that the Walrasian equilibrium in competitive markets is efficient according to his optimality criterion [SZ95]. In [Par94], Pareto formulated the optimality criterion which indicates that an efficient allocation of the resource to the individuals is achieved when a redistribution of the resources reduces the wealth of at least one individual. The interesting property of the Walrasian equilibrium in competitive markets is that given the behavior of the consumers as willing to maximize their profits independently leads to a Pareto optimal allocation of the resources. Pareto found his optimality condition motivated by the multiple optimal points found by Edgeworth [Edg81] in a setting of exchange between individuals.

In his book *Mathematical Psychics* [Edg81] in 1881, Edgeworth studied a voluntary exchange model between economic agents. Each agent is initially endowed with an amount of goods. The agents bargain on the distribution of the goods. Edgeworth showed in a two individual setting that starting at an initial distribution of two goods, there is a set of equilibria at which the two consumers are simultaneously satisfied. He called the set of points at which the bargaining ends the contract curve. The allocations on the contract curve satisfy the Pareto optimality criterion⁵. In Section 4.1, we model the situation in the two-user MISO IFC as an exchange economy and characterize all points on the contract curve. Moreover, we construct a bargaining process between the

⁵The equilibria in the exchange economy of Edgeworth were later discovered by Shubik [Shu59] to coincide with the core of a coalitional game between the individuals. Coalitional games are discussed in Section 1.4.2.

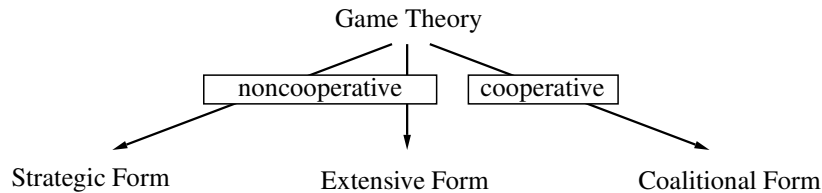


Figure 1.8.: Distinctions in game theory.

MISO links in order to reach a point on the contract curve.

1.4.2. Game Theory

Game theory studies the decisions that individuals, referred to as players, would make in conflict situations. Each player’s decision depends on the decisions of the other players. Accordingly, game theory analyzes the decisions the players would make when they interact. Game theory is built on the assumption that the players are rational and intelligent decision-makers [LR57, Mye84]:

- Rationality: The behavior of a player follows the maximization of his utility function.
- Intelligence: The players are capable to comprehend the conflict situation they are in and know that the other players are also intelligent.

These attributes of the players are understood under the term “rational players” [LR57].

In game theory, the distinction is made under noncooperative and cooperative games. In cooperative games, the players cooperate by choosing their actions jointly to achieve a jointly acceptable solution. Noncooperative games, on the other hand, assume that each player independently chooses his actions taking the actions of the other players as fixed. The foundations of noncooperative games are due to John Nash [Mye99]. While the players can be regarded as either noncooperative or cooperative, the distinction in game theory is made according to the form of the game [OR94]. There exists three game forms: The strategic form, the extensive form, and the coalitional form. Strategic and extensive form games are noncooperative games while coalitional form games are cooperative games. This distinction is illustrated in Figure 1.8. In this thesis, we do not use extensive form games. The interested reader is referred to [OR94, Section 6] for the theory. Next, we will describe noncooperative games in strategic form and cooperative games in coalitional form.

The Strategic Form

A game in strategic form $\langle \mathcal{K}, (\mathcal{A}_k)_{k \in \mathcal{K}}, (u_k)_{k \in \mathcal{K}} \rangle$ [OR94, Section 2.1] is composed of three elements. The set $\mathcal{K} = \{1, \dots, K\}$ consists of the players. Each player k has a strategy space \mathcal{A}_k from which he can select his actions. Each element of \mathcal{A}_k is a pure strategy and resembles a deterministic choice of action of player k . Alternatively, a mixed strategy of a player k is the choice of a pure strategy in \mathcal{A}_k with a certain probability. That is, each player k can randomize between different pure strategies in his strategy set \mathcal{A}_k . In this thesis, we do not consider the possibility of mixed strategies for the players. The utility function of a player k is $u_k : \mathcal{A}_1 \times \dots \times \mathcal{A}_K \rightarrow \mathbb{R}_+$. The utility function describes the preferences of a player depending on the strategies of all players. A player k in a game in strategic form can only choose strategies from his own strategy set \mathcal{A}_k to maximize his utility function.

The solution of a game in strategic form is a Nash equilibrium [Nas50b]. The Nash equilibrium describes the noncooperative outcome between the players as each player maximizes his utility given the actions of others. A pure strategy *Nash equilibrium* [OR94, Definition 14.1] of a strategic game is a strategy profile $(a_1^{\text{NE}}, \dots, a_K^{\text{NE}}) \in \mathcal{A}_1 \times \dots \times \mathcal{A}_K$ such that for every player $k \in \mathcal{K}$

$$u_k(a_1^{\text{NE}}, \dots, a_K^{\text{NE}}) \geq u_k(a_1^{\text{NE}}, \dots, a_{k-1}^{\text{NE}}, a_k, a_{k+1}^{\text{NE}}, \dots, a_K^{\text{NE}}), \text{ for all } a_k \in \mathcal{A}_k. \quad (1.9)$$

A Nash equilibrium is composed of a set of strategies for each player with the property that if one player changes his strategy unilaterally he would reduce his payoff. In Figure 1.9, the Nash equilibrium is illustrated. The illustration shows how the utility point would change if a player changes his strategy alone while the other player chooses the Nash equilibrium strategy. In Section 3.1, we study strategic games in the MISO IFC.

A Nash equilibrium may not always exist in pure strategies. However, the existence of a Nash equilibrium is guaranteed when the players use mixed strategies [Nas50b]. Conditions for existence and uniqueness of a pure strategy Nash equilibrium are provided in [Ros65].

The *best response* of a player k to the strategies of the other players is a strategy or set of strategies from \mathcal{A}_k that maximize player k 's utility function. The Nash equilibrium is a stable state at which each player chooses his best response to the strategies of the other players. Thus, the Nash equilibrium can be reached by a series of best responses. In strategic games, best response dynamics are studied [BO98] in order to examine whether the Nash equilibrium can be reached. Global stability of a Nash equilibrium means that a Nash equilibrium is reached by a series of best responses starting from

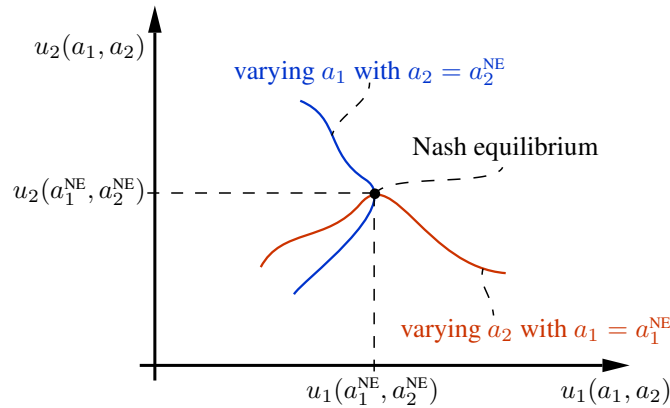


Figure 1.9.: Illustration of a Nash equilibrium.

any strategy profile.

Bayesian games [Mye83] are strategic games in which the players have uncertainty about the other players. A player's incomplete information can be about the utility functions or the strategy spaces of the other players. In these games, each player has private information which the other players do not know. The private information at player k is described by his type t_k . All types of a player k are included in the set T_k . Given his type t_k , player k builds beliefs on what the other players' types are. The subjective probability $\pi_k(t_1, \dots, t_{k-1}, t_{k+1}, \dots, t_K | t_k)$ describes player k 's beliefs about the other players' types given his type is t_k . In Bayesian games, a player chooses the strategy which maximizes his expected utility function over all possible types of the other players. The equilibrium of a game with incomplete information is called a Bayesian equilibrium.

The Coalitional Form

Games in coalitional form describe possible cooperation between players. Unlike in noncooperative games, cooperative games consider joint decisions of the players. A game in coalitional form without transferable utilities $\langle \mathcal{K}, \mathcal{X}, V, (u_k)_{k \in \mathcal{K}} \rangle$ [OR94, Section 13.5] is described by four elements: The set of players is \mathcal{K} and is called the grand coalition. The set \mathcal{X} is the set of consequences which consists of all jointly possible actions of the players. The mapping V assigns to every coalition $\mathcal{S} \subseteq \mathcal{K}$ a subset of the set \mathcal{X} . The utility function of a player k is $u_k : \mathcal{X} \rightarrow \mathbb{R}_+$.

The above definition of a coalitional game is general and can represent any game with transferable utilities. In a coalitional game with transferable utilities, the sum of the payoff of the players in a coalition \mathcal{S} (the worth of a coalition \mathcal{S}) is represented

by the characteristic function $\nu(\mathcal{S}) \in \mathbb{R}$ [LR57, Chapter 8]. In coalitional games with transferable utilities, the worth of a coalition can be divided arbitrarily between its members.

Solution concepts of coalitional games characterize a stable element or set of stable elements in the set of consequences \mathcal{X} . The first criterion for an element of the set \mathcal{X} to be stable is for it to be an imputation. An *imputation* is an element $\mathbf{x} \in \mathcal{X}$ satisfying $u_k(\mathbf{x}) \geq u_k(V(\{k\}))$ for all $k \in \mathcal{K}$ [OR94, Section 14.2]. In words, an imputation is a strategy profile with which each player k gets a higher utility than being noncooperative. If a strategy profile $\mathbf{x} \in \mathcal{X}$ is not an imputation, then there exists a player that would not agree to \mathbf{x} since he can achieve a higher utility when acting on his own. Let $\mathcal{I} \subseteq \mathcal{X}$ be the set of all imputations. An *objection* of coalition \mathcal{S} to the imputation \mathbf{y} is an imputation \mathbf{x} such that $u_k(\mathbf{x}) > u_k(\mathbf{y})$ for all $k \in \mathcal{S}$.

The *core* of a coalitional game is the set of imputations to which there exists no objection by any coalition \mathcal{S} . We use the core solution concept in the MISO IFC in Section 3.2.1. Another solution concept of coalitional games is the *stable set* proposed by von Neumann and Morgenstern [vNM44]. The stable set \mathcal{F} of a coalitional game is a subset of all imputations in \mathcal{I} which satisfies the internal and external stability conditions [OR94, Definition 279.1]:

- Internal stability: If $\mathbf{x} \in \mathcal{F}$ then for no $\mathbf{z} \in \mathcal{F}$ does there exist a coalition \mathcal{S} for which $u_k(\mathbf{z}) > u_k(\mathbf{x})$ for $k \in \mathcal{S}$.
- External stability: If $\mathbf{z} \in \mathcal{F} \setminus \mathcal{I}$ then there exists an element $\mathbf{y} \in \mathcal{F}$ such that $u_k(\mathbf{y}) > u_k(\mathbf{z})$ for $k \in \mathcal{S}$ and for some coalition \mathcal{S} .

While the core solution is a unique set, the stable set might not be unique. That is, there might be several stable sets of a coalitional game. There are other solutions to coalitional games such as the bargaining set, kernel, nucleolus, and the Shapley value. The interested reader is referred to [OR94, Chapter 14] and also to [LJ11] for a brief introduction.

The above described solutions of coalitional games determine joint strategies of the players such that players would cooperate in a grand coalition and no coalition has the incentive to deviate and act on its own. Coalition formation games [AD74, Mar07] describe situations in which the players can dynamically group to form a coalition structure. A *coalition structure* is a partition of the grand coalition \mathcal{K} into a set of disjoint coalitions. In coalition formation games, a partition function assigns to each coalition structure the worth of each coalition. The stability of a coalition structure ensures that no set of players can deviate to form another coalition structure. Different coalition

formation models are mentioned in the survey papers [Gre94, Yi03]. In [vNM44], von Neumann and Morgenstern proposed a coalition formation model, where each player proposes a set of players to build a coalition with. If a set of players have simultaneously proposed each other, then the coalition forms. In [DG80], an individually stable coalition formation model is proposed. In this model, only a single player is allowed to join a coalition in the existing coalition structure. An individually stable contractual equilibrium is formulated which requires that a player could only change coalitions when this is beneficial for him, to all the members of the coalition which he joins, and all the members of the coalition which he leaves. It is shown that this equilibrium always exists and it is possible to design a dynamic process that yields in a finite number of steps an equilibrium. In Section 3.2.2, we use a coalition formation algorithm which is based on merging and splitting of coalitions to reach a stable coalition structure. This coalition formation mechanism has been proposed in [AW09].

Cooperative games can be also solved by bargaining problems⁶. A bargaining problem between K players is defined by $\langle \mathcal{U}, \mathbf{d} \rangle$, where $\mathcal{U} \subset \mathbb{R}^K$ is the utility set and $\mathbf{d} \in \mathcal{U}$ is called the *threat point* or *disagreement point*. If the players could not reach an agreement, then their utilities correspond to the threat point. The solution of a bargaining problem is a unique point in \mathcal{U} . In [Nas50a], Nash formulated a cooperative solution to a two-player bargaining problem with a convex utility set \mathcal{U} . The Nash bargaining solution (NBS) \mathbf{u}^{NBS} is based on four axioms [Pet92]⁷:

- Weak Pareto Optimality (WPO): There exists no $\mathbf{x} \in \mathcal{U}$ such that $\mathbf{x} > \mathbf{u}^{\text{NBS}}$ (the inequality is componentwise). This means that the players cannot jointly improve their outcome from the NBS.
- Symmetry (SYM): If $d_1 = \dots = d_K$ and the utility space \mathcal{U} is symmetric, i.e. for any point $\mathbf{x} \in \mathcal{U}$ the permutation of the coordinates of \mathbf{x} leads to a point $\mathbf{x}' \in \mathcal{U}$, then $u_1^{\text{NBS}} = \dots = u_K^{\text{NBS}}$.
- Scale Transformation Covariance (STC): The bargaining problem $\langle \mathbf{a}\mathcal{U} + \mathbf{b}, \mathbf{a}\mathbf{d} + \mathbf{b} \rangle$ with $\mathbf{a}, \mathbf{b} \in \mathbb{R}^K$ and $\mathbf{a} > 0$ has the NBS $\mathbf{a}\mathbf{u}^{\text{NBS}} + \mathbf{b}$ where \mathbf{u}^{NBS} is the NBS of $\langle \mathcal{U}, \mathbf{d} \rangle$.
- Independence of Irrelevant Alternatives (IIA): Given two bargaining problems $\langle \mathcal{U}, \mathbf{d} \rangle$ and $\langle \tilde{\mathcal{U}}, \tilde{\mathbf{d}} \rangle$ with $\mathbf{d} = \tilde{\mathbf{d}}$ and $\mathcal{U} \subset \tilde{\mathcal{U}}$ and the NBS of $\langle \tilde{\mathcal{U}}, \tilde{\mathbf{d}} \rangle$ is $\tilde{\mathbf{u}}^{\text{NBS}} \in \mathcal{U}$ then the NBS of $\langle \mathcal{U}, \mathbf{d} \rangle$ is also $\tilde{\mathbf{u}}^{\text{NBS}}$.

⁶Bargaining problems can be represented by games in coalitional form [OR94, Chapter 15].

⁷We describe the axioms using the NBS.

The NBS satisfies the above axioms and solves the following problem [Pet92, Definition 2.1]:

$$\begin{aligned} & \text{maximize} && \prod_{k=1, \dots, K} (u_k - d_k) \\ & \text{subject to} && (u_1, \dots, u_K) \in \mathcal{U}. \end{aligned} \tag{1.10}$$

The NBS is the point in the utility set which dominates the threat point and maximizes the volume of the box created with the points \mathbf{d} and \mathbf{u}^{NBS} . Other bargaining solutions from axiomatic bargaining theory, such as the Kalai-Smorodinsky (KS) solution [KS75] and the egalitarian bargaining solution are described in [Pet92].

Chapter 2.

System Model and Problem Formulation

2.1. System and Channel Model

Consider a set $\mathcal{K} := \{1, \dots, K\}$ of transmitter-receiver pairs (links) operating concurrently in the same spectral band. Each transmitter k is equipped with $N_k \geq 2$ antennas, and each receiver with a single antenna. This setting is illustrated in Figure 2.1 and corresponds to the K -user multiple-input single-output (MISO) interference channel (IFC).

The quasi-static block flat-fading channel vector from transmitter k to receiver ℓ is denoted by $\mathbf{h}_{k\ell} \in \mathbb{C}^{N_k \times 1}$. Each transmitter k uses a transmit beamforming vector \mathbf{w}_k from its feasible *strategy space* \mathcal{A}_k defined as

$$\mathbf{w}_k \in \mathcal{A}_k := \{\mathbf{w} \in \mathbb{C}^{N_k \times 1} : \|\mathbf{w}\|^2 \leq 1\}, \quad (2.1)$$

where we assumed a total power constraint of one (w.l.o.g.). The basic model for the matched-filtered, symbol-sampled complex baseband data received at receiver k is¹

$$y_k = \mathbf{h}_{kk}^H \mathbf{w}_k s_k + \sum_{\ell \neq k} \mathbf{h}_{\ell k}^H \mathbf{w}_\ell s_\ell + n_k, \quad (2.2)$$

where $s_k \sim \mathcal{CN}(0, 1)$ is the symbol transmitted by transmitter k and $n_k \sim \mathcal{CN}(0, \sigma^2)$ are the noise terms. Throughout, we define the signal-to-noise ratio (SNR) as $1/\sigma^2$.

A *strategy profile* is a joint choice of strategies of all transmitters defined as

$$(\mathbf{w}_1, \dots, \mathbf{w}_K) \in \mathcal{X} := \mathcal{A}_1 \times \dots \times \mathcal{A}_K. \quad (2.3)$$

Given a strategy profile, the signal-to-interference-and-noise ratio (SINR) of link k is

$$\gamma_k(\mathbf{w}_1, \dots, \mathbf{w}_K) = \frac{|\mathbf{h}_{kk}^H \mathbf{w}_k|^2}{\sigma^2 + \sum_{\ell \neq k} |\mathbf{h}_{\ell k}^H \mathbf{w}_\ell|^2}, \quad (2.4)$$

¹For ease of notation, we conjugate the true channels $\tilde{\mathbf{h}}_{k\ell}$ such that $\mathbf{h}_{k\ell} = \tilde{\mathbf{h}}_{k\ell}^*$.

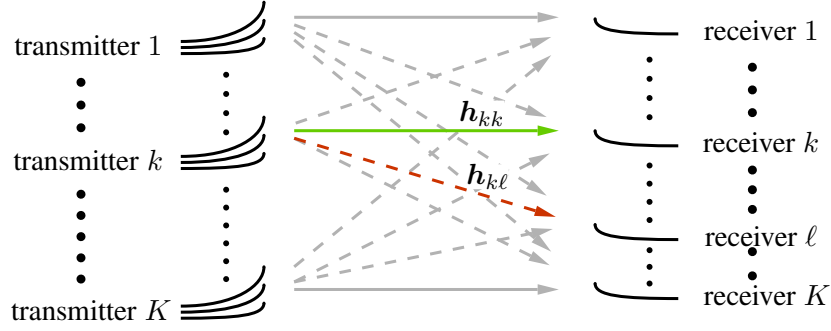


Figure 2.1.: Illustration of a K -user MISO IFC. The transmitters use multiple antennas while each receiver uses a single antenna. The solid arrows represent the links' intended channel vectors. The dashed arrows represent the interference channel vectors.

which results in the achievable rate

$$R_k(\mathbf{w}_1, \dots, \mathbf{w}_K) = \log_2(1 + \gamma_k(\mathbf{w}_1, \dots, \mathbf{w}_K)), \quad (2.5)$$

when single-user decoding (SUD) is assumed at receiver k , i.e., the receiver treats interference as noise. The *achievable rate region* is defined as

$$\mathcal{R} := \left\{ (R_1(\mathbf{w}_1, \dots, \mathbf{w}_K), \dots, R_K(\mathbf{w}_1, \dots, \mathbf{w}_K)) \in \mathbb{R}_+^K : (\mathbf{w}_1, \dots, \mathbf{w}_K) \in \mathcal{X} \right\}, \quad (2.6)$$

which is the set composed of all jointly achievable rates. In the rate region \mathcal{R} , rate tuples can be ranked according to their Pareto efficiency. A rate tuple $(R'_1, \dots, R'_K) \in \mathcal{R}$ is *Pareto superior* to $(R_1, \dots, R_K) \in \mathcal{R}$ if $(R'_1, \dots, R'_K) \geq (R_1, \dots, R_K)$, where the inequality is componentwise and strict for at least one component. The transition from (R_1, \dots, R_K) to (R'_1, \dots, R'_K) is called a *Pareto improvement* [JR03, Chapter 4.3.2]. Situations where Pareto improvements are not possible are called *Pareto optimal*. These points constitute the *Pareto boundary* of the rate region. Formally, the set of Pareto optimal points of \mathcal{R} are defined as [Pet92, p. 18]

$$\mathcal{P}(\mathcal{R}) := \{ \mathbf{x} \in \mathcal{R} : \text{there is no } \mathbf{y} \in \mathcal{R} \text{ with } \mathbf{y} \geq \mathbf{x}, \mathbf{y} \neq \mathbf{x} \}, \quad (2.7)$$

where the inequality in (2.7) is componentwise. The Pareto boundary is a subset of the weak Pareto boundary defined as [Pet92, p. 14]

$$\mathcal{W}(\mathcal{R}) := \{ \mathbf{x} \in \mathcal{R} : \text{there is no } \mathbf{y} \in \mathcal{R} \text{ with } \mathbf{y} > \mathbf{x} \}, \quad (2.8)$$

where the inequality in (2.8) is componentwise.

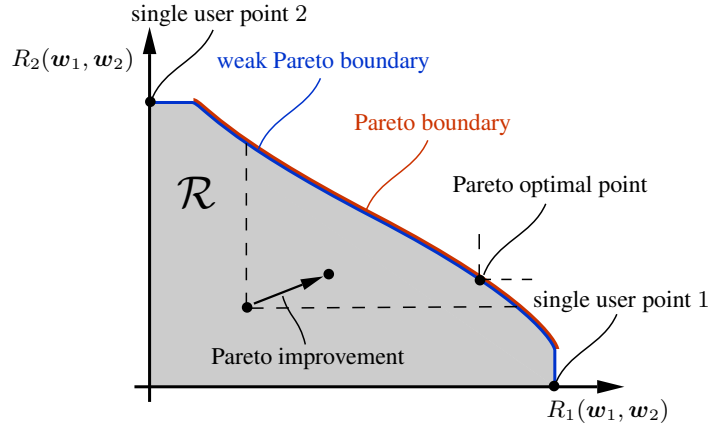


Figure 2.2.: Illustration of a two-user rate region.

In Figure 2.2, a two-user rate region is illustrated. The weak Pareto boundary is the set of outermost points in the rate region. The Pareto boundary is a subset of the weak Pareto boundary which has the additional property that it is impossible to strictly improve the rate of a link from the current operating point without affecting the rates of the other links. Accordingly, Pareto optimality is stronger than weak Pareto optimality. A single user point of a link k is its maximum achievable rate when all other links switch their transmission off. The links' coexistence brings the conflict that the links cannot achieve the rates in their single user points simultaneously. This is mainly due to the interference coupling between the links which degrades their performance. In the MISO IFC rate region, efficient operating points must be Pareto optimal. Otherwise, it is possible to improve the rate of at least one link without affecting the rates of the other links. Next, we will provide the necessary beamforming vectors required to operate at any Pareto optimal point.

By observing that the achievable rate of a link k in (2.5) is monotonically increasing with the direct power gain $|\mathbf{h}_{kk}^H \mathbf{w}_k|^2$ for fixed interference powers $|\mathbf{h}_{\ell k}^H \mathbf{w}_\ell|^2, k \neq \ell$. In addition, the rate of link k is monotonically decreasing with the interference power gain for fixed intended power gain. Pareto optimal beamforming requires a tradeoff between maximizing the intended power gain and minimizing interference gains generated at unintended receivers.

In the two-user MISO IFC, the set of efficient beamforming vectors for each transmitter $k \in \{1, 2\}$ are parameterized by a single real-valued parameter as [JLD08, Corollary 1]

$$\mathbf{w}_k(\lambda_k) = \sqrt{\lambda_k} \frac{\mathbf{\Pi}_{\mathbf{h}_{k\ell}} \mathbf{h}_{kk}}{\|\mathbf{\Pi}_{\mathbf{h}_{k\ell}} \mathbf{h}_{kk}\|} + \sqrt{1 - \lambda_k} \frac{\mathbf{\Pi}_{\mathbf{h}_{k\ell}}^\perp \mathbf{h}_{kk}}{\|\mathbf{\Pi}_{\mathbf{h}_{k\ell}}^\perp \mathbf{h}_{kk}\|}, \quad k \neq \ell, \quad (2.9)$$

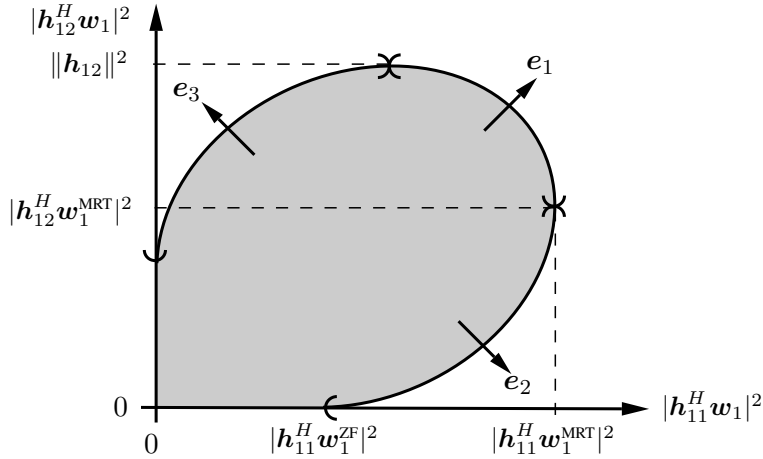


Figure 2.3.: Illustration of a power gain region.

where $\lambda_k \in [0, \lambda_k^{\text{MRT}}]$ with $\lambda_k^{\text{MRT}} = \|\mathbf{\Pi}_{\mathbf{h}_{k\ell}} \mathbf{h}_{kk}\|^2 / \|\mathbf{h}_{kk}\|^2$. The set of beamforming vector in (2.9) includes maximum ratio transmission (MRT) for $\lambda_k = \lambda_k^{\text{MRT}}$ such that

$$\mathbf{w}_k(\lambda_k^{\text{MRT}}) = \mathbf{w}_k^{\text{MRT}} = \frac{\mathbf{h}_{kk}}{\|\mathbf{h}_{kk}\|}, \quad (2.10)$$

and also zero forcing transmission (ZF) for $\lambda_k = 0$ such that

$$\mathbf{w}_k(\lambda_k = 0) = \mathbf{w}_k^{\text{ZF}} = \frac{\mathbf{\Pi}_{\mathbf{h}_{k\ell}}^\perp \mathbf{h}_{kk}}{\|\mathbf{\Pi}_{\mathbf{h}_{k\ell}}^\perp \mathbf{h}_{kk}\|}, \quad k \neq \ell. \quad (2.11)$$

In (2.9), the set of beamforming vectors necessary for Pareto optimal operation are characterized for each transmitter independently. This set includes the two special beamforming vectors, MRT and ZF, where MRT beamforming maximizes the intended power gain, while ZF nulls the interference at the unintended receiver.

In [Jor10], the concept of power gain region associated with a transmitter is developed in order to characterize efficient beamforming in the K -link case. The power gain region of a transmitter k is the set of all achievable power gains from this transmitter to all receivers. In Figure 2.3, a two-dimensional power gain-region is illustrated for transmitter 1. The direction vectors \mathbf{e}_1 , \mathbf{e}_2 , and \mathbf{e}_3 refer to three different parts of the boundary of the power gain region. The boundary part corresponding to \mathbf{e}_2 includes the maximum achievable power gain at receiver 1 and also zero power gain at receiver 2. These extreme points correspond to MRT and ZF transmission strategies, respectively.

Using the power gain region concept, the beamforming vectors necessary to achieve

any Pareto optimal point in the rate region \mathcal{R} are parameterized as [MJ11, Theorem 2]:

$$\mathbf{w}_k(\xi_{k1}, \dots, \xi_{kK}) = p_k \mathbf{v}_{max} \left(\underbrace{\xi_{kk} \mathbf{h}_{kk} \mathbf{h}_{kk}^H - \sum_{\ell \neq k} \xi_{k\ell} \mathbf{h}_{k\ell} \mathbf{h}_{k\ell}^H}_{\mathbf{Z}_k} \right), \quad (2.12)$$

where $\xi_{k\ell}$ are real nonnegative weights satisfying $\sum_{\ell=1}^K \xi_{k\ell} = 1$, and the power allocation is determined by the following conditions:

$$p_k = \begin{cases} 1 & \mu_{max}(\mathbf{Z}_k) > 0 \\ [0, 1] & \mu_{max}(\mathbf{Z}_k) = 0 \\ 0 & \mu_{max}(\mathbf{Z}_k) < 0 \end{cases}. \quad (2.13)$$

The number of required real-valued parameters to determine the efficient beamforming vectors for each transmitter k in (2.12) is $K - 1$. For a transmitter k , power control in (2.13) is needed when the downlink channels $\mathbf{h}_{k\ell}$, $\ell \in \mathcal{K}$, from transmitter k are linearly dependent. In this case, the largest eigenvalue of \mathbf{Z}_k for specific choice of parameters can be less than zero. If the downlink channels from transmitter k are linearly independent, then $\mu_{max}(\mathbf{Z}_k)$ is always strictly larger than zero except for $\xi_{kk} = 0$.

2.2. Problem Formulation and Contributions

In this section, we formulate the problems studied in this thesis and state our contributions accordingly. Moreover, we provide the references to the papers and articles (listed at the end of this section) where the results have been already published.

Our results are motivated by the fact that the Nash equilibrium in the MISO IFC, investigated in Section 3.1.1, is generally inefficient [LDJ08, LJ08]. With this respect, our problem formulations are concerned with the improvement of the performance of the links from the Nash equilibrium through coordination or cooperation mechanisms.

In Chapter 3, noncooperative and cooperative models from game theory for beamforming design in MISO IFC are used. The problem statements of this chapter are formulated in Problem 1 and Problem 2.

Problem 1. *What are the necessary constraints on the strategy space of each transmitter to achieve a Pareto optimal Nash equilibrium?*

Problem 1 is studied in Section 3.1.2. We consider a strategic game between the links in which the strategy space of each transmitter is constrained by null-shaping

constraints. Null-shaping constraints at a transmitter prohibit its transmission in specific spacial dimensions. We characterize the necessary null-shaping constraints for each transmitter such that the Nash equilibrium of the resulting strategic game is Pareto optimal. Here it is assumed that the arbitrator sets the constraints at each transmitter. This result has been published in [MJ11b].

Problem 2. *How would the links cooperate to jointly improve their rates with simple non-iterative transmission schemes such as zero forcing transmission or Wiener filter precoding?*

Problem 2 is studied in Section 3.2. We use coalitional games in the MISO IFC to determine possible cooperation between the links. The conditions for nonempty core of the coalitional game with ZF beamforming are characterized. These conditions state when the links can jointly improve their rates by joint cooperation with ZF transmission. In Section 3.2.2, a coalition formation game is formulated in which distinct sets of links can cooperate with ZF beamforming or Wiener filter precoding. We utilize an algorithm called merge-and-split in Section 3.2.3 to determine stable coalition structures according to which joint performance improvement from the Nash equilibrium is achieved. These results have been published in [MJ11a].

The next problems deal with the two-user MISO IFC and are studied using models from microeconomic theory in Chapter 4.

Problem 3. *What are the necessary and sufficient beamforming vectors that achieve all Pareto optimal points in the two-user MISO IFC SINR region?*

Problem 3 is studied in Section 4.1. We use a model of exchange in the two-user MISO IFC. The links are regarded as consumers that possess goods corresponding to the parameters of the efficient beamforming vectors in (2.9). The consumers in this setting can trade the goods between themselves. We exploit the Edgeworth box to illustrate the distribution of the goods between the consumers. In the Edgeworth box, the contract curve corresponds to the distributions of the goods that lead to Pareto optimal points. We characterize the contract curve in closed-form in Section 4.1.1. Moreover, we determine the exchange equilibria in Section 4.1.2 which are Pareto optimal points that dominate the Nash equilibrium. These results have been published in [MJ11c] and the journal version in [MJ12a].

Problem 4. *How to design a cooperative bargaining process that requires low signaling overhead between two links and terminates at an exchange equilibrium?*

Problem 4 is studied in Section 4.1.3. The exchange equilibria characterized in Section 4.1.2 are candidates for the outcomes of a bargaining process between the two consumers (links). The bargaining process is iterative and structured in bargaining-steps. At each bargaining-step, communication between the transmitters is needed in the form of signaling. Our design of the bargaining process relies on a systematic study of the allocations in the Edgeworth box. Accordingly, we propose a bargaining process which requires two-bit signaling from each transmitter at each bargaining-step and is guaranteed to converge to an outcome arbitrarily close to an exchange equilibrium. This result has been published in [MJHG10].

Problem 5. *How to coordinate the beamforming vectors of the two links to achieve an exchange equilibrium?*

Problem 5 is considered in Section 4.2. The competitive market model in Section 4.2 extends the exchange model in Section 4.1 by defining prices for the goods. The equilibrium of a competitive market is the Walrasian equilibrium and corresponds to the prices that equate the demand to the supply of goods. We characterize the Walrasian equilibrium prices in Section 4.2.2 and prove its uniqueness. In addition, we propose a coordination process, realized by the arbitrator, to reach the Walrasian equilibrium in Section 4.2.3. The Walrasian equilibrium lies in the set of exchange equilibria, i.e., dominates the Nash equilibrium. These results have been published in [MJ11c] and the journal version in [MJ12a].

References

- [MJHG10] R. Mochaourab, E. A. Jorswieck, K. M. Z. Ho, and D. Gesbert, “Bargaining and beamforming in interference channels,” in *Proc. ACSSC*, Jun. 2010, pp. 1–5. invited.
- [MJ11a] R. Mochaourab and E. A. Jorswieck, “Coalition formation in MISO interference channels,” in *Proc. IEEE CAMSAP*, Dec. 2011, pp. 237–240. invited.
- [MJ11b] R. Mochaourab and E. A. Jorswieck, “Optimal beamforming in interference networks with perfect local channel information,” *IEEE Trans. Signal Process.*, vol. 59, no. 3, pp. 1128–1141, Mar. 2011.
- [MJ11c] R. Mochaourab and E. A. Jorswieck, “Walrasian equilibrium in two-user multiple-input single-output interference channel,” in *Proc. IEEE ICC, Workshop on Game Theory and Resource Allocation for 4G*, Jun. 2011, pp. 1–5.

- [MJ12a] R. Mochaourab and E. A. Jorswieck, “Exchange economy in two-user multiple-input single-output interference channels,” *IEEE J. Sel. Topics Signal Process.*, vol. 6, no. 2, pp. 151–164, Apr. 2012.

2.3. Related Work

In this section, we first describe works that characterize Pareto optimal operating points in MISO IFC as well as works that design distributed coordination mechanisms to improve the performance of the links. Afterwards, we mention works that apply tools from game theory and microeconomic theory for resource allocation problems in communication networks.

2.3.1. Beamforming in Interference Channels

The problem of jointly optimizing the transmit beamforming vectors at the transmitters to meet a global objective of system efficiency in the MISO IFC has been the study of several recent works. Achieving a Pareto optimal point in the rate region requires finding the corresponding joint beamforming vectors to be used at the transmitters. The set of feasible beamforming vectors for each transmitter is an N -dimensional complex ball where N is the number of used antennas. In [LDL11], it is found that the complexity of the problem for finding desirable Pareto optimal operating points in the MISO IFC such as the maximum weighted sum-rate and proportional-fair rate points is NP-hard. Therefore, characterizing the necessary beamforming vectors that lead to Pareto optimal points is valuable to reduce the complexity of finding efficient operating points. Works with this objective are discussed next.

Characterization of Pareto Optimal Points

The importance of characterizing the set of beamforming vectors necessary for the links’ Pareto optimal operation is twofold: First, the set of relevant beamforming vectors to consider for finding a Pareto optimal point is reduced to a relatively small subset of all feasible beamforming vectors. Second, this set is parameterized by a number of scalars which reduces the complexity for indicating the required beamforming vectors. The work in [JLD08] was an initiation for characterizing the set of necessary transmission strategies to achieve all Pareto optimal points in the MISO IFC with interference treated as noise at the receivers. The efficient beamforming vectors are parameterized by $K(K-1)$ complex-valued parameters, where K is the number of links. The proposed parametrization reveals that only a small subset of all feasible beamforming vectors are

necessary for Pareto optimal beamforming. For the special two-user case, the efficient beamforming vectors are proven to be a linear combination of MRT and ZF. Thus, two real-valued parameters are required each between zero and one to characterize all Pareto optimal operating points. Based on this characterization, a monotonic optimization framework is developed in [JL10] for the two-user case to find the maximum weighted sum-rate, proportional-fair rate, and max-min solution that lie on the Pareto boundary of the rate region.

In [KL10], the problem of maximizing the rate of one link while fixing the rate of the other link in the two-user MISO IFC is solved by a feasibility second order cone program (SOCP). Accordingly, only points on the Pareto boundary of the two-user MISO IFC are obtained. Recently in [LKL11a], the parametrization for the two-user case in [JLD08] is used to characterize in closed form the beamforming vectors necessary and sufficient to achieve all Pareto optimal points, i.e. a single real-valued parameter is needed to characterize all Pareto optimal points in the two-user MISO IFC.

In [ZG09], the Pareto boundary of the two-user MISO IFC rate region is parameterized by two real-valued parameters each between zero and infinity. This parametrization relies on the virtual SINR framework proposed in [RFLT98] and relates to the parametrization in [JL10]. The virtual SINR framework in [RFLT98] is based on a duality between the uplink and the downlink in the MISO IFC. This framework is exploited for solving the problem of minimizing total network transmit power subject to SINR requirements at the receivers. A more general duality between the uplink and downlink in MISO channels is constructed in [DY10] for a multicell setting with multiple users served in each cell. The problem of minimizing transmitted power subject to receiver SINR requirements is solved considering different types of transmit power constraints.

The $K(K - 1)$ complex-valued parametrization in [JL10] for the K -user case has been recently improved to a $K(K - 1)$ real-valued parametrization in [SCP11, ZC10, MJ11]. In [SCP11], the K -user MISO IFC is considered with the capabilities of time-sharing (scheduling) the resources between the links. The optimality of single-stream beamforming to achieve all Pareto optimal points is proven. Moreover, a parametrization of the beamforming vectors that achieve all points on the Pareto boundary of the MISO IFC rate region is provided requiring $K(K - 1)$ real-valued parameters each between 0 and π . In [ZC10], the authors characterize the Pareto boundary of the MISO IFC through controlling interference levels at the receivers. The necessary beamforming vectors to achieve all Pareto optimal points are parameterized by $K(K - 1)$ real-valued parameters each between zero and infinity. Interestingly, the acquired parametrization for K users in [ZC10] is similar as in [ZG09] for the case of full power transmission.

However, the optimality of the proposed parametrization in [ZG09] is only studied for the two-user case. The necessary beamforming vectors to achieve all Pareto optimal points in a general MISO setting is characterized in [Jor10, MJ11]. The characterization exploits the concept of power gain region associated with a transmitter. The power gain region illustrates the efficient tradeoff between maximizing intended power gains and minimizing interference at unintended receivers. Accordingly, efficient transmission can be characterized in any setting in which the utility functions are monotonic in received power gains. The number of required parameters in a MISO setting with T transmitters and K receivers is $T(K - 1)$ where each parameter is between zero and one.

Specific points on the Pareto boundary of the MISO IFC rate region can be computed using monotonic optimization techniques [Tuy00]. These methods exploit the monotonicity properties of a global objective function. The optimal solution is found by systematically partitioning the utility space and removing regions where the solution may not lie. Monotonic optimization techniques require high computational complexity. However, they provide computational structure to solve nonconvex optimization problems which possess the monotonicity properties in the optimization variables. In [RTSH11], a global objective function is used which incorporates as special cases the maximum weighted sum-rate, proportional-fair rate, and max-min solutions. These points are found by a branch and bound algorithm in the MISO IFC and MISO BC. Monotonic optimization has been recently applied in [LZC12] to calculate the maximum weighted sum-rate in the SISO, SIMO, and MISO IFC. Moreover, monotonic optimization is exploited in [UB12] to calculate the maximum weighted sum-rate, proportional-fair rate, and max-min points in a multicell setting with multiple users in each cell. The framework also solves the problem of optimal time-sharing between the users.

Characterization of Pareto optimal points in cooperative multicell settings is conducted in [BZGO10, BBO12, BJBO11]. In cooperative multicell settings, signals intended for the users can be transmitted from multiple base stations in order to enhance the overall system performance. In [BZGO10], all Pareto optimal beamforming vectors for both cases of perfect and partial CSI at the transmitters are parameterized by $K(K - 1)$ complex-valued parameters. For perfect CSI at the transmitters and including dynamic transmitter cooperation for common receiver transmission, a parametrization of the efficient beamforming vector is provided in [BBO12] with general linear transmit power constraint at the transmitters. The number of required parameters is $K + L - 1$, where L is the number of linear transmit power constraints. For per transmitter power constraint, $2K - 1$ parameters are required each between zero and one. Thus, an improvement to the parameterizations requiring $K(K - 1)$ real-values is achieved. Also in

[BBO12], the calculation of each point on the Pareto boundary is done by using a bisection method and a quasi-convex feasibility problem. In [BJBO11], a general framework for multicell multicarrier transmission with dynamic cooperation between the transmitters is provided with general transmit power constraints. Optimality properties such as single-stream beamforming and the conditions for full power transmission are characterized. Moreover, a parametrization of the Pareto optimal beamforming vectors is provided with $KC + L$ real-valued parameters each between zero and one, where C and L are the number of subcarriers and the number of linear transmit power constraints, respectively. Considering a single carrier and per transmitter power constraints, the number of parameters in [BJBO11] is $2K$. In a multicell MISO setting with uncertainty in CSI at the transmitters, robust Pareto optimal beamforming is obtained by robust fairness-profile optimization in [BZBO12]. All Pareto optimal points in the performance region are achieved requiring $K - 1$ real-valued parameters. In addition, a monotonic optimization algorithm is applied to achieve specific Pareto optimal points such as maximum sum and proportional fair performance points.

In the case of partial CSI at the transmitters, characterization of the Pareto optimal transmit covariance matrices for the two-user MISO IFC is done in [LLJ10]. In [LKL09], it is shown that the characterization in [LLJ10] with the restriction of single-stream beamforming is a combination of MRT and ZF beamforming. Also with the restriction of single-stream beamforming, the Pareto boundary of the two-user MISO IFC with partial CSI at the transmitters is calculated in [KGLL09] using semidefinite relaxation and semidefinite programming (SDP). The problem is cast as maximizing the rate of one link while fixing the rate of the other.

All the results mentioned above hold for the case of single-user decoding (SUD) capabilities at the receiver, i.e., the receivers treat interference as noise. Considering multi-user decoding (MUD) capable receivers, the necessary Pareto optimal beamforming vectors in the two-user MISO IFC is characterized in [HGJM11]. In [LKL11b], an efficient algorithm is proposed for the computation of Pareto optimal points in the rate region with MUD capabilities.

Coordination Mechanisms

The real-valued parametrization for the two-user case in [JLD08] has been important for designing efficient distributed resource allocation schemes. In [HG08], this parametrization is utilized to propose a bargaining algorithm that requires two-bit signaling between the transmitters. Starting in joint MRT (Nash equilibrium), the transmitters reduce their beamforming parameters in each iteration by an equal step-length leading to joint

increase in the links' rates. In [LK10], a similar algorithm is proposed for the cases of perfect and imperfect CSI. At each iteration, each transmitter optimizes its transmission to reduce a fixed amount of interference power at unintended receivers. Both algorithms in [HG08] and [LK10] terminate when at least one link experiences reduction in its outcome. While both algorithms improve the joint performance of the systems from the Nash equilibrium, these outcomes are not Pareto optimal. Extension to the precoding design in MIMO IFC is done in [HG10].

In [ZC10], a distributed algorithm is proposed that is performed between link pairs in the MISO IFC. The transmitters exchange interference levels in each iteration and optimize their transmission such that these interference levels are met at unintended receivers. The interference levels are updated based on a necessary condition for Pareto optimality. Although this condition is not proven to be also sufficient, numerical evidence shows that the algorithm converges to a Pareto optimal outcome almost surely. In [LDL11], after deriving the complexity results on finding specific Pareto optimal points in the MISO IFC, a distributed algorithm is proposed to find Pareto optimal points such as the maximum sum-rate. The proposed algorithm requires perfect local CSI at transmitters as well as the exchange of scalar values regarding received powers in each iteration. The algorithm is guaranteed to converge to a local optimum. In [QZLC11], distributed algorithms are proposed where the computational load of Pareto optimal beamforming vectors is distributed and carried out sequentially at the transmitters. The algorithms terminate at Pareto optimal points requiring the exchange of the optimization parameters between the transmitters.

In the K -user MISO IFC, a low complexity one-shot coordination mechanism is proposed in [ZG09] in which each transmitter independently maximizes its virtual SINR. The virtual SINR of a transmitter is the SINR achieved when virtually regarding the single antenna receivers as transmitters and the actual transmitters as the multi-antenna receivers. The virtual SINR is maximized by an MMSE beamforming structure. For the two-user case, the proposed mechanism is proven to be Pareto optimal. The work in [ZG09] is extended to the precoding design in MIMO settings in [ZHG09]. Furthermore, the extension to cooperative multicell settings is studied in [ZG10] in which all transmitters know the signals intended to all receivers.

The appealing property of MMSE transmit beamforming is that it only requires local CSI at a transmitter. Moreover, in cases of low and high SNR, joint MMSE beamforming is sum-rate optimal because the MMSE beamforming vector converges to MRT beamforming at low SNR and to ZF at high SNR. This explains the fact that MMSE transmit beamforming design as in [ZG09] has been proposed in several works

[HSHS08, LNR⁺09, LPNV10, PPL11]. In [HSHS08], MMSE beamforming maximizes the signal-to-leakage plus noise ratio. In [LNR⁺09], the high SNR approximation of the sum-rate in a two-user MISO IFC is optimized leading to an MMSE beamforming design. Extension of [LNR⁺09] to MISO multicarrier settings is done in [LRB⁺10]. In [PPL10], using the high SNR approximation of the weighted sum-rate, suboptimal distributed beamforming techniques are provided. There, the parametrization in [ZG09] is utilized to propose a heuristic algorithm which iteratively updates the parameters to improve the links' sum-rate. In [VPNL11], the authors study the reciprocity of the uplink and downlink channels in the MISO IFC when automatic gain control at the receivers is considered. Automatic gain control adapts the signal power at the receiver to meet a specifically defined value. The corresponding transmit beamforming design in the MISO IFC is termed EIG beamforming. In [PNLV11], EIG beamforming is used with transmit power adaptation such that maximum restricted power levels at each receiver are not exceeded.

The works in [BN10, DUD11] provide heuristic ZF beamforming schemes in multicell settings. The objective is to efficiently select a subset of receivers at which interference is nulled by applying ZF transmission. In [BN10], the transmitters perform ZF to receivers which are mostly affected by interference. In [DUD11], a successive greedy user selection approach is applied with the objective of maximizing the system sum-rate.

2.3.2. Game Theoretic and Microeconomic Theory Applications

In this section, related work that applies models from game theory and microeconomic theory are discussed. While game theoretic models have been used plentifully for resource allocation problems in wireless networks, there exists relatively little work that apply microeconomic models.

Game Theory for Resource Allocation in Wireless Networks

Game theoretic models for resource allocation in wireless networks have been successfully applied in numerous works. In this section, we only mention a few results to highlight the advantages in the game theoretic approaches. First, we mention applications of noncooperative games for distributed resource allocation problems. These include games in strategic form and in extensive form. Afterwards, we present works that consider cooperative game theoretic models.

Two-player zero-sum games are considered in [PCL03, JB04] to find robust transmission strategies for a MIMO link. In [PCL03], worst-case transmission is investigated

by studying a game between the MIMO link and nature. Nature chooses the channel matrix, and the transmitter optimizes its strategy to maximize the link capacity. It is found that robust transmission, corresponding to the Nash equilibrium (min-max solution), is a transmit covariance matrix with uniform power allocation. In [JB04], robust transmission according to worst-case interference is studied. Here, nature chooses the interference covariance matrix from a set of alternatives, and the link optimizes the transmitter and receiver covariance matrices accordingly. Robust transmission is determined by the min-max solution.

In distributed resource allocation schemes, each user exploits available local information to optimize his utility function independently. Noncooperative game models are consistent with this approach. If the users (players) independently choose their best response to the strategies of the other players, the Nash equilibrium is the stable state at which no player can improve his utility by choosing another strategy. Accordingly, distributed operating points are Nash equilibria.

In multicarrier SISO IFC, waterfilling power allocation maximizes the rate of a link for given power allocations of the other transmitters. The global stability of distributed iterative waterfilling is the stability of the Nash equilibrium of a strategic game between the links. In [SPB08], conditions for the uniqueness of the Nash equilibrium and global convergence of iterative waterfilling are characterized. In the MIMO IFC, analysis of the Nash equilibrium regarding uniqueness and global stability is done in [SPB09].

Pricing is a mechanism used to enforce distributed system efficiency. For example, energy-efficiency can be acquired if the utility function of a transmitter is constructed such that excessive transmission powers are penalized [SMG01, JBN10]. An overview of distributed energy efficient power control in multiuser systems can be found in [MPS07]. In [SMG01], pricing to reduce transmission powers is applied to achieve joint performance improvements in the distributed system. In [JBN10], the Pareto boundaries of multiple access channels are characterized where the user utilities include linear pricing terms. In SISO MAC, linear pricing has been applied in [SMG02] to improve the outcome of the users without pricing. The authors in [SMG02] prove the existence and global stability of the Nash equilibrium by showing that the considered game is a supermodular game [Top98]. Supermodular games are a class of noncooperative games which have interesting properties regarding the structure of the Nash equilibria as well as the convergence properties of distributed algorithms [AA03]. The properties of supermodular games have been also exploited in [HBH06, SSB⁺09]. In [HBH06], distributed power control in ad hoc networks is studied with pricing determined according to the generated interference. In [SSB⁺09], distributed power allocation and beamforming is

proposed in multi-antenna IFCs. Each link independently maximizes its utility function taking into account a pricing term which depends on the interference generated at unintended receivers. Accordingly, the performance of the system is improved in a distributed fashion.

Games in extensive form have been applied in [LEG08, EPT07, LE11]². In [LEG08], a Stackelberg game is proposed in multiple access channels. The base station is the leader which decides first for the decoding order of the users. The users are the followers which choose their transmission strategies after the base station. The Stackelberg equilibrium is shown to achieve the corner points of the capacity region. Moreover in [LEG08], a repeated game is formulated to achieve points on the Pareto boundary of the capacity region. In [EPT07], after showing that the Nash equilibrium in spectrum sharing settings is generally inefficient, a repeated game is formulated to provide incentives for the transmitters to choose their strategies such that the outcome is Pareto optimal. The bargaining model of alternating offers [Rub82] is successfully applied in [LE11] to achieve Pareto optimal points in interference channels.

Noncooperative and cooperative game theoretic models for conflict analysis in the interference channel are discussed in [LJLM09]. In [LJ08], it is shown that MRT is a dominant strategy for each transmitter in the MISO IFC. That is, each noncooperative transmitter chooses MRT independent of the beamforming vectors used at the other transmitters. The Nash equilibrium, corresponding to joint MRT, is shown to be inefficient in general. Therefore, a cooperative Pareto optimal solution is proposed according to the Nash bargaining solution (NBS). In [LZ08], the NBS has been characterized for the multicarrier SISO IFC. The NBS is acceptable for all links since it provides rates jointly larger than at the Nash equilibrium. Another solution from axiomatic bargaining theory is the Kalai-Smorodinsky (KS) solution. In [NS09], the KS is studied in the MISO IFC and an algorithm is provided to reach the solution. Both the NBS and KS are desirable outcomes because they are Pareto optimal and give for each player utilities higher than without cooperation.

Games in coalitional form provide cooperative solutions for resource allocation problems. A tutorial on the application of coalitional games in wireless networks is given in [SHD⁺09]. In [MSM08], transmitter and receiver cooperation of single-antenna links is considered. Coalitions between transmitters and receivers lead to multi-antenna systems which enhance the performance of the links. Coalition formation in multiuser systems is studied in [SHDH09]. Users with single-antennas, initially assigned orthogonal re-

²Stackelberg games, repeated games as well as the game of alternating offers are games in extensive form [OR94].

sources, cooperate to form multi-antenna systems. Significant gains are achieved by using tools from coalitional game theory which provide structured cooperation methods between the users.

Microeconomic Theory for Resource Allocation in Communication Networks

Models from microeconomic theory have found a few applications for resource allocation problems in communication networks. In [Ye07], the competitive market model is considered for allocating transmit powers to the links sharing a common frequency band. The links purchase their transmit power subject to budget constraints. An agent, referred to as the market, determines the unit prices of the power spectra. Existence of the Walrasian equilibrium is proven and conditions for its uniqueness are provided. In [LTY09], the work in [Ye07] is extended to the problem of determining the budgets of the links to satisfy specific user requirements. For example, the links' budgets are determined such that all users achieve equal utilities in equilibrium. In [XAY10], the Walrasian equilibrium is formulated as a linear complementarity problem (LCP) for a multicarrier setting, and a decentralized price-adjustment process is proposed to reach the equilibrium. In each iteration, the links send their power demands to the spectrum manager which adjusts the prices according to the total demand and supply of power. The work in [XAY10] supports both works in [Ye07, LTY09] in providing a mechanism to reach the Walrasian equilibrium.

Spectrum trading in cognitive radio is analyzed using microeconomic models in [NH08]. In this setting, primary users sell their owned spectrum to secondary users. Three models to determine the prices of the spectrum are considered: The first model corresponds to a competitive market in which the prices are determined according to the Walrasian equilibrium. The second model is a Cournot oligopoly in which the primary service providers compete with each other to determine their prices. The equilibrium in this model corresponds to a Nash equilibrium. The third model considers cooperative primary users which jointly determine the spectrum prices to maximize their total profit. Also in cognitive radio settings, hierarchical spectrum sharing is modeled as an inter-related market in [NH10]. The service in one tier of the hierarchical system sells its spectrum to the service in the lower tier. The pricing mechanism for the bandwidth allocations between the services corresponds to the Walrasian equilibrium, i.e. the supply equates the demand of the resources. In [TGC10], the Walrasian equilibrium is used for simultaneous bitrate allocation for multiple video streams. There, the Edgeworth box [Wal74] is used as a tool to illustrate the efficient allocation of the streams.

Chapter 3.

Game Theoretic Applications

This chapter deals with the application of game theory for conflict analysis and resource allocation in the MISO IFC. The links are assumed to be rational and intelligent as discussed in Section 1.4.2. In the first section of this chapter, the links are assumed to be noncooperative. In this case, either there is no possibility of communication between the links, or an arbitrator is connected to the links to coordinate their actions. In the second section, we assume that the links can directly communicate with each other. For this case, cooperative games are applied to determine cooperative solutions between the links.

3.1. Noncooperative Games

In game theory, games in strategic form determine outcomes of a conflict situation between noncooperative players. The noncooperative outcome corresponds to strategies the players would choose if cooperation among them is not feasible. The complexity of implementing a noncooperative outcome is much less than a cooperative outcome since the former requires no overhead in communication between the players. If cooperation between the players is feasible, the noncooperative outcome can be considered as a threat point or a disagreement point in case cooperation fails. That is, each player cooperates with another player under the condition that its performance improves from the noncooperative outcome.

3.1.1. Game in Strategic Form

The players in our setting are the links and a game in strategic form between them is defined by the tuple [OR94, Definition 11.1]

$$\langle \mathcal{K}, (\mathcal{A}_k)_{k \in \mathcal{K}}, (R_k)_{k \in \mathcal{K}} \rangle, \quad (3.1)$$

where \mathcal{K} is the set of players, \mathcal{A}_k is the strategy space of player k in (2.1), and R_k is the achievable rate function of player k in (2.5).

The solution of the strategic game in (3.1) is a Nash equilibrium¹.

Definition 1. A Nash equilibrium [OR94, Definition 14.1] of a strategic game

$$\langle \mathcal{K}, (\mathcal{A}_k)_{k \in \mathcal{K}}, (R_k)_{k \in \mathcal{K}} \rangle \quad (3.2)$$

is a strategy profile $(\mathbf{w}_1^{NE}, \dots, \mathbf{w}_K^{NE}) \in \mathcal{A}_1 \times \dots \times \mathcal{A}_K$ such that for every player $k \in \mathcal{K}$

$$R_k(\mathbf{w}_1^{NE}, \dots, \mathbf{w}_K^{NE}) \geq R_k(\mathbf{w}_1^{NE}, \dots, \mathbf{w}_{k-1}^{NE}, \mathbf{w}_k, \mathbf{w}_{k+1}^{NE}, \dots, \mathbf{w}_K^{NE}), \text{ for all } \mathbf{w}_k \in \mathcal{A}_k. \quad (3.3)$$

In words, a Nash equilibrium is a strategy profile in which no player has the incentive to change his strategy if all other players choose their Nash equilibrium strategy. From Definition 1, each player would always choose his *best response strategy* to the strategies chosen by the other player. That is, each player decides for the strategy in his strategy set which maximizes his utility given the strategies of the other players. Consequently, the Nash equilibrium is a state of mutual best responses.

Given a set of beamforming vectors of all other players $(\mathbf{w}_1, \dots, \mathbf{w}_{k-1}, \mathbf{w}_{k+1}, \dots, \mathbf{w}_K)$, transmitter k 's best response is the beamforming vector \mathbf{w}_k which maximizes his achievable rate as

$$\underset{\mathbf{w}_k \in \mathcal{A}_k}{\text{maximize}} \log_2 \left(1 + \frac{|\mathbf{h}_{kk}^H \mathbf{w}_k|^2}{\sigma^2 + \sum_{j \neq k} |\mathbf{h}_{jk}^H \mathbf{w}_j|^2} \right). \quad (3.4)$$

The solution of the above problem is maximum ratio transmission (MRT) written as

$$\mathbf{w}_k^{\text{MRT}} = \frac{\mathbf{h}_{kk}}{\|\mathbf{h}_{kk}\|}. \quad (3.5)$$

The MRT beamforming strategy of player k in (3.5) does not depend on the strategies of the other players. Thus, each transmitter chooses its MRT beamforming vector to maximize its achievable rate irrespective of the strategy choice of the other transmitters. Consequently, the Nash equilibrium of our strategic game is unique and corresponds to joint MRT $(\mathbf{w}_1^{\text{MRT}}, \dots, \mathbf{w}_K^{\text{MRT}})$. In addition, the Nash equilibrium of our game belongs to a strong notion of equilibrium called dominant strategy equilibrium.

Definition 2. A dominant strategy equilibrium [OR94, Definition 181.1] of a strategic game

$$\langle \mathcal{K}, (\mathcal{A}_k)_{k \in \mathcal{K}}, (R_k)_{k \in \mathcal{K}} \rangle \quad (3.6)$$

¹The Nash equilibrium in the MISO IFC has been studied in [LDJ08].

is a strategy profile $(\mathbf{w}_1^*, \dots, \mathbf{w}_K^*) \in \mathcal{A}_1 \times \dots \times \mathcal{A}_K$ such that for every player $k \in \mathcal{K}$

$$R_k(\mathbf{w}_1, \dots, \mathbf{w}_{k-1}, \mathbf{w}_k^*, \mathbf{w}_{k+1}, \dots, \mathbf{w}_K) \geq R_k(\mathbf{w}_1, \dots, \mathbf{w}_K),$$

for all $(\mathbf{w}_1, \dots, \mathbf{w}_K) \in \mathcal{A}_1 \times \dots \times \mathcal{A}_K$. (3.7)

In words, a dominant strategy equilibrium consists of the strategies of the players, where each player chooses his best response strategy irrespective of the strategies chosen by the other players.

The Nash equilibrium in our game is a state in which the links would operate without requiring any overhead for communication with one another. However, if the outcome in Nash equilibrium is not efficient, methods for cooperation or coordination between the links have to be provided.

The best response of a player k in (3.4) maximizes the intended power gain without taking into account the interference it generates at the other receivers. Consequently, interference which is treated as additive noise at the receivers can be uncontrollably high to degrade the performance of the noncooperative systems. Generally, in spectrum sharing scenarios the Nash equilibrium is not efficient because each noncooperative transmitter is indifferent to the amount of interference it generates at the other receivers [EPT07]. Coexisting noncooperative links can end up in high mutual interference which leads to saturation in the rates of each system with increasing transmission power.

The efficiency of the Nash equilibrium outcome depends on its distance to the Pareto boundary of the rate region. In [LJ08], it is shown that the Nash equilibrium is close to the Pareto boundary in the low SNR regime. In the high SNR regime, zero forcing (ZF) transmission is near Pareto optimal, while the Nash equilibrium has poor performance [LDJ08].

In Figure 3.1, Figure 3.2, and Figure 3.3, we plot two-user rate regions² for -10 , 5 and 20 dB SNR, respectively. In Figure 3.1, the Nash equilibrium is near Pareto optimal while joint ZF has worse performance. In the low SNR regime, noise power dominates the interference power at each receiver. Hence, the users must maximize the intended power gain with MRT with which the interference is negligible with respect to noise. In Figure 3.2, the Nash equilibrium and joint ZF are away from the Pareto boundary. In Figure 3.3, the Nash equilibrium has bad performance while joint ZF is near Pareto optimal. At high SNR, the noise power is negligible in comparison to interference and therefore nulling the interference at unintended receivers with ZF brings joint improvement to the links' performance.

²The Pareto boundary of the two-user rate region is plotted using the closed form solution presented later in Chapter 4.1.

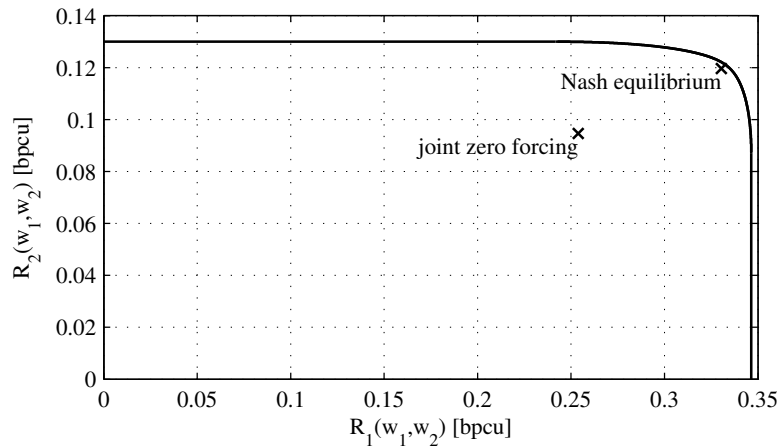


Figure 3.1.: Two-user rate region at -10 dB SNR.

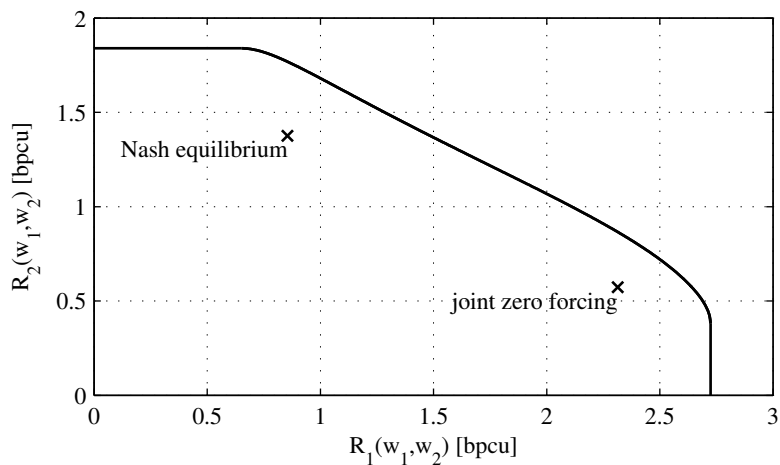


Figure 3.2.: Two-user rate region at 5 dB SNR.

A measure called the Price of Anarchy (PoA) quantifies the efficiency of the Nash equilibrium³. The PoA is defined as the ratio of the maximum sum utility to the sum utility in the worst-case Nash equilibrium [KP99, Pap01]:

$$\text{PoA} = \frac{\text{maximum sum utility}}{\text{worst-case sum utility in Nash equilibrium}}. \quad (3.8)$$

If the PoA is one, then the Nash equilibrium coincides with the maximum sum utility point. If the PoA is two, then two times the sum utility in Nash equilibrium can be achieved if coordination overhead is made to improve the efficiency of the noncooperative state. A high PoA is an indication for the necessity of cooperation or coordination between the players. We compare the Nash equilibrium in our setting to the maximum

³The analysis of the Price of Anarchy in the MISO IFC has been done in [LJLM09].

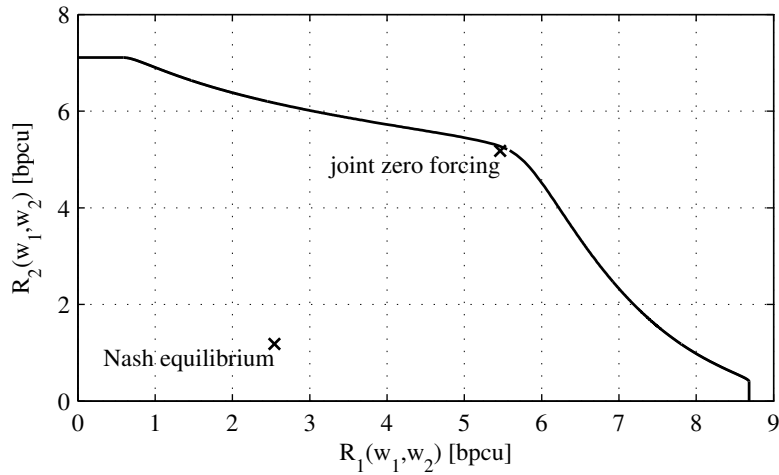


Figure 3.3.: Two-user rate region at 20 dB SNR.

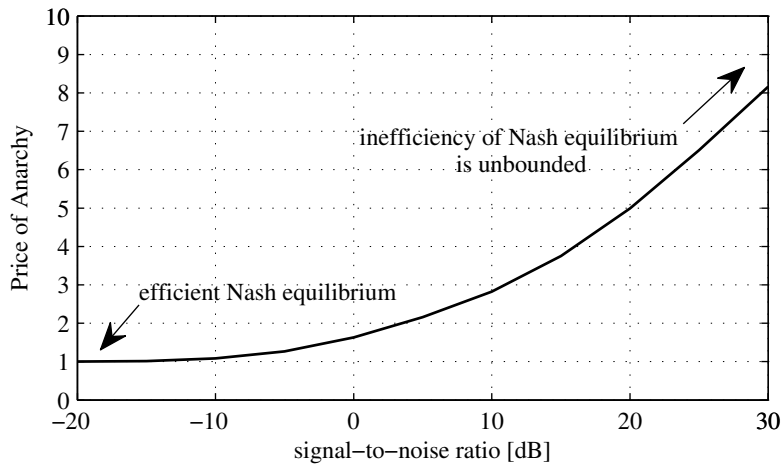


Figure 3.4.: Plot of the Price of Anarchy in the MISO IFC for increasing SNR.

achievable sum rate found by grid search for different SNR values in Figure 3.4. In the low SNR regime, the Nash equilibrium is sum rate optimal. The inefficiency of the sum rate in Nash equilibrium increases for increasing SNR.

3.1.2. Constraints for Efficient Nash Equilibrium

The previous section has shown that the Nash equilibrium is generally not Pareto efficient. In this section, we assume that there exists an arbitrator which coordinates the actions of the players. Specifically, the arbitrator puts null-shaping constraints on the strategy sets of the players. We characterize the necessary constraints to achieve all Pareto optimal points in the rate region as Nash equilibria. A null-shaping constraint is

a term used in underlay cognitive radio scenarios [GJMS09]. In an underlay cognitive radio scenario, secondary users can share the communication resources with primary users under the condition they do not impose quality of service (QoS) degradation to the primary systems. A limited QoS degradation to the primary users is described by interference temperature constraints (ITC) [Hay05]. When no interference on the primary users is allowed, the constraint is said to be a null-shaping constraint [SPPF09].

Let \mathbf{w}_k be the beamforming vector used at transmitter k , null-shaping constraints in the directions $\mathbf{v}_{k1}, \dots, \mathbf{v}_{kL}$ are written as

$$|\mathbf{w}_k^H \mathbf{v}_{ki}| = 0, \quad i = 1, \dots, L. \quad (3.9)$$

In order to be able to fulfill the L null-shaping constraints simultaneously, the number of applied antennas at the transmitter has to be greater than L .

We apply the null-shaping constraints on the transmissions in our setting. However, these constraints do not correspond to directions of primary users but are virtually selected by the arbitrator in order to improve the efficiency of the Nash equilibrium. The game in strategic form with null-shaping constraints is

$$\langle \mathcal{K}, (\tilde{\mathcal{A}}_k)_{k \in \mathcal{K}}, (R_k)_{k \in \mathcal{K}} \rangle, \quad (3.10)$$

where the strategy set of each player k includes the null-shaping constraints as

$$\tilde{\mathcal{A}}_k = \{\mathbf{w}_k \in \mathcal{A}_k : |\mathbf{w}_k^H \mathbf{v}_{ki}| = 0, i = 1, \dots, L\}. \quad (3.11)$$

Accordingly, the null-shaping constraints for a player k reduce his strategy space from \mathcal{A}_k in (2.1) to $\tilde{\mathcal{A}}_k$. Player k 's dominant strategy, which solves the following problem:

$$\underset{\mathbf{w}_k \in \tilde{\mathcal{A}}_k}{\text{maximize}} \log_2 \left(1 + \frac{|\mathbf{h}_{kk}^H \mathbf{w}_k|^2}{\sigma^2 + \sum_{j \neq k} |\mathbf{h}_{jk}^H \mathbf{w}_j|^2} \right), \quad (3.12)$$

is

$$\mathbf{w}_k = \frac{\Pi_{\mathbf{V}_k}^\perp \mathbf{h}_{kk}}{\|\Pi_{\mathbf{V}_k}^\perp \mathbf{h}_{kk}\|}. \quad (3.13)$$

where $\mathbf{V}_k = [\mathbf{v}_{k1}, \dots, \mathbf{v}_{kL}]$. Consequently, the beamforming vector in (3.13) is the Nash equilibrium strategy of the strategic game with null-shaping constraints in (3.10).

Efficient design of null-shaping constraints leads to Pareto optimal points in the achievable rate region with the applied beamforming vectors having the form of (3.13).

Corollary 1. *Assume that the number of antennas at each transmitter is larger than or equal to the number of links, i.e. $N_k \geq K$ for all $k = 1, \dots, K$, and define*

$$\mathbf{Z}_k(\xi_{k1}, \dots, \xi_{kK}) = [\mathbf{z}_{k1}(\xi_{k1}, \dots, \xi_{kK}), \dots, \mathbf{z}_{kK-1}(\xi_{k1}, \dots, \xi_{kK})], \quad (3.14)$$

with

$$\mathbf{z}_{ki}(\xi_{k1}, \dots, \xi_{kK}) = \mathbf{v}_i \left(\xi_{kk} \mathbf{h}_{kk} \mathbf{h}_{kk}^H - \sum_{\ell \neq k} \xi_{k\ell} \mathbf{h}_{k\ell} \mathbf{h}_{k\ell}^H \right), \quad (3.15)$$

where $\xi_{k\ell}$ are nonnegative real weights satisfying $\sum_{\ell=1}^K \xi_{k\ell} = 1$. All points on the Pareto boundary of the rate region \mathcal{R} can be achieved by the beamforming vectors

$$\mathbf{w}_k(\xi_{k1}, \dots, \xi_{kK}) = \frac{\mathbf{\Pi}_{\mathbf{Z}_k(\xi_{k1}, \dots, \xi_{kK})}^\perp \mathbf{h}_{kk}}{\|\mathbf{\Pi}_{\mathbf{Z}_k(\xi_{k1}, \dots, \xi_{kK})}^\perp \mathbf{h}_{kk}\|}, \quad k = 1, \dots, K. \quad (3.16)$$

Proof. The proof is provided in Section 3.3.1. □

In Corollary 1, the design of the null-shaping constraints is given in (3.14), and the efficient transmission strategies are in (3.16). Here, $K - 1$ null-shaping constraints are to be applied on each transmitter, and the number of required real-valued parameters is the same as in (2.12). Hence, the complexity of parameterizing the efficient beamforming vectors is similar in Corollary 1 to the parametrization in (2.12).

Through the design of the null-shaping constraints in Corollary 1, all Pareto optimal points of the rate region are characterized by transmission strategies that are Nash equilibria. The interesting observations are as follows. Null-shaping constraints are sufficient to characterize the Pareto boundary of the MISO IFC rate region. Moreover, given the null-shaping constraints, the transmitters are required to be noncooperative in order to achieve efficient operating points. Alternatively, the noncooperative outcome of the players is more efficient when the players' strategy sets are made smaller. This is in analogy with the Braess paradox [Bra68] in traffic planning where investing in new roads for a traffic network in Nash equilibrium can increase the delay time for each driver.

3.2. Cooperative Games

In this section, cooperation between the links is studied using coalitional games. The links can directly communicate with each other to develop possible cooperation. While noncooperative transmission of a link corresponds to MRT, we choose two cooperative transmission schemes which take into account the interference generated at the unintended receivers. These cooperative transmission schemes are zero forcing transmission and Wiener filter precoding.

3.2.1. Game in Coalitional Form

In game theory, cooperative games are described by games in coalitional form. A game in coalitional form [OR94, Definition 268.2] is defined by the tuple

$$\langle \mathcal{K}, \mathcal{X}, V, (R_k)_{k \in \mathcal{K}} \rangle, \quad (3.17)$$

where \mathcal{K} is the set of players, \mathcal{X} is the set of possible joint actions of the players in (2.3), V assigns to every coalition \mathcal{S} (a nonempty subset of \mathcal{K}) a set $V(\mathcal{S}) \subseteq \mathcal{X}$, and R_k is the utility of player k given in (2.5). A coalition \mathcal{S} is a set of players that are willing to cooperate, and $V(\mathcal{S})$ defines their joint feasible strategies. In this game, the payoff of a player cannot be transferred to other players in his coalition. The game is said to have *nontransferable utilities*.

A coalitional game⁴ between the links determines the strategy profiles with which all the links have the incentive to cooperate jointly. This set of strategy profiles makes up the *core* of the coalitional game.

Definition 3. *The core of a coalitional game [OR94, Definition 268.3] is the set of all strategy profiles $(\mathbf{x}_k)_{k \in \mathcal{K}} \in V(\mathcal{K})$ for which there is no coalition \mathcal{S} and $(\mathbf{y}_k)_{k \in \mathcal{S}} \in V(\mathcal{S})$ for which $R_k(\mathbf{y}_1, \dots, \mathbf{y}_K) > R_k(\mathbf{x}_1, \dots, \mathbf{x}_K)$ for all $k \in \mathcal{S}$.*

The core is *not empty* if there exists no coalition $\mathcal{S} \subset \mathcal{K}$ which can deviate from the grand coalition and provide its members with payoffs higher than in the grand coalition. In Definition 3, the players outside coalition \mathcal{S} are not explicitly considered in terms of their choices of strategies. Several models exist that describe the behavior of the players in $\mathcal{K} \setminus \mathcal{S}$ [Mar07]. Originally, von Neumann and Morgenstern in [vNM44] and later elaborated upon in [Aum67], was to consider worst-case behavior. The members of a coalition \mathcal{S} should consider their payoffs which $\mathcal{K} \setminus \mathcal{S}$ cannot prevent them from

⁴A tutorial on the application of coalitional games in communication networks can be found in [SHD⁺09].

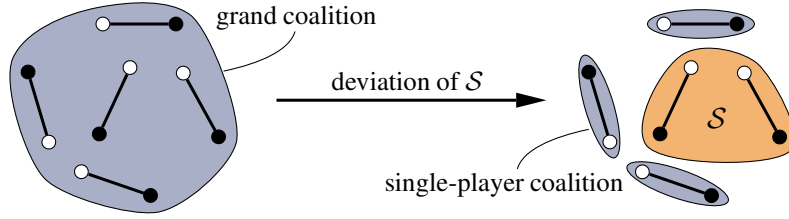


Figure 3.5.: In the γ -core, no coalition \mathcal{S} has the incentive to deviate from the grand coalition.

achieving (β -core) or alternatively the payoffs that they can guarantee for themselves (α -core). For our model, it is unusual to think that the links outside a coalition \mathcal{S} would choose their strategies jointly to minimize the payoff of the members of \mathcal{S} . We adopt the γ -model from [HK83] and assume that all players outside a coalition \mathcal{S} do not cooperate, i.e., build *single-player coalitions*. Coalition deviation in the γ -core is illustrated in Figure 3.5.

For the cooperation strategies in a coalition \mathcal{S} , we consider two simple non-iterative transmission schemes which can be applied in a distributed manner. These are ZF transmission and transmit Wiener filter (WF) [JUN05].

Coalitional Game with Zero Forcing Beamforming

The transmitters choose MRT if they are not cooperative, i.e. are in single-player coalitions. If a transmitter cooperates with a set of links, then it performs ZF in the directions of the corresponding receivers. Hence, we define the mapping

$$V^{\text{ZF}}(\mathcal{S}) = \{(\mathbf{w}_k)_{k \in \mathcal{K}} \in \mathcal{X} : \mathbf{w}_k = \mathbf{w}_{k \rightarrow \mathcal{S}}^{\text{ZF}} \text{ for } k \in \mathcal{S}, \mathbf{w}_\ell = \mathbf{w}_\ell^{\text{MRT}} \text{ for } \ell \in \mathcal{K} \setminus \mathcal{S}\}, \quad (3.18)$$

where $\mathbf{w}_{k \rightarrow \mathcal{S}}^{\text{ZF}}$ is transmitter k 's ZF beamforming vector to the links in \mathcal{S} written as

$$\mathbf{w}_{k \rightarrow \mathcal{S}}^{\text{ZF}} = \frac{\Pi_{\mathbf{Z}_{k \rightarrow \mathcal{S}}}^\perp \mathbf{h}_{kk}}{\|\Pi_{\mathbf{Z}_{k \rightarrow \mathcal{S}}}^\perp \mathbf{h}_{kk}\|}, \quad \mathbf{Z}_{k \rightarrow \mathcal{S}} = (\mathbf{h}_{k\ell})_{\ell \in \mathcal{S} \setminus \{k\}}. \quad (3.19)$$

Observe that if the number of antennas $N_k < |\mathcal{S}|$, then ZF in (3.19) is the zero vector, i.e. transmitter k switches its transmission off. Similar to the definition of the strategy profile $V^{\text{ZF}}(\mathcal{S})$ in (3.18), it is possible to consider different cooperative transmit beamforming than ZF in a coalition. The game in coalitional form with ZF cooperation is

$$\langle \mathcal{K}, \mathcal{X}, V^{\text{ZF}}, (R_k)_{k \in \mathcal{K}} \rangle. \quad (3.20)$$

According to Definition 3, the γ -core is not empty if and only if

$$R_k(V^{\text{ZF}}(\mathcal{S})) \leq R_k(V^{\text{ZF}}(\mathcal{K})), \quad \text{for all } k \in \mathcal{S}, \text{ for all } \mathcal{S} \subset \mathcal{K}. \quad (3.21)$$

The next result provides the condition under which the γ -core of our game is not empty.

Proposition 1. *The γ -core of the coalitional game in (3.20) is not empty if and only if*

$$\sigma^2 \leq \bar{\sigma}^2 := \min_{\mathcal{S} \subset \mathcal{K}} \min_{k \in \mathcal{S}} \left\{ \frac{\sum_{\ell \in \mathcal{K} \setminus \mathcal{S}} |\mathbf{h}_{\ell k}^H \mathbf{w}_{\ell}^{\text{MRT}}|^2 |\mathbf{h}_{kk}^H \mathbf{w}_{k \rightarrow \mathcal{K}}^{\text{ZF}}|^2}{|\mathbf{h}_{kk}^H \mathbf{w}_{k \rightarrow \mathcal{S}}^{\text{ZF}}|^2 - |\mathbf{h}_{kk}^H \mathbf{w}_{k \rightarrow \mathcal{K}}^{\text{ZF}}|^2} \right\}. \quad (3.22)$$

Proof. The proof is provided in Section 3.3.2. \square

Proposition 1 implies that for all SNR values $1/\sigma^2 \geq 1/\bar{\sigma}^2$, it is profitable for all players to jointly perform ZF. If a transmitter's number of antennas is less than the number of receivers in the network, $\bar{\sigma}^2$ will be zero since there exists a transmitter which cannot perform ZF to all receivers. This means that the grand coalition will not form in this case.

Next, we determine the condition under which no player has the incentive to build a coalition with other players. In this case, the following must hold:

$$R_k(V^{\text{ZF}}(\{k\})) > R_k(V^{\text{ZF}}(\mathcal{S})), \quad \text{for all } k \in \mathcal{S}, \text{ for all } \mathcal{S} \subseteq \mathcal{K}, |\mathcal{S}| > 1. \quad (3.23)$$

Notice that $V^{\text{ZF}}(\{k\}) = (\mathbf{w}_1^{\text{MRT}}, \dots, \mathbf{w}_K^{\text{MRT}})$ from (3.18). The condition on σ^2 for (3.23) to hold is given in the next result. The proof uses similar steps as the proof of Proposition 1.

Proposition 2. *No player has an incentive to build a coalition with another player using ZF transmission if*

$$\sigma^2 > \underline{\sigma}^2 := \max_{\mathcal{S} \subseteq \mathcal{K}} \max_{k \in \mathcal{S}} \left\{ \frac{|\mathbf{h}_{kk}^H \mathbf{w}_{k \rightarrow \mathcal{S}}^{\text{ZF}}|^2 \sum_{\ell \in \mathcal{K} \setminus \{k\}} |\mathbf{h}_{\ell k}^H \mathbf{w}_{\ell}^{\text{MRT}}|^2 - \|\mathbf{h}_{kk}\|^2 \sum_{\ell \in \mathcal{K} \setminus \mathcal{S}} |\mathbf{h}_{\ell k}^H \mathbf{w}_{\ell}^{\text{MRT}}|^2}{\|\mathbf{h}_{kk}\|^2 - |\mathbf{h}_{kk}^H \mathbf{w}_{k \rightarrow \mathcal{S}}^{\text{ZF}}|^2} \right\}. \quad (3.24)$$

From Proposition 2, we have that for all SNR values $1/\sigma^2 < 1/\underline{\sigma}^2$, it is not profitable for any user to cooperate with ZF. Figure 3.6 summarizes the results from Proposition 1 and Proposition 2. It can be observed that there is an SNR range in which distinct subsets of the links can group to build coalitions. This mechanism is studied under games in partition form in Section 3.2.2.

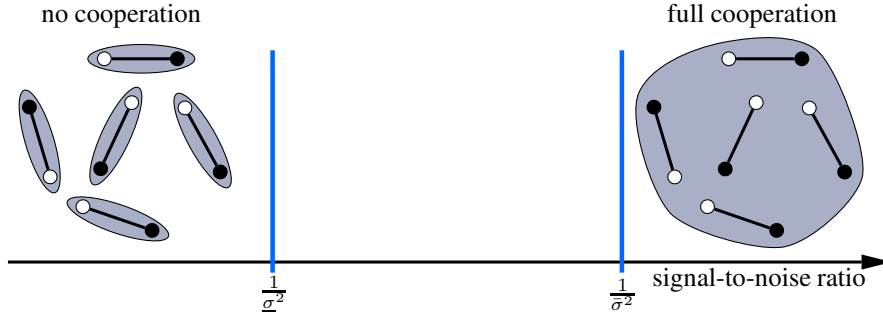


Figure 3.6.: Illustration of the conditions for full cooperation (nonempty core) and conditions for no cooperation (single-player coalitions) for ZF coalitional game.

Coalitional Game with Wiener Filter Precoding

Generally, different cooperative transmission scheme can be applied for cooperation between the links in a coalitional game. In this section, we assume the players cooperate by performing WF precoding to the players in their own coalition. A transmitter k 's WF beamforming vector for coalition \mathcal{S} is written as

$$\mathbf{w}_{k \rightarrow \mathcal{S}}^{\text{WF}} = \frac{(\mathbf{I}\sigma^2 + \sum_{\ell \in \mathcal{S} \setminus \{k\}} \mathbf{h}_{k\ell} \mathbf{h}_{k\ell}^H)^{-1} \mathbf{h}_{kk}}{\|(\mathbf{I}\sigma^2 + \sum_{\ell \in \mathcal{S} \setminus \{k\}} \mathbf{h}_{k\ell} \mathbf{h}_{k\ell}^H)^{-1} \mathbf{h}_{kk}\|}. \quad (3.25)$$

The WF beamforming vector in (3.25) has interesting behavior for asymptotic SNR cases [JUN05]. In the high SNR regime ($\sigma^2 \rightarrow 0$), $\mathbf{w}_{k \rightarrow \mathcal{S}}^{\text{WF}}$ converges to $\mathbf{w}_{k \rightarrow \mathcal{S}}^{\text{ZF}}$ in (3.19). In the low SNR regime ($\sigma^2 \rightarrow \infty$), $\mathbf{w}_{k \rightarrow \mathcal{S}}^{\text{WF}}$ converges to $\mathbf{w}_k^{\text{MRT}}$ in (3.5).

The game in coalitional form with WF precoding is

$$\langle \mathcal{K}, \mathcal{X}, V^{\text{WF}}, (R_k)_{k \in \mathcal{K}} \rangle. \quad (3.26)$$

where the mapping V^{WF} which defines the strategy profile according to WF cooperation scheme is

$$V^{\text{WF}}(\mathcal{S}) = \{(\mathbf{w}_k)_{k \in \mathcal{K}} \in \mathcal{X} : \mathbf{w}_k = \mathbf{w}_{k \rightarrow \mathcal{S}}^{\text{WF}} \text{ for } k \in \mathcal{S}, \mathbf{w}_\ell = \mathbf{w}_\ell^{\text{MRT}} \text{ for } \ell \in \mathcal{K} \setminus \mathcal{S}\}. \quad (3.27)$$

Conditions for nonempty γ -core of the coalitional game in (3.26) in terms of an SNR threshold is hard to characterize because the noise power in (3.25) is inside the matrix inverse. However, according to numerical simulations, we find that the SNR threshold above which the γ -core of the coalitional game with WF precoding is nonempty is always less than that with ZF cooperation. In other words, the SNR range in which the players have the incentive to jointly cooperate with WF precoding is according to numerical evidence larger than the SNR range in which the players will jointly cooperate with ZF.

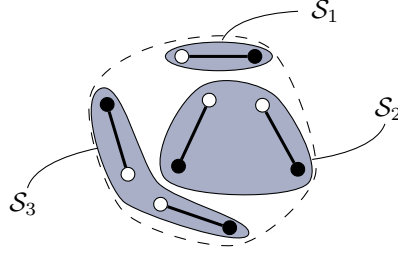


Figure 3.7.: Illustration of a coalition structure $\mathcal{C} = \{\mathcal{S}_1, \mathcal{S}_2, \mathcal{S}_3\}$.

3.2.2. Coalition Formation

In the previous section, we have described the γ -core which reveals the feasibility for the formation of the grand coalition. In this section, we consider coalition formation games [AD74, Mar07]. These games describe situations in which the players can group to form a coalition structure. A *coalition structure* \mathcal{C} is a partition of the grand coalition \mathcal{K} into a set of disjoint coalitions $\{\mathcal{S}_1, \dots, \mathcal{S}_L\}$ where $\bigcup_{j=1}^L \mathcal{S}_j = \mathcal{K}$ and $\bigcap_{j=1}^L \mathcal{S}_j = \emptyset$. In Figure 3.7, an example coalition structure is illustrated.

We consider two scenarios for player cooperation in a coalition. These scenarios correspond to ZF and WF transmissions. Given a coalition structure $\mathcal{C} = \{\mathcal{S}_1, \dots, \mathcal{S}_L\}$, the strategy profile of the players according to ZF or WF is defined by

$$F^{\text{bf}}(\mathcal{C} = \{\mathcal{S}_1, \dots, \mathcal{S}_L\}) := \{(\mathbf{w}_k)_{k \in \mathcal{K}} \in \mathcal{X} : \mathbf{w}_k = \mathbf{w}_{k \rightarrow \mathcal{S}_j}^{\text{bf}} \text{ for } k \in \mathcal{S}_j, j = 1, \dots, L\}, \quad (3.28)$$

where $\text{bf} \in \{\text{ZF}, \text{WF}\}$ with $\mathbf{w}_{k \rightarrow \mathcal{S}_j}^{\text{ZF}}$ and $\mathbf{w}_{k \rightarrow \mathcal{S}_j}^{\text{WF}}$ defined in (3.19) and (3.25), respectively. Notice that if $|\mathcal{S}_j| = 1$ and $k \in \mathcal{S}_j$, then $\mathbf{w}_{k \rightarrow \mathcal{S}_j}^{\text{ZF}} = \mathbf{w}_{k \rightarrow \mathcal{S}_j}^{\text{WF}} = \mathbf{w}_k^{\text{MRT}}$. For a coalition structure \mathcal{C} , $F^{\text{ZF}}(\mathcal{C})$ is a strategy profile in which each player chooses ZF to the players in his coalition. Similarly, $F^{\text{WF}}(\mathcal{C})$ is the strategy profile when WF is applied.

A *comparison relation* \triangleright compares two coalition structures \mathcal{C}_1 and \mathcal{C}_2 . The notation $\mathcal{C}_1 \triangleright \mathcal{C}_2$ means that coalition structure \mathcal{C}_1 is preferred to \mathcal{C}_2 . In [AW09], several comparison relations are discussed. We use the *Pareto order relation* defined as

$$\mathcal{C}_1 \triangleright \mathcal{C}_2 \Leftrightarrow \left\{ R_k(F^{\text{bf}}(\mathcal{C}_1)) \geq R_k(F^{\text{bf}}(\mathcal{C}_2)), \text{ for all } k \in \mathcal{K} \right\}, \quad (3.29)$$

where the inequality in (3.29) is strict for at least one player k .

In coalition formation games, the stability of a coalition structure is important. A coalition structure is stable if no set of players has the incentive to deviate and form a different coalition structure. Coalition deviation is described by a *defection function* which maps a coalition structure with all preferable alternatives. In [AW09], a defection function \mathbb{D}_{hp} is proposed which is based on simple rules of coalitions merging and splitting. A coalition structure \mathcal{C} is \mathbb{D}_{hp} -stable if the players are not interested in changing \mathcal{C}

through merge and split operations. The merge and split rules thus define a procedure for coalition formation. This procedure has been applied in [SHDH09] for a wireless multiple access network.

3.2.3. Merge-and-Split Algorithm

We shortly describe the merge-and-split algorithm [AW09, SHDH09]. The algorithm is divided into two operations which are executed iteratively. Given $\mathcal{C}_1 = \{\mathcal{S}_1, \dots, \mathcal{S}_L\}$, the *merge rule* merges a set of coalitions $\mathcal{T} \subseteq \mathcal{C}_1$ to a single coalition if the formed coalition structure \mathcal{C}_2 satisfies the Pareto order relation $\mathcal{C}_2 \triangleright \mathcal{C}_1$. This operation is repeated until no merges are possible.

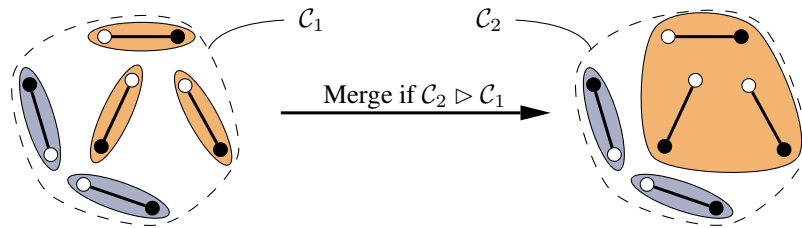


Figure 3.8.: An illustration of the merge operation.

In the *split rule*, a coalition $\mathcal{S}_k \in \mathcal{C}_1$ splits into smaller coalitions if the obtained coalition structure \mathcal{C}_2 satisfies $\mathcal{C}_2 \triangleright \mathcal{C}_1$. The split rule terminates when no further splits in any coalition are possible.

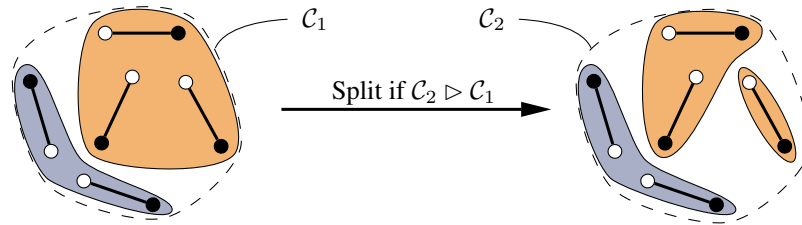


Figure 3.9.: An illustration of the split operation.

The convergence of the algorithm is guaranteed due to the adopted Pareto order relation in (3.29). Distributed implementation as well as a discussion on the complexity of the merge-and-split algorithm can be found in [SHDH09].

We apply the merge-and-split algorithm for coalition formation in our setting. In order to include the effect of distances between the links on the received power gains, we use the path loss model in which the signal between a transmitter and a receiver reduces in power in the rate of a path loss exponent. The path loss exponent depends on

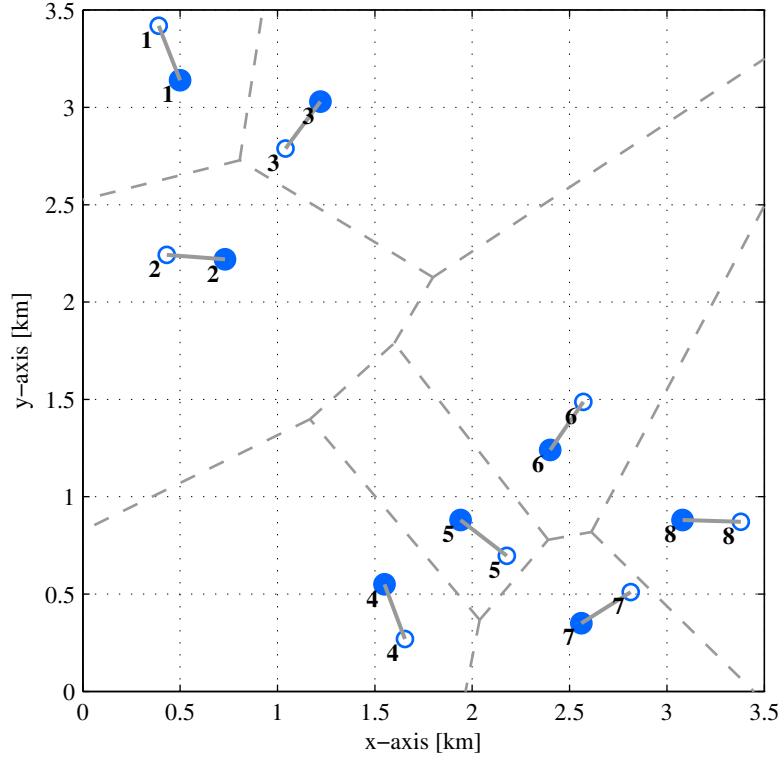


Figure 3.10.: Distribution of the links in the plane.

the propagation model and takes values between two and four. Let $d_{k\ell}$ be the distance between transmitter k and a receiver ℓ in meters and α be the path loss exponent, we write the channel vector $\mathbf{h}_{k\ell} = d_{k\ell}^{-\alpha/2} \bar{\mathbf{h}}_{k\ell}$ with $\|\bar{\mathbf{h}}_{k\ell}\| = 1$. In Figure 3.10, we generate a sample distribution of 8 links in the plane. The transmitters are randomly placed in a 3 km by 3 km square area. Each receiver k is placed randomly at a distance $d_{kk} = 300$ meters away from its transmitter k . We define the SNR as $\text{SNR} = d_{kk}^{-\alpha} / \sigma^2$. Each transmitter uses 12 antennas and the path loss exponent is set to $\alpha = 3$. Using the merge-and-split algorithm, we calculate the user rates at 15 dB SNR in Figure 3.11. At $\text{SNR} = 15$ dB, the grand coalition forms with WF precoding and the coalition structure with ZF beamforming is $\{\{4, 5, 6, 7, 8\}, \{1\}, \{2\}, \{3\}\}$, where the coalition $\{4, 5, 6, 7, 8\}$ is the cluster of links in the bottom right side of Figure 3.10. With both ZF and WF cooperation schemes, joint improvement in the rates of the links is achieved from the Nash equilibrium by link coalition formation.

Using the merge-and-split algorithm, the average rate of the 8 links is plotted for increasing SNR in Figure 3.12. In the low SNR regime, single-player coalitions exist with the ZF cooperation scheme supporting the result in Proposition 2. Moreover, at low SNR it is observed that some players cooperate with WF transmission. This is

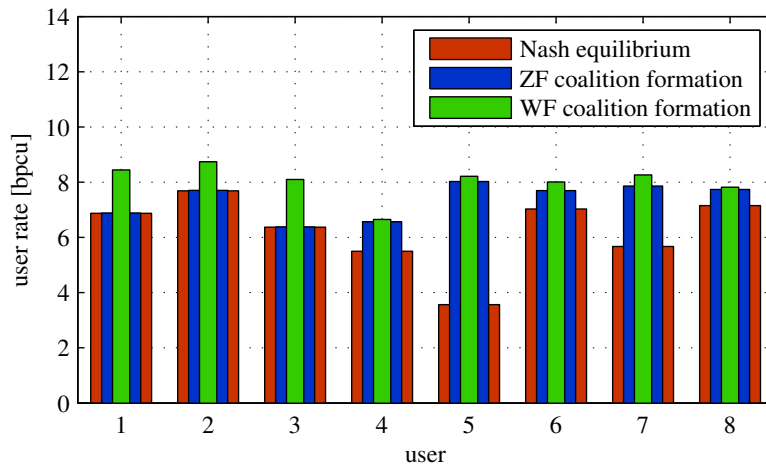


Figure 3.11.: Link rates at 15 dB SNR.

because WF precoding converges to MRT transmission at low SNR. Note that in the low SNR regime, the outcome with joint MRT is efficient as is revealed in Section 3.1.1. In the mid SNR regime, coalition formation improves the joint performance of the links from the Nash equilibrium. It is observed that with WF precoding, larger coalitions form at lower SNR values than with ZF beamforming which explains the higher performance gains with WF than with ZF. The optimal ZF and WF coalition structures that achieve the maximum average user rate are found by exhaustive search. The average user rate in Nash equilibrium saturates in the high SNR regime. This is contrary to ZF and WF coalition formation where the average user rate increases linearly due to the formation of the grand coalition. The formation of the grand coalition at high SNR supports the result in Proposition 1. It is evident from Figure 3.11 and Figure 3.12 that enabling link coalition formation, even with simple cooperative transmission schemes, leads to joint performance improvement in the network.

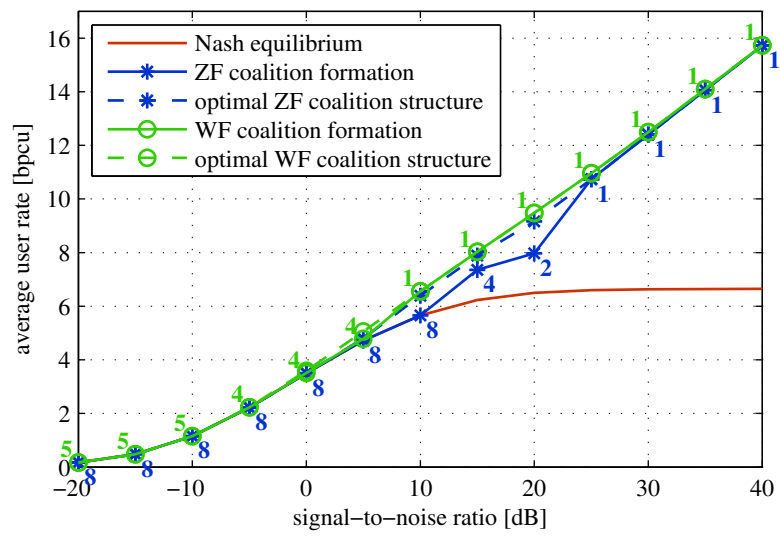


Figure 3.12.: Average rate of the 8 links. The number under (above) the curve is the number of coalitions with ZF (WF).

3.3. Proofs

3.3.1. Proof of Corollary 1

We prove that the gains achieved by the beamforming vectors in (3.16) are equal to the gains achieved by the beamforming vectors given in (2.12). Define the matrix \mathbf{M}_k as

$$\mathbf{M}_k = \underbrace{\xi_{kk} \mathbf{h}_{kk} \mathbf{h}_{kk}^H}_{\mathbf{A}_k} + \underbrace{\sum_{\ell \neq k} -\xi_{k\ell} \mathbf{h}_{k\ell} \mathbf{h}_{k\ell}^H}_{\mathbf{B}_k}. \quad (3.30)$$

The matrices \mathbf{M}_k , \mathbf{A}_k and \mathbf{B}_k are Hermitian matrices of size $N_k \times N_k$. The eigenvalues of \mathbf{M}_k are real and we always consider them ordered in nondecreasing order, i.e., $\mu_1(\mathbf{M}_k) \leq \mu_2(\mathbf{M}_k) \leq \dots \leq \mu_{N_k}(\mathbf{M}_k)$. \mathbf{A}_k is a positive semidefinite matrix, $\mathbf{A}_k \succeq 0$, and $\text{rank}(\mathbf{A}_k) = 1$, i.e.,

$$0 = \mu_1(\mathbf{A}_k) = \dots = \mu_{N_k-1}(\mathbf{A}_k) \leq \mu_{N_k}(\mathbf{A}_k). \quad (3.31)$$

\mathbf{B}_k consists of the sum of the negative of positive semidefinite matrices. Hence, $\mathbf{B}_k \preceq 0$ and $\text{rank}(\mathbf{B}_k) \leq K - 1$, which leads to the following properties on the eigenvalues:

$$\mu_1(\mathbf{B}_k) \leq \dots \leq \mu_{K-1}(\mathbf{B}_k) \leq 0, \quad (3.32)$$

and

$$\mu_K(\mathbf{B}_k) = \dots = \mu_{N_k}(\mathbf{B}_k) = 0. \quad (3.33)$$

Next, we study the eigenvalues of $\mathbf{M}_k = \mathbf{A}_k + \mathbf{B}_k$. According to Weyl's inequality of the eigenvalues of the sum of Hermitian matrices [HJ85, Theorem 4.3.7] we have

$$\mu_{N_k-1}(\mathbf{M}_k) \leq \mu_{N_k-1}(\mathbf{A}_k) + \mu_{N_k}(\mathbf{B}_k) = 0, \quad (3.34)$$

$$\mu_K(\mathbf{M}_k) \geq \mu_1(\mathbf{A}_k) + \mu_K(\mathbf{B}_k) = 0. \quad (3.35)$$

The eigenvalues of \mathbf{M}_k are ordered in nondecreasing order. Therefore, the following eigenvalues of \mathbf{M}_k are always equal to zero: $\mu_K(\mathbf{M}_k) = \dots = \mu_{N_k-1}(\mathbf{M}_k) = 0$. In addition, the smallest $K - 1$ eigenvalues of \mathbf{M}_k are nonpositive.

If the dimension of space is larger than the number of receivers, i.e., $N_k \geq K - 1$, then there would be at least $N_k - (K - 1) - 1$ eigenvalues of \mathbf{M}_k that are zero. For the eigenvectors corresponding to those eigenvalues, the eigenvalue equation is written as

$$\left(\xi_{kk} \mathbf{h}_{kk} \mathbf{h}_{kk}^H + \sum_{\ell \neq k} -\xi_{k\ell} \mathbf{h}_{k\ell} \mathbf{h}_{k\ell}^H \right) \mathbf{v}_i = \mathbf{0}, \quad (3.36)$$

holds for all $i = K, \dots, N_k - 1$. Then, for all $\ell \in \mathcal{K}$,

$$\left(\xi_{k\ell} \mathbf{h}_{k\ell} \mathbf{h}_{k\ell}^H\right) \mathbf{v}_i = \mathbf{0}, \quad \text{for all } i = K, \dots, N_k - 1. \quad (3.37)$$

The set of eigenvectors $\{\mathbf{v}_1, \dots, \mathbf{v}_{N_k}\}$ of \mathbf{M}_k in (3.30), form an orthonormal set, i.e. $\|\mathbf{v}_i\| = 1$ for all $i = 1, \dots, N_k$ and $\mathbf{v}_i^H \mathbf{v}_j = 0$ for $i \neq j$. Therefore, we can write $\sum_{\ell=1}^{N_k} \mathbf{v}_\ell \mathbf{v}_\ell^H = \mathbf{I}$, which gives

$$\begin{aligned} \mathbf{v}_{N_k} \mathbf{v}_{N_k}^H &= \mathbf{I} - \sum_{\ell=1}^{N_k-1} \mathbf{v}_\ell \mathbf{v}_\ell^H \\ &= \mathbf{I} - \mathbf{G}_k \mathbf{G}_k^H = \mathbf{\Pi}_{\mathbf{G}_k}^\perp, \end{aligned} \quad (3.38)$$

where $\mathbf{G}_k = [\mathbf{v}_1, \dots, \mathbf{v}_{N_k-1}]$. Let the matrix \mathbf{Z}_k consist of the eigenvectors of \mathbf{G}_k excluding the eigenvectors that satisfy (3.37), i.e.,

$$\mathbf{Z}_k = [\mathbf{v}_1, \dots, \mathbf{v}_{K-1}], \quad (3.39)$$

then for any $\mathbf{g} \in \mathbb{C}^{N_k}$ in the space of the channels $[\mathbf{h}_{k1}, \dots, \mathbf{h}_{kK}]$ we can write

$$\left| \mathbf{g}^H \frac{\mathbf{\Pi}_{\mathbf{Z}_k}^\perp \mathbf{h}_{k\ell}}{\|\mathbf{\Pi}_{\mathbf{Z}_k}^\perp \mathbf{h}_{k\ell}\|} \right|^2 = \left| \mathbf{g}^H \frac{\mathbf{\Pi}_{\mathbf{G}_k}^\perp \mathbf{h}_{k\ell}}{\|\mathbf{\Pi}_{\mathbf{G}_k}^\perp \mathbf{h}_{k\ell}\|} \right|^2 \quad (3.40)$$

$$= \left| \mathbf{g}^H \frac{\mathbf{v}_{N_k} \mathbf{v}_{N_k}^H \mathbf{h}_{k\ell}}{\|\mathbf{v}_{N_k} \mathbf{v}_{N_k}^H \mathbf{h}_{k\ell}\|} \right|^2 \quad (3.41)$$

$$= |\mathbf{g}^H \mathbf{v}_{N_k}|^2, \quad (3.42)$$

where $\ell \in \mathcal{K}$. Hence, the same power gains are achieved with the beamforming vectors $\frac{\mathbf{\Pi}_{\mathbf{Z}_k}^\perp \mathbf{h}_{k\ell}}{\|\mathbf{\Pi}_{\mathbf{Z}_k}^\perp \mathbf{h}_{k\ell}\|}$ and \mathbf{v}_{N_k} used in (2.12) for the downlink channels $[\mathbf{h}_{k1}, \dots, \mathbf{h}_{kK}]$.

3.3.2. Proof of Proposition 1

Considering an arbitrary player i in an arbitrary coalition \mathcal{S} , we write the condition in (3.21) as

$$\frac{|\mathbf{h}_{kk}^H \mathbf{w}_{k \rightarrow \mathcal{S}}^{\text{ZF}}|^2}{\sigma^2 + \sum_{\ell \in \mathcal{K} \setminus \mathcal{S}} |\mathbf{h}_{\ell k}^H \mathbf{w}_\ell^{\text{MRT}}|^2} \leq \frac{|\mathbf{h}_{kk}^H \mathbf{w}_{k \rightarrow \mathcal{K}}^{\text{ZF}}|^2}{\sigma^2}, \quad (3.43)$$

where we used the signal-to-interference plus noise ratio (SINR) expression in (2.5) knowing that the logarithm function is monotonically increasing in the SINR. Cross multiplying the terms in (3.43) and solving for σ^2 we get

$$\sigma^2 \leq \frac{\sum_{\ell \in \mathcal{K} \setminus \mathcal{S}} |\mathbf{h}_{\ell k}^H \mathbf{w}_\ell^{\text{MRT}}|^2 |\mathbf{h}_{kk}^H \mathbf{w}_{k \rightarrow \mathcal{K}}^{\text{ZF}}|^2}{|\mathbf{h}_{kk}^H \mathbf{w}_{k \rightarrow \mathcal{S}}^{\text{ZF}}|^2 - |\mathbf{h}_{kk}^H \mathbf{w}_{k \rightarrow \mathcal{K}}^{\text{ZF}}|^2}, \quad (3.44)$$

which is the condition that a player k in a coalition \mathcal{S} prefers the grand coalition \mathcal{K} to \mathcal{S} . Note that $|\mathbf{h}_{kk}^H \mathbf{w}_{k \rightarrow \mathcal{S}}^{\text{ZF}}|^2 - |\mathbf{h}_{kk}^H \mathbf{w}_{k \rightarrow \mathcal{K}}^{\text{ZF}}|^2$ in (3.44) is always positive because ZF

beamforming nulls more spatial dimensions in \mathcal{K} than in $\mathcal{S} \subset \mathcal{K}$. Since the condition in (3.21) has to hold for all $k \in \mathcal{S}$ and all proper subsets \mathcal{S} of \mathcal{K} , we get the expression in (3.22).

Chapter 4.

Microeconomic Theory Applications

In this chapter, models from microeconomic theory are used to characterize equilibria which are Pareto optimal in the two-user MISO IFC. In the first section of this chapter, an exchange economy model between the links is studied. The parametrization of the efficient beamforming vectors are regarded as goods which the links, referred to as consumers, can exchange between themselves. The exchange equilibria are the possible distribution of the goods at which the consumers are jointly satisfied. These equilibria are Pareto optimal and dominate the Nash equilibrium of a strategic game between the links (studied in Section 3.1.1). In order to reach an exchange equilibrium, we construct a bargaining process between the two links which sequentially updates the amounts of goods traded between the consumers. In the second section of this chapter, we use a competitive market model which additionally associates prices to the goods. We characterize the Walrasian equilibrium in this competitive market which is Pareto optimal and lies in the set of exchange equilibria. In order to implement the Walrasian equilibrium, a coordination mechanism is proposed which relies on communication between the consumers and the arbitrator.

4.1. Exchange Economy

In this section, a model of voluntary exchange of goods between two consumers is described. Each consumer is assumed to be initially endowed with amounts of divisible goods. The consumers exchange the goods between themselves because this leads to joint improvement in their utilities. We make the necessary transformation from the two-user MISO IFC to a setting in which the links are the consumers, and the parameterized set of efficient beamforming vectors are regarded as goods.

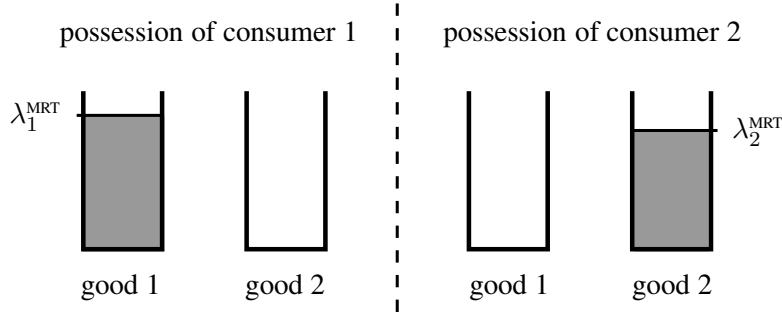


Figure 4.1.: Illustration of the initial distribution of the two goods.

4.1.1. Model of Exchange

In the model of exchange proposed by Edgeworth in 1881 [Edg81], there exists a set of consumers which voluntarily exchange goods they possess to jointly increase their payoff. The set of consumers corresponds to the two MISO links in our setting. The goods correspond to the parameters of the beamforming vectors in (2.9), restated here¹

$$\mathbf{w}_k(\lambda_k) = \sqrt{\lambda_k} \frac{\mathbf{\Pi}_{\mathbf{h}_{k\ell}} \mathbf{h}_{kk}}{\|\mathbf{\Pi}_{\mathbf{h}_{k\ell}} \mathbf{h}_{kk}\|} + \sqrt{1 - \lambda_k} \frac{\mathbf{\Pi}_{\mathbf{h}_{k\ell}}^\perp \mathbf{h}_{kk}}{\|\mathbf{\Pi}_{\mathbf{h}_{k\ell}}^\perp \mathbf{h}_{kk}\|}, \quad k \neq \ell, \quad (4.1)$$

where $\lambda_k \in [0, \lambda_k^{\text{MRT}}]$ with $\lambda_k^{\text{MRT}} = \|\mathbf{\Pi}_{\mathbf{h}_{k\ell}} \mathbf{h}_{kk}\|^2 / \|\mathbf{h}_{kk}\|^2$. These beamforming vectors are necessary to achieve all Pareto optimal points in the two-user rate region \mathcal{R} in (2.6).

According to the parametrization of the efficient beamforming vectors in (4.1), there are two goods and λ_1 will stand for good 1 and λ_2 for good 2. The consumers are initially endowed with amounts of these goods. We will assume that the links start the trade in Nash equilibrium. Thus, consumer k is initially endowed with λ_k^{MRT} from his good and nothing from the good of the other consumer. Specifically, we define $(\lambda_1^{\text{MRT}}, 0)$ and $(0, \lambda_2^{\text{MRT}})$ as the *endowments* of consumers 1 and 2, respectively. In Figure 4.1, the initial endowments of the consumers are illustrated.

Since during exchange each consumer will possess different amounts from both available goods, we introduce new variables that indicate these. When consumer k trades an amount of his good k to consumer $\ell \neq k$, this amount will be represented by $x_k^{(\ell)} \leq \lambda_k^{\text{MRT}}$. The amount left for consumer k from his good is $x_k^{(k)} = \lambda_k^{\text{MRT}} - x_k^{(\ell)}$. In connection to the parametrization in (4.1), we define the amounts of possessed goods as

$$x_k^{(k)} = \lambda_k, \quad x_\ell^{(k)} = \lambda_\ell^{\text{MRT}} - \lambda_\ell, \quad \ell \neq k. \quad (4.2)$$

If consumer k gives $x_k^{(\ell)}$ to the other consumer, this means that transmitter k uses the beamforming vector in (4.1) which corresponds to $\lambda_k^{\text{MRT}} - x_k^{(\ell)}$. Hence, if $x_k^{(\ell)}$ increases,

¹Throughout this chapter, the indices k, ℓ are restricted to be in the set $\{1, 2\}$.

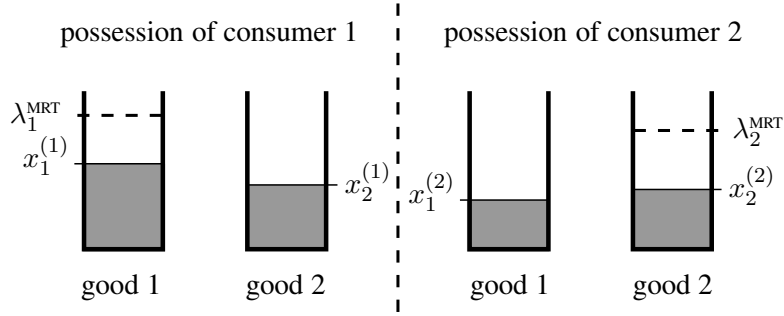


Figure 4.2.: Illustration of the distribution of the two goods during exchange.

transmitter k reduces the interference at receiver ℓ by using a beamforming vector nearer to ZF. In Figure 4.2, the distribution of the goods during exchange is depicted.

Consumer Preference

The utility function of a consumer represents his preference over the goods. We use the SINR expression in (2.4) as the utility function of a consumer k . Because consumer preference is invariant to positive monotonic transforms [JR03, Theorem 1.2], the results in this chapter hold for any SINR based utility function such as the achievable rate function in (2.5). We define the two-user SINR region as

$$\Phi := \left\{ (\gamma_1(\mathbf{w}_1, \mathbf{w}_2), \gamma_2(\mathbf{w}_1, \mathbf{w}_2)) \in \mathbb{R}_+^2 : \|\mathbf{w}_1\|^2 \leq 1, \|\mathbf{w}_2\|^2 \leq 1 \right\}, \quad (4.3)$$

where the SINR γ_k of link k is defined in (2.4). Note that any SINR tuple which is Pareto optimal corresponds to a Pareto optimal point in the rate region in (2.6). Since the set of beamforming vectors in (4.1) are necessary to achieve all Pareto optimal points, we express the SINR of a link k in terms of the parameters λ_k in (4.1). First, we formulate the power gains at the receivers depending on the parameters.

Lemma 1. *The power gains at the receivers in terms of the parametrization in (4.1) are*

$$|\mathbf{h}_{kk}^H \mathbf{w}_k(\lambda_k)|^2 = \left(\sqrt{\lambda_k g_k} + \sqrt{(1 - \lambda_k) \check{g}_k} \right)^2, \quad (4.4)$$

$$|\mathbf{h}_{k\ell}^H \mathbf{w}_k(\lambda_k)|^2 = \lambda_k g_{k\ell}, \quad k \neq \ell, \quad (4.5)$$

where $\lambda_k \in [0, \lambda_k^{MRT}]$ and $g_k := \|\mathbf{\Pi}_{\mathbf{h}_{k\ell}} \mathbf{h}_{kk}\|^2$, $\check{g}_k := \|\mathbf{\Pi}_{\mathbf{h}_{k\ell}}^\perp \mathbf{h}_{kk}\|^2$, $g_{k\ell} := \|\mathbf{h}_{k\ell}\|^2$, $k \neq \ell$.

Proof. The proof is provided in Section 4.3.1. □

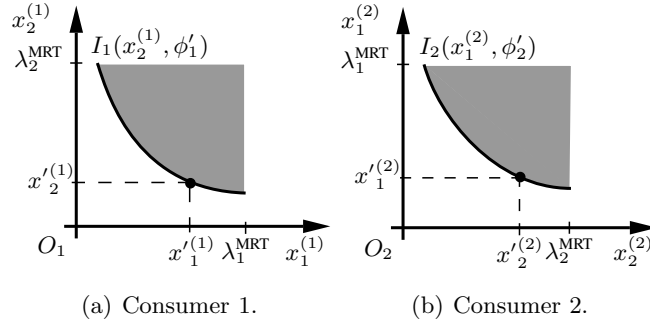


Figure 4.3.: Preference representation of the consumers. I_1 and I_2 are indifference curves of consumer 1 and 2, respectively.

Notice in (4.5) that the interference gain $\lambda_k g_{k\ell}$ scales linearly with λ_k . With this respect, increasing λ_k increases the interference at the unintended receiver. We rewrite the SINR of a link k in terms of the goods as²

$$\phi_k(x_1^{(k)}, x_2^{(k)}) = \frac{\left(\sqrt{x_k^{(k)}} g_k + \sqrt{(1 - x_k^{(k)}) \check{g}_k}\right)^2}{\sigma^2 + \lambda_\ell^{\text{MRT}} g_{\ell k} - x_\ell^{(k)} g_{\ell k}}, \quad (4.6)$$

where we substituted $\lambda_k = x_k^{(k)}$ and $\lambda_\ell = \lambda_\ell^{\text{MRT}} - x_\ell^{(k)}$, $\ell \neq k$, from (4.2). Next, we prove an important property of the SINR function in (4.6) in relation to the goods.

Theorem 1. $\phi_k(x_1^{(k)}, x_2^{(k)})$ in (4.6) is continuous, strongly increasing, and strictly quasiconcave on $[0, \lambda_1^{\text{MRT}}] \times [0, \lambda_2^{\text{MRT}}]$.

Proof. The proof is provided in Section 4.3.2. \square

According to Theorem 1, the SINR $\phi_k(x_1^{(k)}, x_2^{(k)})$ is strongly increasing [JR03, Definition A1.17] means that for³ $(x_1'^{(k)}, x_2'^{(k)}) \geq (x_1^{(k)}, x_2^{(k)})$ and $(x_1'^{(k)}, x_2'^{(k)}) \neq (x_1^{(k)}, x_2^{(k)})$, it holds that $\phi_k(x_1'^{(k)}, x_2'^{(k)}) > \phi_k(x_1^{(k)}, x_2^{(k)})$. Moreover, the SINR $\phi_k(x_1^{(k)}, x_2^{(k)})$ is strictly quasiconcave [JR03, Definition A1.25] means that for all $(x_1'^{(k)}, x_2'^{(k)}) \neq (x_1^{(k)}, x_2^{(k)})$ and for all $t \in (0, 1)$, the following holds

$$\phi_k\left(t(x_1'^{(k)}, x_2'^{(k)}) + (1-t)(x_1^{(k)}, x_2^{(k)})\right) > \min\left\{\phi_k(x_1'^{(k)}, x_2'^{(k)}), \phi_k(x_1^{(k)}, x_2^{(k)})\right\}. \quad (4.7)$$

The properties in Theorem 1 imply that the SINR function has a unique maximum over the set $[0, \lambda_1^{\text{MRT}}] \times [0, \lambda_2^{\text{MRT}}]$.

²We give a new notation for the SINR as ϕ_k because it depends on the goods while the SINR function γ_k is a function of the beamforming vectors.

³The inequalities in the following are componentwise.

The preference of consumers 1 and 2 over the goods is illustrated in Figure 4.3(a) and Figure 4.3(b), respectively. For consumer 1 (analogously consumer 2), O_1 is the origin of the coordinate system which has $x_1^{(1)}$, the amount of good 1, on the x-axis and $x_2^{(1)}$, the amount of good 2, on the y-axis. I_k is the *indifference curve* of consumer k which represents the pairs $(x_1^{(k)}, x_2^{(k)})$ such that the consumer achieves the same utility as with $(x_1^{\prime(k)}, x_2^{\prime(k)})$, i.e., $\phi_k(x_1^{(k)}, x_2^{(k)}) = \phi_k^{\prime} := \phi_k(x_1^{\prime(k)}, x_2^{\prime(k)})$. The indifference curves correspond to the boundaries of the level sets [BV04] of $\phi_k(x_1^{(k)}, x_2^{(k)})$. According to the properties of the utility function in Theorem 1, the indifference curves are convex. The dark region above I_k , corresponds to the pairs $(x_1^{(k)}, x_2^{(k)})$ where the consumer achieves higher payoff than at the indifference curve. The region below I_k corresponds to less payoff for consumer k .

We provide a formulation for the consumer indifference curves. This formulation is essential for the bargaining process between the consumers later described in Section 4.1.3.

Proposition 3. *The indifference curves $I_k(x_k^{(k)})$ as a function of $x_\ell^{(k)}$, for given fixed SINRs ϕ_k^{\prime} are*

$$I_1(x_2^{(1)}, \phi_1^{\prime}) = f\left(\lambda_1^{\text{MRT}}, \frac{\phi_1^{\prime}}{\phi_1(\lambda_1^{\text{MRT}}, x_2^{(1)})}\right), \quad (4.8)$$

$$I_2(x_1^{(2)}, \phi_2^{\prime}) = f\left(\lambda_2^{\text{MRT}}, \frac{\phi_2^{\prime}}{\phi_2(x_1^{(2)}, \lambda_2^{\text{MRT}})}\right), \quad (4.9)$$

where $f(a, b) := (\sqrt{ab} - \sqrt{(1-a)(1-b)})^2$.

Proof. The proof is provided in Section 4.3.3. □

Note that Proposition 3 characterizes a family of indifference curves. Each indifference curve has a domain and range which depends on the fixed SINR value ϕ_k^{\prime} . For given fixed SINRs, the indifference curves should be restricted to take values in the feasible parameter set from (4.1), i.e., $I_1(x_2^{(1)}, \phi_1^{\prime}) \in [0, \lambda_1^{\text{MRT}}]$ and $I_2(x_1^{(2)}, \phi_2^{\prime}) \in [0, \lambda_2^{\text{MRT}}]$.

The Edgeworth Box

The Edgeworth box [Edg81], [JR03, Chapter 5], illustrated in Figure 4.4, is a graphical representation that is useful for the analysis of an exchange economy. The box is constructed by joining Figure 4.3(a) and Figure 4.3(b). Thus, the Edgeworth box has two points of origin, O_1 and O_2 , corresponding to consumer 1 and 2, respectively. The initial endowments of the consumers define the size of the box. The width of the box is

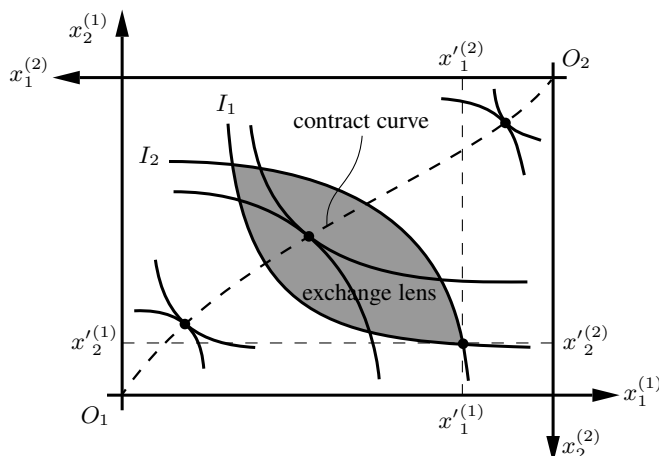


Figure 4.4.: An illustration of an Edgeworth box.

λ_1^{MRT} , and the height is λ_2^{MRT} . Let $(x_1^{(1)}, x_2^{(1)})$ and $(x_1^{(2)}, x_2^{(2)})$ be the possessions of consumer 1 and consumer 2 during exchange. The point $((x_1^{(1)}, x_2^{(1)}), (x_1^{(2)}, x_2^{(2)}))$ is the corresponding *allocation* in the Edgeworth box. Every allocation in the box is an assignment of a possession vector to each consumer. The consumers' preferences in the Edgeworth box can be revealed according to their indifference curves. The dark region in Figure 4.4 is called the *exchange lens* and contains all allocations that are Pareto improvements to the outcome in $((x_1^{(1)}, x_2^{(1)}), (x_1^{(2)}, x_2^{(2)}))$.

The locus of all Pareto optimal points in the Edgeworth box is called the *contract curve* [Edg81]. On these points, the indifference curves are tangent, and are characterized by the following condition⁴ [Edg81, MNS53]:

$$\frac{\partial \phi_1(x_1^{(1)}, x_2^{(1)})}{\partial x_1^{(1)}} \frac{\partial \phi_2(x_1^{(2)}, x_2^{(2)})}{\partial x_2^{(2)}} = \frac{\partial \phi_2(x_1^{(2)}, x_2^{(2)})}{\partial x_1^{(2)}} \frac{\partial \phi_1(x_1^{(1)}, x_2^{(1)})}{\partial x_2^{(1)}}. \quad (4.10)$$

The convexity of the consumers' indifference curves according to Theorem 1 implies that these can only be tangent at a single point. Thus, the condition in (4.10) is necessary and sufficient for an allocation to be on the contract curve.

Theorem 2. *The contract curve $cc : [0, \lambda_2^{\text{MRT}}] \rightarrow [0, \lambda_1^{\text{MRT}}]$ ($x_1^{(1)}$ as a function of $x_2^{(2)}$) is a solution of the following cubic equation⁵*

$$a[x_1^{(1)}]^3 + b[x_1^{(1)}]^2 + c[x_1^{(1)}] + d = 0, \quad (4.11)$$

⁴In multiple consumer settings, the condition provided by Edgeworth in (4.10) should hold for every consumer pair.

⁵This result is independently obtained in [LKL11a].

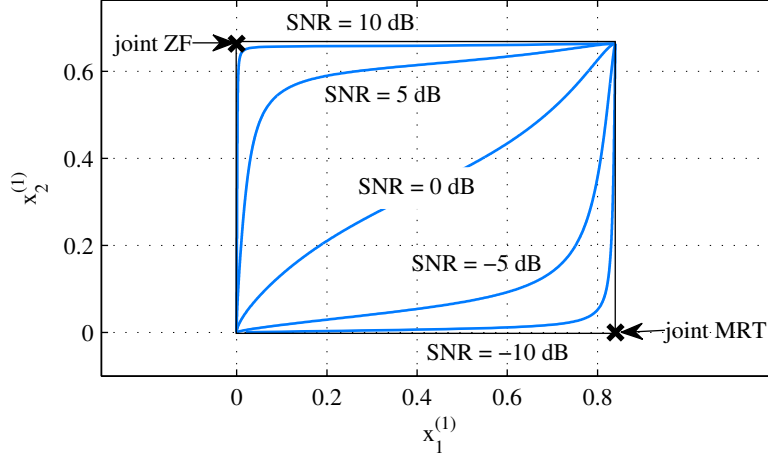


Figure 4.5.: Course of the contract curve in the Edgeworth box for different SNR values.

where

$$a = -(g_1 + \check{g}_1)(C - g_{12})^2, \quad d = g_1\sigma^4, \quad (4.12)$$

$$b = (C - g_{12})\left(2\check{g}_1(C + \sigma^2) + g_1(2\sigma^2 + C - g_{12})\right), \quad (4.13)$$

$$c = -\check{g}_1(C + \sigma^2)^2 + \sigma^2 g_1(2g_{12} - 2C - \sigma^2), \quad (4.14)$$

and C is a function of $x_2^{(2)}$ given as

$$C = \frac{\left(\sqrt{x_2^{(2)} g_2} + \sqrt{(1 - x_2^{(2)}) \check{g}_2}\right)}{\left(\sqrt{\frac{g_2}{x_2^{(2)}}} - \sqrt{\frac{\check{g}_2}{1 - x_2^{(2)}}}\right) \left(\frac{\sigma^2}{g_{21}} + \lambda_2^{MRT} - x_2^{(1)}\right)}. \quad (4.15)$$

The root of interest in (4.11) lies in $[0, \lambda_1^{MRT}]$ and satisfies

$$\text{sign}\left(\sigma^2/g_{12} + x_1^{(1)} - Cx_1^{(1)}\right) = \text{sign}\left(\sigma^2/g_{12} + x_1^{(1)} + C(1 - x_1^{(1)})\right). \quad (4.16)$$

Proof. The proof is provided in Section 4.3.4. \square

The contract curve characterized in Theorem 2 are all allocations in the Edgeworth box which are Pareto optimal in the SINR region. Thus, Theorem 2 provides all Pareto optimal points in closed-form requiring a single real-valued parameter. In Figure 4.5, the contract curve is plotted in the Edgeworth box for different SNR values. The number of antennas at the transmitters is two and we generate sample channel vectors. The contract curve is calculated by taking 10^3 samples of $x_2^{(2)}$ uniformly spaced in $(0, \lambda_2^{MRT})$ to obtain values of $x_1^{(1)}$. The course of the contract curve for 10 dB SNR is near to the edge of the Edgeworth box where joint ZF is marked. This means that Pareto optimal

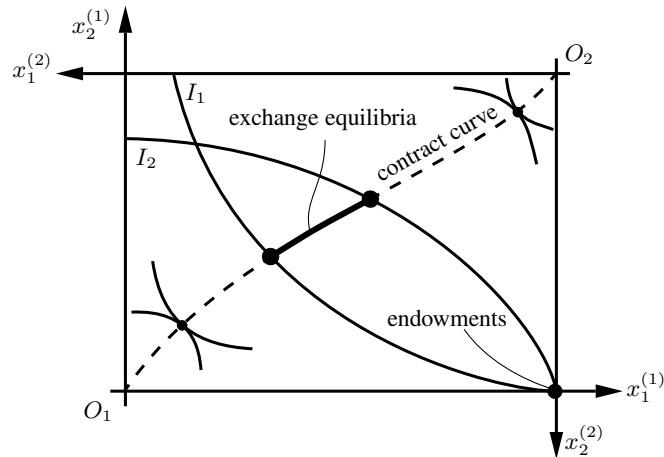


Figure 4.6.: An illustration of the exchange equilibria in the Edgeworth box.

allocations require either transmitter to choose beamforming vectors near to ZF. For decreasing SNR, the contract curve moves away from the ZF edge. For low SNR, the contract curve is then close to the edge with joint MRT. These observations conform with the analysis in [LJ08] where maximum sum rate transmission is studied in low and high SNR regimes.

4.1.2. Exchange Equilibria

According to Edgeworth [Edg81], the outcome of an exchange between the consumers must lie on the contract curve. The set of outcomes at which exchange would settle are called *exchange equilibria* and are illustrated in Figure 4.6. The exchange equilibria are the set of allocations on the contract curve which are bounded by the indifference curves corresponding to the initial endowments. That is, the exchange equilibria allocations correspond to all Pareto optimal points which dominate the Nash equilibrium in the SINR region. With the initial endowments corresponding to the Nash equilibrium, the corresponding indifference curves can be calculated from Proposition 3. The bounds for the exchange equilibria, as illustrated in Figure 4.6, can be calculated as the intersection of the indifference curves starting at the allocations in Nash equilibrium and the contract curve characterized in Theorem 2.

Relation to the Core

The solution concept by Edgeworth is related to that of coalitional games called the core [Shu61]. The exchange economy between the two links can be represented as a coalitional game without transferable payoff [OR94, Chapter 13.5]. A game in coalitional

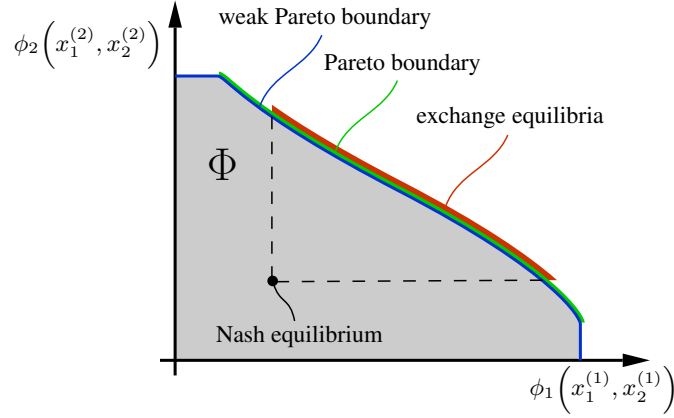


Figure 4.7.: An illustration of the exchange equilibria in the SINR region.

form [OR94, Definition 268.2] between the two links is defined by the tuple

$$\langle \mathcal{K}, \mathcal{G}, V, (\phi_k)_{k \in \mathcal{K}} \rangle. \quad (4.17)$$

In (4.17), $\mathcal{K} = \{1, 2\}$ is the set of players which consists of the two links. \mathcal{G} is called the set of consequences defined as

$$\mathcal{G} = \left\{ \left((x_1^{(1)}, x_2^{(1)}), (x_1^{(2)}, x_2^{(2)}) \right) : (x_1^{(k)}, x_2^{(k)}) \in [0, \lambda_1^{\text{MRT}}] \times [0, \lambda_2^{\text{MRT}}] \right\}. \quad (4.18)$$

The mapping V assigns to every coalition \mathcal{S} (a nonempty subset of \mathcal{K}) a set $V(\mathcal{S}) \subseteq \mathcal{G}$, such that

- $V(\{1\}) = V(\{2\}) = ((\lambda_1^{\text{MRT}}, 0), (0, \lambda_2^{\text{MRT}}))$,
- $V(\{1, 2\}) = \left\{ \left((x_1^{(1)}, x_2^{(1)}), (x_1^{(2)}, x_2^{(2)}) \right) \in \mathcal{G} : x_k^{(1)} + x_k^{(2)} = \lambda_k^{\text{MRT}} \right\}$,

and ϕ_k is the SINR of player k in (4.6).

The core [OR94, Definition 268.3] of the coalitional game in (4.17) is the set of all allocations $\left((x_1^{(1)}, x_2^{(1)}), (x_1^{(2)}, x_2^{(2)}) \right) \in V(\mathcal{K})$ for which there exists no coalition $\mathcal{S} \subseteq \mathcal{K}$ and an allocation $\left((x_1^{\prime(1)}, x_2^{\prime(1)}), (x_1^{\prime(2)}, x_2^{\prime(2)}) \right) \in V(\mathcal{S})$ for which $\phi_k(x_1^{\prime(k)}, x_2^{\prime(k)}) > \phi_k(x_1^{(k)}, x_2^{(k)})$ for all $k \in \mathcal{S}$. Therefore, the core consists of the allocations which lead to points on the Pareto boundary of the SINR region and dominate the Nash equilibrium. Consequently, the core of a coalitional game between the links is the set of exchange equilibria. The exchange equilibria in the SINR region are illustrated in Figure 4.7.

4.1.3. Bargaining

In this section, we propose a bargaining process between the consumers. The consumers iteratively exchange amounts of goods within themselves until they reach an exchange

equilibrium. The bargaining process requires that the consumers be able to communicate directly with each other and exchange signaling bits. Updating the amounts of goods at each consumer as well as specifying the signals between the consumers is done by using the Edgeworth box representation. We systematically study all achievable allocations in the Edgeworth box taking into account the possible signaling between the transmitters. Moreover, we take into account that each consumer can only update the distribution of its own good. That is, each link can only change its own beamforming parameters.

Multistage Bargaining

The bargaining process is sequential and is divided into bargaining-steps. At each bargaining-step, each consumer chooses an amount of his good to propose to the other consumer. At a bargaining-step t , consumer 1 proposes $x_1^{(2)(t)}$ to consumer 2, and consumer 2 proposes $x_2^{(1)(t)}$ to consumer 1. In addition, the consumers exchange messages in order to calculate the proposals in the next bargaining-step. The *possession* of consumer 1 at a bargaining-step t is $(x_1^{(1)(t)}, x_2^{(1)(t)})$, where $x_1^{(1)(t)}$ is the amount of his good and $x_2^{(1)(t)}$ is the amount of good from consumer 2. Similarly, $(x_1^{(2)(t)}, x_2^{(2)(t)})$ is the possession of consumer 2 at bargaining-step t . We denote an allocation in the Edgeworth box at a bargaining-step t as

$$\mathbf{x}^{(t)} := \left((x_1^{(1)(t)}, x_2^{(1)(t)}), (x_1^{(2)(t)}, x_2^{(2)(t)}) \right). \quad (4.19)$$

Recall that each allocation in the Edgeworth box is a distribution of the goods which corresponds to a beamforming vector for each transmitter in the parameterized set in (4.1).

The bargaining process is structured in stages. A bargaining-stage, indexed with s , can span several bargaining-steps as illustrated in Figure 4.8. If at a bargaining-step $t, t > s$, a Pareto improvement is achieved to the SINRs in the current bargaining-stage, then we set $s = t$. This means that a new bargaining-stage begins each time a Pareto improvement is achieved. At each bargaining-step, the consumers compare their outcomes to their current stage outcome (corresponding to bargaining-step s). In the first stage, $s = 0$, the possessions of the consumers correspond to the Nash equilibrium.

Next, we describe how the consumers choose their proposals at each bargaining-step and also what messages are they to signal to each other.

Bargaining Process

We assume that each consumer k knows his SINR $\phi_k(x_1^{(k)(t)}, x_2^{(k)(t)})$ at bargaining-step t as well as his SINR $\phi_k(x_1^{(k)(s)}, x_2^{(k)(s)})$ for the current stage s . We define the following

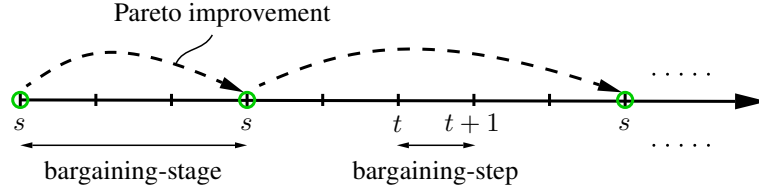


Figure 4.8.: An illustration of the bargaining steps and stages during the bargaining process.

capabilities for each consumer:

- consumer k keeps track of a step-length $\delta_k^{(t)} < \lambda_k^{\text{MRT}}$ at each bargaining-step t . The step-length is required in order to increment or decrement the amount of good proposed to the other consumer. The initial value of the step-length is set prior to the bargaining process as $\delta_k^{(0)} < \lambda_k^{\text{MRT}}$.
- consumer k can change the sign of the step-length $\delta_k^{(t)}$ and also reduce its length by multiplying it with $\theta_k \in (0, 1)$.
- consumer k can choose three types of proposals to consumer $\ell, \ell \neq k$, at bargaining-step $t + 1$. These are:

- (I) $x_k^{(\ell)(t+1)} = x_k^{(\ell)(t)}$
- (II) $x_k^{(\ell)(t+1)} = x_k^{(\ell)(t)} + \delta_k^{(t+1)}$
- (III) $x_k^{(\ell)(t+1)} = \lambda_k^{\text{MRT}} - I_k(x_\ell^{(k)(t)}, \phi_k(x_1^{(k)(s)}, x_2^{(k)(s)}))$

Proposal type (I) does not change the amount of good k proposed to consumer $\ell \neq k$ from the previous bargaining-step. Proposal type (II) increases or decreases the proposed amount of good k depending on the sign of $\delta_k^{(t+1)}$. Proposal type (III) achieves for consumer k the same SINR value as his current stage outcome $\phi_k(x_1^{(k)(s)}, x_2^{(k)(s)})$ when consumer ℓ proposes $x_\ell^{(k)(t)}$. The indifference curve function I_k is defined in Proposition 3.

- consumer k sets $\Gamma_\ell = \text{true}$ if consumer $\ell, \ell \neq k$, chooses proposal type (III) at the current bargaining-step. Otherwise, consumer k sets $\Gamma_\ell = \text{false}$ unless he also chooses proposal type (III).

In Figure 4.9, six Edgeworth boxes are illustrated. In all boxes, the indifference curves correspond to the stage allocation $\mathbf{x}^{(s)}$. The marked regions in Figure 4.9 resemble the regions where the allocations $\mathbf{x}^{(t)}, t > s$, are possible with respect to the indifference curves. Note that all regions in the Edgeworth box are covered in the cases in Figure 4.9,

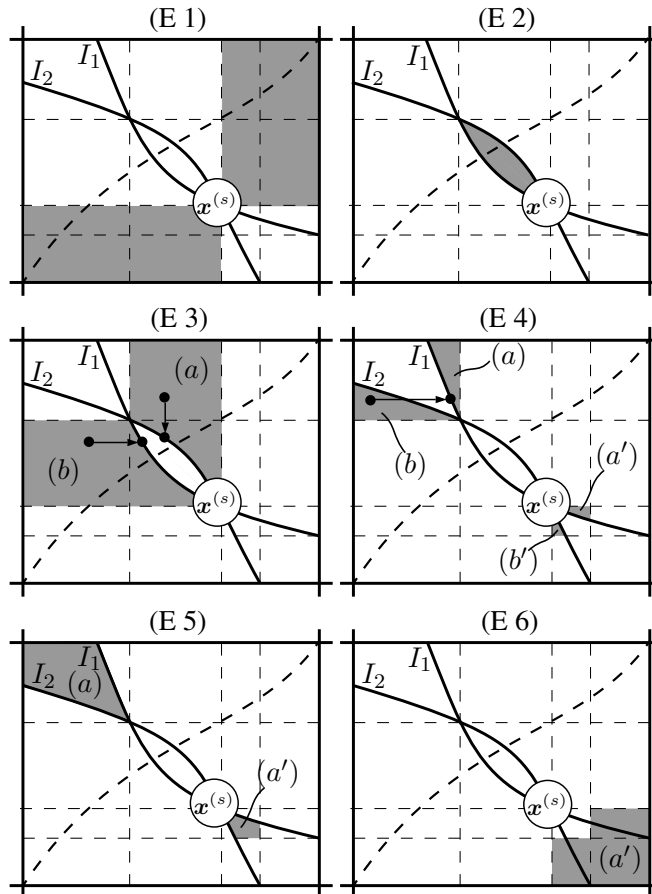


Figure 4.9.: Six Edgeworth boxes which illustrate the possible positions of the allocation $\mathbf{x}^{(t)}$ of a bargaining-step.

hence all possible positions of $\mathbf{x}^{(t)}$ are treated. These cases will aid in the description of our bargaining process.

Each consumer k can signal to the other consumer one of four signals. This requires two bits of information to be sent to the other transmitter at each bargaining-step. The four types of signals are:

- Accept (A_k): A consumer k signals A_k to the other consumer if his SINR has increased in the current bargaining-step.
- Reject (R_k): A consumer k signals R_k to the other consumer if his SINR has decreased in the current bargaining-step.
- Not Possible (N_k): A consumer k signals N_k to the other consumer if it is not possible for consumer k to find a proposal which gives him the same SINR as the stage SINR.

- Back (B_k): A consumer k signals B_k to the other consumer if he detects that the sign of the step-length has to be changed. In this case, if the consumers previously were incrementing their proposals, after signaling B_k they would start decrementing their proposals in the next bargaining-steps.

The choice of consumer 1's proposal (analogously consumer 2) is described in the flowchart in Figure 4.13. In Figure 4.13, consumer 1 chooses the signaling to consumer 2 based on conditions D_1, D_2 , and D_3 (analogously for consumer 2). Condition D_1 is true if the current step-length $\delta_1^{(t)}$ is below an accuracy measure ϵ . If consumer k signals B_k , then all consumers alter their initial step-length as $\delta_k^{(0)} = -\theta_k \delta_k^{(0)}$ and set $\delta_k^{(t+1)} = \delta_k^{(0)}$. The new proposals are of type (II). This adaptation is necessary since $\mathbf{x}^{(t)}$ can be in the opposite direction to the exchange lens (proposals in the regions marked with a prime in Figure 4.9 (E 4)-(E 6)). Since $\delta_1^{(t)}$ and $\delta_2^{(t)}$ always have the same sign, $\mathbf{x}^{(t)}$ will never be in the marked regions in Figure 4.9 (E 1).

Condition D_2 is true if consumer 1 achieves an improvement in his payoff. Thus, consumer 1 accepts the proposal by signaling A_1 to consumer 2. Now, consumer 1's proposal depends on the signal from consumer 2: If consumer 2 signals A_2 , then the allocation $\mathbf{x}^{(t)}$ is necessarily in the exchange lens in Figure 4.9 (E 2), i.e., a Pareto improvement from the stage allocation is achieved. The new stage allocation is set as $\mathbf{x}^{(s)} = \mathbf{x}^{(t)}$ and both consumers choose proposal type (II) without altering the step-lengths. If consumer 2 signals R_2 , then $\mathbf{x}^{(t)}$ is in region (a) in Figure 4.9 (E 3). Consumer 2 chooses proposal type (III) and consumer 1 chooses proposal type (I). This adaptation is illustrated in Figure 4.9 (E 3) as projecting the allocation $\mathbf{x}^{(t)}$ onto I_2 . Consumer 1 then sets $\Gamma_2 = \mathbf{true}$. If consumer 2 signals N_2 , then $\mathbf{x}^{(t)}$ is in region (a') in Figure 4.9 (E 6) and above I_1 . Both consumers then choose proposal type (II) which makes $\mathbf{x}^{(t+1)}$ closer to $\mathbf{x}^{(s)}$ than $\mathbf{x}^{(t)}$.

Condition D_3 is true if consumer 1 cannot find $x_1^{(2)(t+1)}$, given $x_2^{(1)(t)}$, to achieve the SINR $\phi_1(x_1^{(1)(s)}, x_2^{(1)(s)})$ of the current stage. Having that consumer 1 can choose the proposals $x_1^{(2)(t+1)} \in [0, \lambda_k^{\text{MRT}}]$, then $\phi_1(x_1^{(1)(s)}, x_2^{(1)(s)})$ is feasible if it is in the set $\mathcal{F}_1(x_2^{(1)(t)})$ defined as

$$\mathcal{F}_1(x_2^{(1)(t)}) := [\phi_1(0, x_2^{(1)(t)}), \phi_1(\lambda_1^{\text{MRT}}, x_2^{(1)(t)})]. \quad (4.20)$$

Similarly for consumer 2, we define the set

$$\mathcal{F}_2(x_1^{(2)(t)}) := [\phi_2(x_1^{(2)(t)}, 0), \phi_2(x_1^{(2)(t)}, \lambda_2^{\text{MRT}})]. \quad (4.21)$$

The above defined sets determine whether it is feasible to find a beamforming vector for a transmitter which achieves an SINR equal to the bargaining stage outcome. This case

occurs if $\mathbf{x}^{(t)}$ is in the region marked in Figure 4.9 (E 6), where $\mathbf{x}^{(t)}$ cannot be projected onto I_1 for constant $x_1^{(2)(t)}$. Condition D_3 is also true if Γ_2 is true, i.e., consumer 2 has chosen proposal type (III) in the previous step. This case reveals that the previous allocation $\mathbf{x}^{(t-1)}$ has been in any of the marked regions in Figure 4.9 (E 4). Each consumer chooses proposal types (II) after reducing their step-lengths. Hence, $\mathbf{x}^{(t+1)}$ will be closer to $\mathbf{x}^{(s)}$. If D_3 is false, consumer 1 chooses his proposal according to the signal from consumer 2: If consumer 2 signals (A_2), then this case is analogous to the case described before when consumer 1 signals A_1 and consumer 2 R_2 . If consumer 2 signals (R_2), then $\mathbf{x}^{(t)}$ can only be in regions (a) or (a') in Figure 4.9 (E 5). Both consumers use proposal types (II) after reducing their step-lengths.

The bargaining process terminates when $|\delta_1^{(0)}| < \epsilon$ or $|\delta_2^{(0)}| < \epsilon$. The initial step-length $\delta_k^{(0)}$ is reduced each time B_k is signaled, i.e., when $|\delta_k^{(t)}| < \epsilon$. The step-length of at least one consumer is reduced in each bargaining-step, except when Pareto improvements are achieved. Pareto improvements lead to a reduction in the size of the exchange lens. The exchange lens vanishes when the indifference curves are tangent, i.e., the allocation is on the contract curve. Therefore, the bargaining process converges after a finite number of steps to an outcome arbitrarily close to the contract curve. In the SINR region, the bargaining outcome is then arbitrarily close to an exchange equilibrium on the Pareto boundary.

Simulation Results

In Figure 4.10, the Pareto boundary of an SINR region for sample channel realizations is plotted using the set of efficient beamforming vectors in (4.1) (100 samples are taken uniformly in $[0, \lambda_k^{\text{MRT}}]$). Joint ZF and the Nash equilibrium (joint MRT) outcomes are plotted. The Nash equilibrium is the starting point for our bargaining process. Three different bargaining outcomes achieved by our bargaining process are marked with squares. The bargaining trajectories from the Nash equilibrium to these outcomes corresponds to the stages during the bargaining process. The bargaining outcome cannot be determined prior to the bargaining process and depends on the initializing parameters such as the initial step-lengths $\delta_k^{(0)}$ and θ_k . The bargaining outcomes always dominate the Nash equilibrium, e.g. BO_1, BO_2 , and BO_3 . The dashed line connecting joint MRT and joint ZF points is the trajectory curve of the bargaining algorithm proposed in [HG08]. In this algorithm both consumers start at the Nash equilibrium (or joint ZF) and reduce their proposals in equal step-lengths. The algorithm terminates when at least one link experiences reduction in its payoff. The outcome of this algorithm starting in Nash equilibrium is marked with a circle.

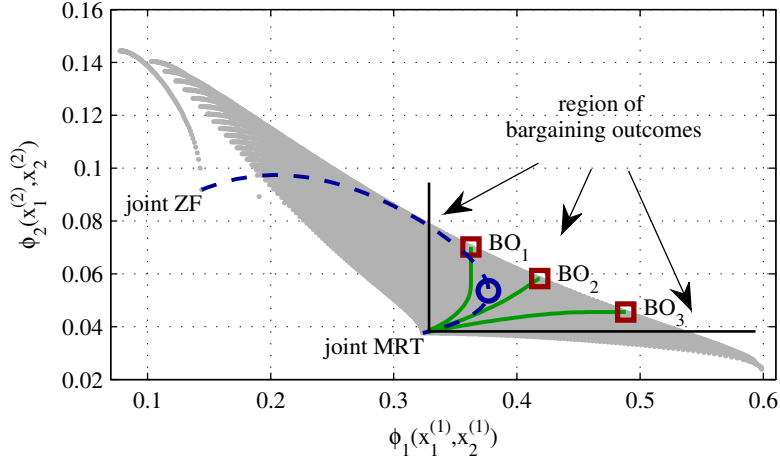


Figure 4.10.: SINR region of a two-user MISO IFC with $\text{SNR} = 0$ dB. The bargaining outcomes are marked with squares for three different initial step-lengths $(\delta_1^{(0)}, \delta_2^{(0)})$. $BO_1 : (0.02, 0.01)$, $BO_2 : (0.015, 0.01)$, $BO_3 : (0.01, 0.01)$.

In Figure 4.11, an Edgeworth box is plotted for the bargaining process in which the step-lengths are initialized with $(\delta_1^0, \delta_2^0) = (0.1, 0.1)$ and the accuracy measure is $\epsilon = 10^{-5}$. The stage allocations are marked with crosses, and the exchange lens is bounded by the corresponding indifference curves. The exchange lens reduces in size after each bargaining-stage until the indifference curves are tangent at the bargaining outcome. This indicates that the outcome is Pareto optimal. In Figure 4.12, the SINR values for the same setting as of Figure 4.11 are plotted for increasing bargaining-steps. The stage outcomes are marked with circles. These are the SINR pairs that the consumers jointly accept during the bargaining process. The algorithm terminates after 40 bargaining-steps. However, since the SINRs only increase slightly after half the bargaining-steps, the bargaining process could be stopped at bargaining-step 20 requiring a total of 80 signaling bits.

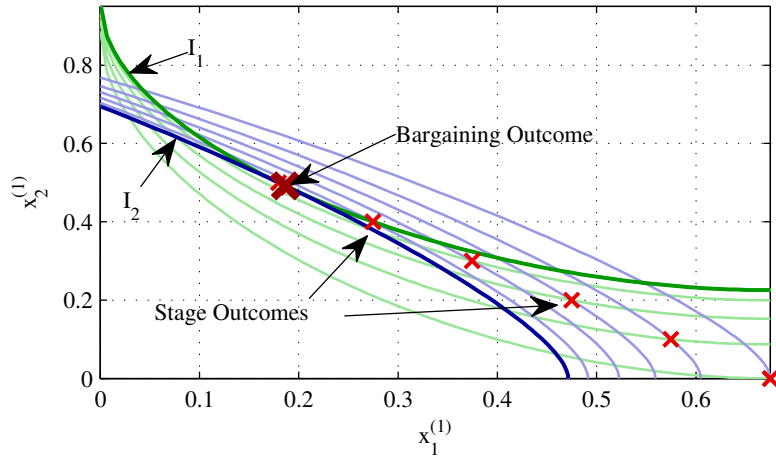


Figure 4.11.: Edgeworth box representation of the bargaining process for $(\delta_1^{(0)}, \delta_2^{(0)}) = (0.1, 0.1)$. Two antennas are used at each transmitter and SNR = 0 dB.

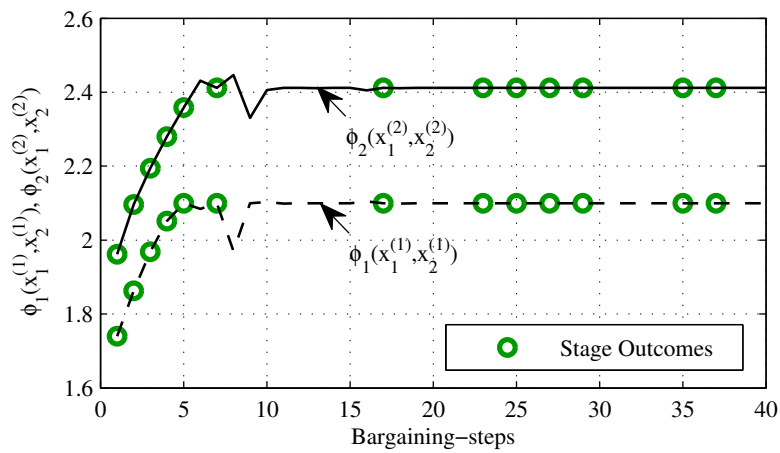


Figure 4.12.: SINR values over the bargaining-steps for $(\delta_1^{(0)}, \delta_2^{(0)}) = (0.1, 0.1)$. Two antennas are used at each transmitter and SNR = 0 dB.

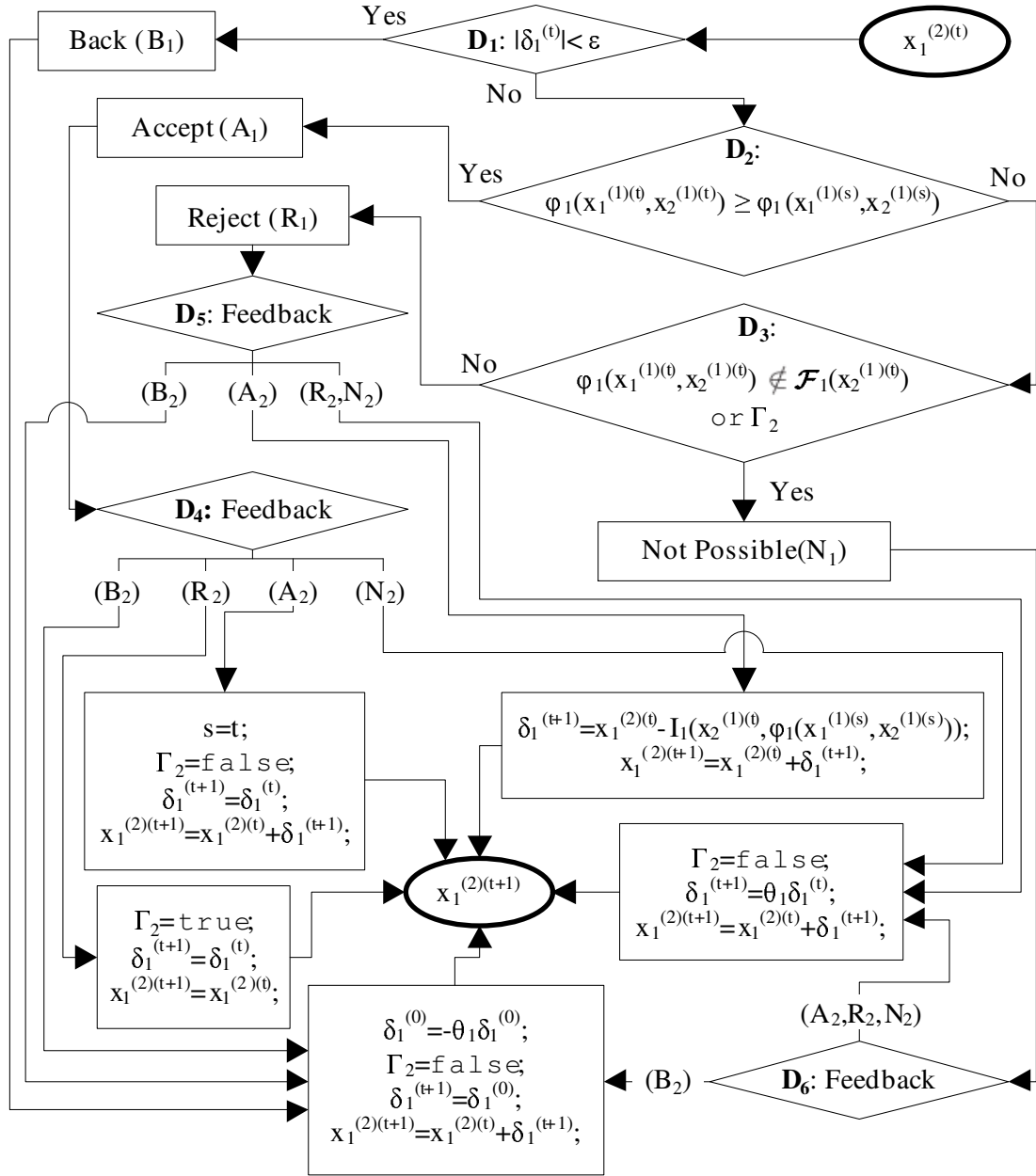


Figure 4.13.: Flowchart for consumer 1 (analogously consumer 2) for a new proposal.

4.2. Competitive Markets

In this section, we model the situation between two MISO links as a competitive market. The stable state of a competitive market is called Walrasian equilibrium and lies in the set of exchange equilibria characterized in the previous section. We continue to interpret the efficient beamforming parameters as goods in this section. However, opposed to the previous section where the goods were directly exchanged between the consumers, the goods in a competitive market are bought and sold by the consumers at given prices.

4.2.1. Competitive Market Model

In a competitive market, the consumers buy quantities of goods and also sell goods they possess such that they maximize their profit. Each good has a price and every consumer takes the prices as given. The prices of the goods are not determined by consumers, but arbitrated by markets. In our case, the arbitrator determines the prices of the goods. The goods in (4.2) correspond to the parameterizations of the efficient beamforming vectors. Let p_k denote the unit price of good k . In order to be able to buy goods, each consumer k is endowed with a budget $\lambda_k^{\text{MRT}} p_k$ which is the worth of his initial amounts of goods⁶. The *budget set* of consumer k is the set of bundles of goods he can afford to buy defined as

$$\mathcal{B}_k := \left\{ (x_1^{(k)}, x_2^{(k)}) \in \mathbb{R}_+^2 : x_1^{(k)} p_1 + x_2^{(k)} p_2 \leq \lambda_k^{\text{MRT}} p_k \right\}. \quad (4.22)$$

The budget set of consumer 1 is illustrated by the grey area in Figure 4.14. The boundary of the budget set is a line which connects the points $(\lambda_1^{\text{MRT}}, 0)$ and $(0, \lambda_1^{\text{MRT}} p_1/p_2)$. Thus, the boundary has a slope of $-p_1/p_2$.

For the consumers, the prices of the goods are measures for their qualitative valuation. If p_1 is greater than p_2 , then good 1 has more value than good 2. Given the prices p_1 and p_2 , consumer 1 demands the amounts of goods $x_1^{(1)}$ and $x_2^{(1)}$ such that these maximize his SINR utility function in (4.6). Thus, consumer k solves the following problem:

$$\begin{aligned} & \text{maximize} && \phi_k(x_1^{(k)}, x_2^{(k)}) \\ & \text{subject to} && p_1 x_1^{(k)} + p_2 x_2^{(k)} \leq \lambda_k^{\text{MRT}} p_k. \end{aligned} \quad (4.23)$$

In the above consumer problem, the objective function is the SINR of link k in (4.6), and the constraint is defined by the budget set of consumer k in (4.22). The physical interpretation of the budget set constraint can be related to an interference constraint.

⁶This case corresponds to the Arrow-Debreu market model [Ye07].

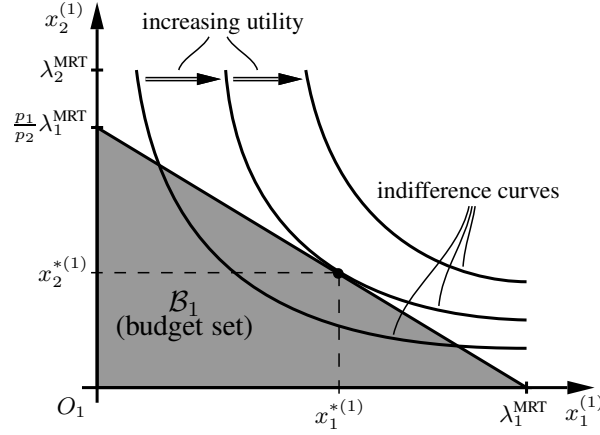


Figure 4.14.: An illustration of the budget set of consumer 1.

Considering consumer 1, the constraint in (4.23) can be reformulated to

$$x_1^{(1)} \leq \lambda_1^{\text{MRT}} - \frac{p_2}{p_1} x_2^{(1)}, \quad (4.24)$$

where, as mentioned before, $x_1^{(1)} = \lambda_1 \in [0, \lambda_1^{\text{MRT}}]$ is the scaling of interference transmitter 1 produces at receiver 2. Analogously, $x_2^{(1)} = \lambda_2^{\text{MRT}} - \lambda_2$ is the scaling for interference reduction from transmitter 2 at receiver 1. Hence, the constraint in (4.24) dictates the tradeoff between the amount of interference transmitter 1 can generate at receiver 2 and the amount of interference receiver 1 is to tolerate. The prices p_1 and p_2 can be interpreted as parameters to control the fairness between the links by regulating the amount of interference the links generate on each other.

Theorem 3. *The unique solution to the problem in (4.23) is*

$$x_1^{*(1)}(p_1, p_2) = \left[1 + \frac{\check{g}_1}{g_1} \left(1 + \frac{g_{21} \frac{p_1}{p_2}}{\sigma^2 + \lambda_2^{\text{MRT}} g_{21} - \lambda_1^{\text{MRT}} g_{21} \frac{p_1}{p_2}} \right)^2 \right]^{-1}, \quad (4.25)$$

$$x_2^{*(1)}(p_1, p_2) = \frac{p_1}{p_2} (\lambda_1^{\text{MRT}} - x_1^{*(1)}), \quad (4.26)$$

for consumer 1, and

$$x_2^{*(2)}(p_1, p_2) = \left[1 + \frac{\check{g}_2}{g_2} \left(1 + \frac{g_{12} \frac{p_2}{p_1}}{\sigma^2 + \lambda_1^{\text{MRT}} g_{12} - \lambda_2^{\text{MRT}} g_{12} \frac{p_2}{p_1}} \right)^2 \right]^{-1}, \quad (4.27)$$

$$x_1^{*(2)}(p_1, p_2) = \frac{p_2}{p_1} (\lambda_2^{\text{MRT}} - x_2^{*(2)}), \quad (4.28)$$

for consumer 2, where \check{g}_k, g_k, g_{kl} are defined in Lemma 1. The feasible prices ratio is in the range:

$$\underline{\beta} := \frac{\lambda_2^{\text{MRT}} g_{12}}{\sigma^2 + \lambda_1^{\text{MRT}} g_{12}} \leq \frac{p_1}{p_2} \leq \bar{\beta} := \frac{\sigma^2 + \lambda_2^{\text{MRT}} g_{21}}{\lambda_1^{\text{MRT}} g_{21}}. \quad (4.29)$$

Proof. The proof is provided in Appendix 4.3.5. \square

Theorem 3 characterizes the demand functions of each consumer. In economic theory, these functions are called *Marshallian demand functions* [JR03] or *Walrasian demand functions* [MCWG95]. Note that each consumer calculates his demands independently without knowing the other consumer's demands. From Theorem 3, consumer 1 (analogously consumer 2) needs to know the constants g_1 , \check{g}_1 , and g_{21} defined in Lemma 1. The measure $\sigma^2 + \lambda_2^{\text{MRT}} g_{21}$ in (4.6) is the noise plus interference power in Nash equilibrium. This measure is reported from receiver 1 to its transmitter in Nash equilibrium which is the links' initial state before coordination takes place.

The demand functions of the consumers in Theorem 3 are *homogenous of degree zero* [JR03, Definition A2.2] with the prices p_1 and p_2 . That is, the demand of consumer 1 for good 1 (analogously consumer 2 for good 2) satisfies $x_1^{*(1)}(tp_1, tp_2) = x_1^{*(1)}(p_1, p_2)$ for $t > 0$. Hence, given only a prices ratio \bar{p}_1/\bar{p}_2 , we can calculate a prices pair as $p_1 = \bar{p}_1/\bar{p}_2$ and $p_2 = 1$ which leads to the same demand as with \bar{p}_1 and \bar{p}_2 . With this respect, a consumer need only know the prices ratio p_1/p_2 from the arbitrator to calculate his demands. In Figure 4.14, the demand of consumer 1 is illustrated as the point where the corresponding indifference curve is tangent to the boundary of the budget set.

The next result provides a significant property that the goods in our setting possess. Later in Section 4.2.2 and Section 4.2.3, this property is required to prove the uniqueness of the Walrasian equilibrium and also to guarantee the global convergence of the price adjustment process.

Lemma 2. *The goods in our setting are gross substitutes, i.e., increasing the price of one good increases the demand of the other good.*

Proof. Decreasing the ratio p_1/p_2 can be interpreted as decreasing p_1 or increasing p_2 . Consider the *aggregate excess demand* of good 1 defined as

$$z_1(p_1, p_2) = x_1^{*(1)}(p_1, p_2) + x_1^{*(2)}(p_1, p_2) - \lambda_1^{\text{MRT}}, \quad (4.30)$$

where $x_1^{*(1)}(p_1, p_2)$ and $x_1^{*(2)}(p_1, p_2)$ are the demand functions of good 1 in (4.25) and (4.28) from Theorem 3. If p_1/p_2 decreases, then $x_1^{*(1)}(p_1, p_2)$ increases. If p_1/p_2 decreases, then $x_1^{*(2)}(p_1, p_2)$ also increases since p_2/p_1 increases and $x_2^{*(2)}(p_1, p_2)$ decreases. Thus, the aggregate excess demand of good 1 in (4.30) increases if p_1/p_2 decreases. The analysis is analogous for the second good. \square

If each consumer is to demand amounts of goods without considering the demands of the other consumer, then it is important that the consumers' demands equal the

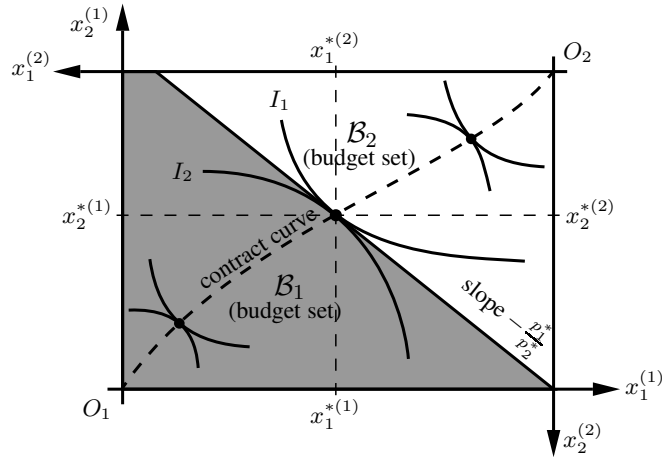


Figure 4.15.: An illustration of an Edgeworth box. I_1 and I_2 are indifference curves of consumer 1 and 2 respectively. The line with slope $-p_1^*/p_2^*$ separates the budget sets of the consumers in Walrasian equilibrium.

consumers' supply of goods. Prices which fulfill this requirement are called *Walrasian* and are calculated next.

4.2.2. Walrasian Equilibrium

In a Walrasian equilibrium, the demand equals the supply of each good [JR03, Definition 5.5]. According to the properties of the utility function in Theorem 1, there exists at least one Walrasian equilibrium [JR03, Theorem 5.5]. The Walrasian prices (p_1^*, p_2^*) that lead to a Walrasian equilibrium satisfy

$$x_1^{*(1)}(p_1, p_2) + x_1^{*(2)}(p_1, p_2) = \lambda_1^{\text{MRT}}, \quad (4.31)$$

$$\text{and } x_2^{*(1)}(p_1, p_2) + x_2^{*(2)}(p_1, p_2) = \lambda_2^{\text{MRT}}. \quad (4.32)$$

In our setting in which only two goods exist, Walras' law [JR03, Chapter 5.2] provides the property that if the demand equals the supply of one good, then the demand would equal the supply of the other good. Hence, in order to calculate the Walrasian prices, it is sufficient to consider only one of the conditions in (4.31) and (4.32).

Theorem 4. *The ratio of the Walrasian prices is the unique root of*

$$a \left[\frac{p_1}{p_2} \right]^5 + b \left[\frac{p_1}{p_2} \right]^4 + c \left[\frac{p_1}{p_2} \right]^3 + d \left[\frac{p_1}{p_2} \right]^2 + e \left[\frac{p_1}{p_2} \right] + f = 0, \quad (4.33)$$

that satisfies the condition in (4.29). The constant coefficients are

$$\begin{aligned} a &= T_1 T_2^2 T_3, & b &= -2T_3 T_2 (T_2 S_2 + T_1 S_1), \\ c &= 2T_4 T_2 S_3 + 4S_1 S_2 T_2 T_3 + T_1 S_4 T_3, \\ d &= -2S_4 S_2 T_3 - 4T_1 T_2 S_2 S_3 - S_1 T_4 S_3, \\ e &= 2S_3 S_2 (T_2 S_2 + T_1 S_1), & f &= -S_1 S_2^2 S_3, \end{aligned}$$

where

$$\begin{aligned} T_1 &= (g_1 - \check{g}_1)/(g_1 + \check{g}_1), & T_2 &= \lambda_1^{MRT} + \sigma^2/g_{12}, \\ T_3 &= (1 - \lambda_1^{MRT})\lambda_1^{MRT}, & T_4 &= (\check{g}_1^2 - \check{g}_1 g_1 + g_1^2)/(g_1 + \check{g}_1)^2, \\ S_1 &= (g_2 - \check{g}_2)/(g_2 + \check{g}_2), & S_2 &= \lambda_2^{MRT} + \sigma^2/g_{21}, \\ S_3 &= (1 - \lambda_2^{MRT})\lambda_2^{MRT}, & S_4 &= (\check{g}_2^2 - \check{g}_2 g_2 + g_2^2)/(g_2 + \check{g}_2)^2, \end{aligned}$$

and \check{g}_k, g_k, g_{kl} are defined in Lemma 1.

Proof. Substituting (4.25) and (4.28) in (4.31) and collecting p_1/p_2 we get the expression in (4.33). The condition in (4.29) states the set of feasible prices such that the demands of the consumers are feasible. At least one price pair is in this set since a Walrasian equilibrium always exists in our setting. In addition, having the property that the goods are gross substitutes in Lemma 2, implies that the Walrasian equilibrium in our setting is unique [MCWG95, Proposition 17.F.3]. Note that the roots in (4.33) can be easily calculated using a Newton method. And due to the uniqueness of the Walrasian prices, only one root satisfies the condition in (4.29). \square

According to the First Welfare Theorem [JR03, Theorem 5.7], the Walrasian equilibrium is Pareto optimal. Moreover, linking to the results in the previous section, the Walrasian equilibrium is an exchange equilibrium [JR03, Theorem 5.6]. In other words, the Walrasian equilibrium dominates the Nash equilibrium outcome. In Figure 4.15, the allocation in Walrasian equilibrium which corresponds to the Walrasian prices ratio p_1^*/p_2^* is illustrated in the Edgeworth box. It is the point on the contract curve which intersects the line that passes through the endowment point (Nash equilibrium) with slope $-p_1^*/p_2^*$ (with respect to the coordinate system of consumer 1). The grey area in Figure 4.15 is the budget set of consumer 1 as described in Figure 4.14. The white area in the Edgeworth box is the budget set of consumer 2. According to the axis transformation in constructing the Edgeworth box, the boundaries of the consumers' budget sets coincide. The indifference curves of the consumers are tangent to this line and also tangent to one another which illustrates the Pareto optimality of the Walrasian equilibrium.

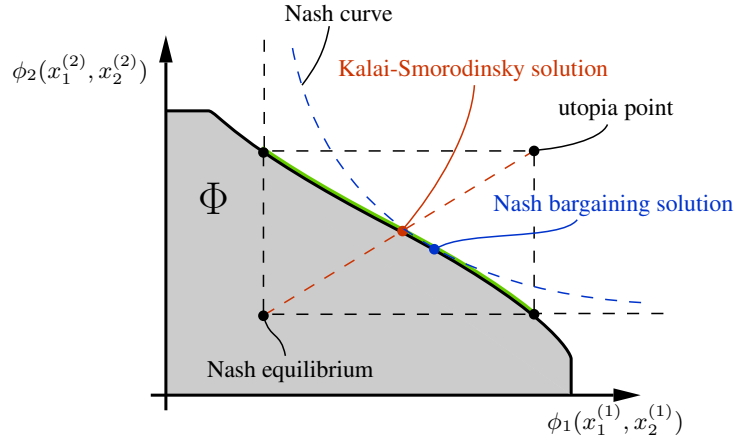


Figure 4.16.: An illustration of the Kalai-Smorodinsky and Nash bargaining solutions in the SINR region.

Relation to Axiomatic Bargaining

Two solutions from axiomatic bargaining theory, namely the Nash bargaining solution (NBS) [Nas50a] and the Kalai-Smorodinsky (KS) solution [KS75] are also exchange equilibria. These solutions differ by the axioms that define them. The interested reader is referred to [Pet92] for a comprehensive theory on axiomatic bargaining. A bargaining problem is defined by⁷ $\langle \Phi, (\phi_1^{\text{NE}}, \phi_2^{\text{NE}}) \rangle$, where Φ is the SINR region in (4.3) and $(\phi_1^{\text{NE}}, \phi_2^{\text{NE}})$ is called the *threat point* which corresponds to the SINR tuple in Nash equilibrium. The threat point is a state reached if cooperation between the players does not succeed.

The NBS [OR94, Chapter 15] of $\langle \Phi, (\phi_1^{\text{NE}}, \phi_2^{\text{NE}}) \rangle$ solves the following problem:

$$\begin{aligned} & \text{maximize} && (\phi_1 - \phi_1^{\text{NE}})(\phi_2 - \phi_2^{\text{NE}}) \\ & \text{subject to} && (\phi_1, \phi_2) \in \Phi. \end{aligned} \tag{4.34}$$

In [LJ08], the NBS solution is selected as a cooperative solution between the two MISO links. The solution is found graphically by checking the intersection of the Pareto boundary and the Nash curves. A *Nash curve* is a set of SINR tuples that satisfy

$$c = (\phi_1 - \phi_1^{\text{NE}})(\phi_2 - \phi_2^{\text{NE}}) \tag{4.35}$$

for a given constant value c . The NBS is the SINR tuple at which the Nash curve touches the boundary of the SINR region at a single point as is illustrated in Figure 4.16. Note

⁷In order to simplify the description of the bargaining solutions, we do not explicitly state the dependence of the utility functions on the goods.

that the NBS is only defined for convex utility regions which ensures a unique solution. The SINR region Φ in our case is not necessarily convex and therefore multiple solutions can exist for the problem in (4.34).

The KS solution of the bargaining problem $\langle \Phi, (\phi_1^{\text{NE}}, \phi_2^{\text{NE}}) \rangle$ solves the following problem [KS75]:

$$\begin{aligned} & \text{maximize} && \min \left(\frac{\phi_1 - \phi_1^{\text{NE}}}{\phi_1^{\text{UP}} - \phi_1^{\text{NE}}}, \frac{\phi_2 - \phi_2^{\text{NE}}}{\phi_2^{\text{UP}} - \phi_2^{\text{NE}}} \right) \\ & \text{subject to} && (\phi_1, \phi_2) \in \Phi, \end{aligned} \tag{4.36}$$

where ϕ_1^{UP} (analogously ϕ_2^{UP}) is the solution of the following problem:

$$\begin{aligned} & \text{maximize} && \phi_1 \\ & \text{subject to} && (\phi_1, \phi_2^{\text{NE}}) \in \Phi. \end{aligned} \tag{4.37}$$

The point $(\phi_1^{\text{UP}}, \phi_2^{\text{UP}})$ is called the *utopia point*. As illustrated in Figure 4.16, the two Pareto optimal points $(\phi_1^{\text{UP}}, \phi_2^{\text{NE}})$ and $(\phi_2^{\text{NE}}, \phi_1^{\text{UP}})$ are the bounds to the set of exchange equilibria from Section 4.1.2. Graphically, the KS solution is the intersection of the Pareto boundary with the line connecting the Nash equilibrium and the utopia point. In [NS09], the KS solution is found in the MISO IFC by solving a set of convex feasibility problems.

The properties that the Walrasian equilibrium and the NBS or KS solution have in common are that they are exchange equilibria, i.e., each user achieves higher utility than at the Nash equilibrium. The difference between the solutions is the fairness aspects in allocating the Pareto optimal utilities to the players. The current advantage in the Walrasian equilibrium over NBS and KS solutions is that it can be characterized in closed-form using Theorem 3 and Theorem 4. In addition, in the next section we devise two coordination mechanism to implement the Walrasian equilibrium.

4.2.3. Coordination Mechanism

In this section, we provide two coordination mechanisms which require different amount of information at the arbitrator. If the arbitrator has full knowledge of all parameters of the setting, then he can calculate the Walrasian prices from Theorem 4 and forward these to the transmitters. The transmitters calculate their demands from Theorem 3 and choose the beamforming vectors accordingly. This mechanism that uses the results in Theorem 3 and Theorem 4 leads directly to the Walrasian equilibrium. In Table 4.1, the required information at the arbitrator and the transmitters to implement this one-shot mechanism are listed. We assume that each transmitter forwards the

	Information
Arbitrator	$\mathbf{h}_{11}, \mathbf{h}_{12}, \mathbf{h}_{21}, \mathbf{h}_{22}, \sigma^2$
Transmitter 1	$\mathbf{h}_{11}, \mathbf{h}_{12}, \sigma^2 + \lambda_2^{\text{MRT}} \ \mathbf{h}_{21}\ ^2, \ \mathbf{h}_{21}\ ^2$
Transmitter 2	$\mathbf{h}_{22}, \mathbf{h}_{21}, \sigma^2 + \lambda_1^{\text{MRT}} \ \mathbf{h}_{12}\ ^2, \ \mathbf{h}_{12}\ ^2$

Table 4.1.: Required information at the arbitrator and transmitters to implement the Walrassian equilibrium in one-shot.

	Information
Arbitrator	$\ \mathbf{h}_{21}\ ^2, \ \mathbf{h}_{12}\ ^2, \lambda_1^{\text{MRT}}, \lambda_2^{\text{MRT}}, \sigma^2$
Transmitter 1	$\mathbf{h}_{11}, \mathbf{h}_{12}, \sigma^2 + \lambda_2^{\text{MRT}} \ \mathbf{h}_{21}\ ^2, \ \mathbf{h}_{21}\ ^2$
Transmitter 2	$\mathbf{h}_{22}, \mathbf{h}_{21}, \sigma^2 + \lambda_1^{\text{MRT}} \ \mathbf{h}_{12}\ ^2, \ \mathbf{h}_{12}\ ^2$

Table 4.2.: Required information at the arbitrator and transmitters for the price adjustment process.

channel information it has to the arbitrator. Note that each transmitter k initially knows the channel vectors \mathbf{h}_{kk} and $\mathbf{h}_{k\ell}, k \neq \ell$, which are required to calculate the efficient beamforming vectors in (2.9). Also, transmitter k knows the sum $\sigma^2 + \lambda_\ell^{\text{MRT}} \|\mathbf{h}_{\ell k}\|^2, k \neq \ell$, since this is the noise plus interference in Nash equilibrium forwarded through feedback from the intended receiver. The arbitrator, which now has full knowledge of all channels, can then forward the missing information on the channel gain $\|\mathbf{h}_{\ell k}\|^2$ to a transmitter k .

If the arbitrator has limited information about the setting, we could still achieve the Walrasian prices through an iterative price adjustment process. For fixed arbitrary initial prices, the transmitters can calculate their demands and forward these to the arbitrator. The arbitrator exploits the demand information to update the prices of the goods. Specifically, the arbitrator would increase the price of the good which has higher demand than its supply. Due to the properties of the goods in Lemma 2, this price adjustment process, also called tâtonnement, is globally convergent to the Walrasian prices given in Theorem 4 [ABH59]. The price adjustment process requires the information listed in Table 4.2 to be available at the arbitrator and the transmitters. In contrast to Table 4.1, the arbitrator requires aside from the noise power σ^2 only the cross channel gains $\|\mathbf{h}_{21}\|^2, \|\mathbf{h}_{12}\|^2$ and the parameters $\lambda_1^{\text{MRT}}, \lambda_2^{\text{MRT}}$ from the transmitters. This information is required only at the beginning of the price adjustment process in order to calculate the bounds for the feasible prices $\underline{\beta}$ and $\bar{\beta}$ given in (4.29).

In Algorithm 1, the price adjustment process is described. This process is essentially

Algorithm 1: Distributed price adjustment process.

Input: $x_1^{(1)}, x_1^{(2)}, x_2^{(1)}, x_2^{(2)}$

1 initialize: accuracy ϵ , $n = 0$, $\bar{\beta}^{(0)} = \bar{\beta}$, $\underline{\beta}^{(0)} = \underline{\beta}$ in (4.29), $\frac{p_1^{(0)}}{p_2^{(0)}} = \frac{\bar{\beta}^{(0)}}{2} + \frac{\underline{\beta}^{(0)}}{2}$;

2 **while** $\bar{\beta}^{(n)} - \underline{\beta}^{(n)} > \epsilon$ **do**

3 receive demands $x_1^{(1)}, x_1^{(2)}, x_2^{(1)}, x_2^{(2)}$;

4 $n = n + 1$;

5 **if** $x_1^{(1)} + x_1^{(2)} > \lambda_1^{MRT}$ **then**

6 $\underline{\beta}^{(n)} = \frac{p_1^{(n-1)}}{p_2^{(n-1)}}$, $\bar{\beta}^{(n)} = \bar{\beta}^{(n-1)}$;

7 $\frac{p_1^{(n)}}{p_2^{(n)}} = \frac{\bar{\beta}^{(n)} + \underline{\beta}^{(n)}}{2}$;

8 **else**

9 $\underline{\beta}^{(n)} = \underline{\beta}^{(n-1)}$, $\bar{\beta}^{(n)} = \frac{p_1^{(n-1)}}{p_2^{(n-1)}}$;

10 $\frac{p_1^{(n)}}{p_2^{(n)}} = \frac{\bar{\beta}^{(n)} + \underline{\beta}^{(n)}}{2}$;

Output: $p_1^{(n)}/p_2^{(n)}$

a bisection method which finds the roots of the excess demand function described in the proof of Lemma 2. The accuracy measure conditioning the termination of the algorithm is defined as ϵ . The terms $\underline{\beta}$ and $\bar{\beta}$ are the lower and upper bounds on the prices ratio given in (4.29), respectively. The prices ratio is initialized to the middle value of these bounds and forwarded to the links. The links send their demands calculated from Theorem 3 to the arbitrator. If the demand of good 1 is greater than its supply, then the arbitrator increases the ratio of the prices to half the distance to the upper bound $\bar{\beta}$. Thus, the price of good 1 relative to the price of good 2 increases. The lower bound on the prices ratio $\underline{\beta}$ is updated to the prices ratio of the previous iteration. If the demand of good 1 is less than its supply, the prices ratio is decremented half the distance to the lower bound $\underline{\beta}$. The upper bound $\bar{\beta}$ is set to the prices ratio of the previous iteration. The algorithm terminates when the distance between the updated upper and lower bounds on the prices ratio is below the accuracy measure ϵ .

In Figure 4.17, the prices ratio in the price adjustment process is marked with a cross and is shown to converge after a few iterations to the Walrasian prices ratio from Theorem 4. The dashed lines correspond to the upper and lower bounds in (4.29).

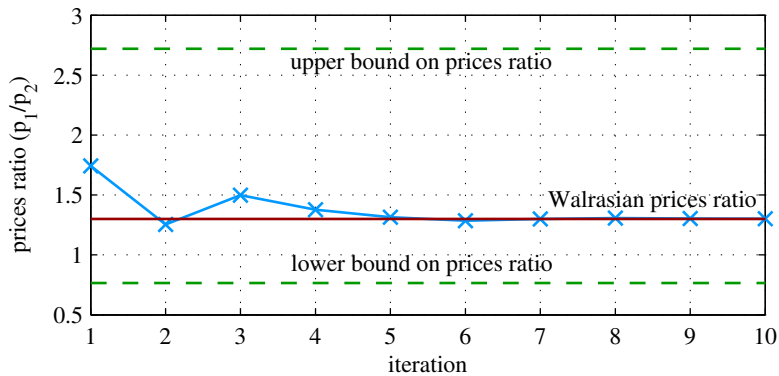


Figure 4.17.: Convergence of the price ratio in the price adjustment process to the Walrasian price ratio.

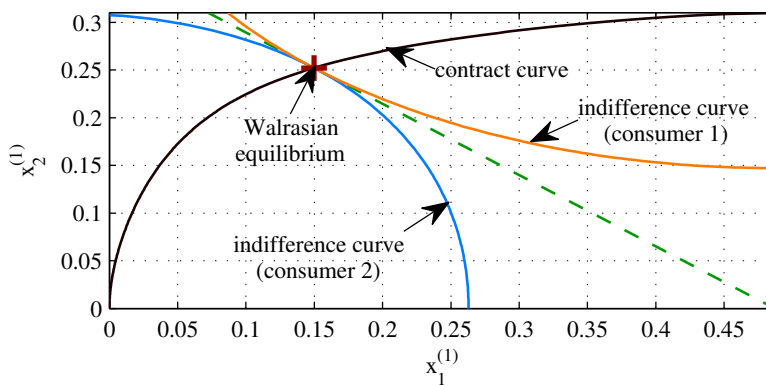


Figure 4.18.: Edgeworth box which depicts the allocation for the Walrasian prices.

Simulation Results

In Figure 4.18, an Edgeworth box is plotted for sample channel realizations with two transmit antennas at each transmitter. For the prices calculated from Theorem 4 we obtain the Walrasian equilibrium allocation on the contract curve where the corresponding indifference curves are tangent. The indifference curves are obtained from Proposition 3. The line passing through the Walrasian equilibrium allocation defines the budget sets of the consumers as is illustrated in Figure 4.15.

In Figure 4.19, the SINR region is plotted. The points lying inside the SINR region correspond to the beamforming vectors in (4.1), where a subset of these points are Pareto optimal. The Pareto boundary corresponds to the allocations on the contract curve calculated in Theorem 2. The exchange equilibria are all Pareto optimal points that dominate the Nash equilibrium (joint MRT). Assuming the links are rational, only exchange equilibria are of interest for the links. In other words, the links will not cooper-

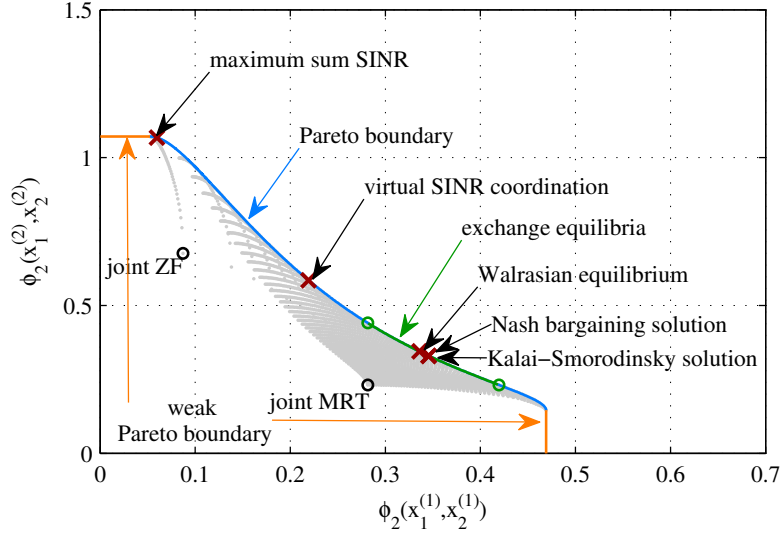


Figure 4.19.: SINR region of a two-user MISO IFC with $\text{SNR} = 0$ dB and two antennas at the transmitters.

ate if one link would achieve lower payoff than at the Nash equilibrium. The Walrasian equilibrium from Theorem 4 is an exchange equilibrium. In Figure 4.19, we also plot the maximum sum SINR which is obtained by grid search over the allocations on the Pareto boundary. The virtual SINR coordination point corresponds to the coordination mechanism in [ZG09], where the minimum mean square error (MMSE) transmit beamforming vectors

$$\mathbf{w}_k^{\text{MMSE}} = \frac{[\sigma^2 \mathbf{I} + \mathbf{h}_{k\ell} \mathbf{h}_{k\ell}^H]^{-1} \mathbf{h}_{kk}}{\|[\sigma^2 \mathbf{I} + \mathbf{h}_{k\ell} \mathbf{h}_{k\ell}^H]^{-1} \mathbf{h}_{kk}\|}, \quad k \neq \ell, \quad (4.38)$$

are proven to achieve a Pareto optimal point. These beamforming vectors require only local CSI at the transmitters which is an appealing property in terms of the low overhead in information exchange between the links. In Figure 4.19, it can be seen that the virtual SINR coordination and the maximum sum SINR points are both not necessarily exchange equilibria. Hence, these points are not suitable for distributed implementation between the rational links.

In Figure 4.19, the NBS and KS solution are plotted. These solutions are exchange equilibria and according to simulations, these two solutions are not far from each other. Note that the NBS is defined for convex utility regions only, and the SINR region Φ in our case is not necessarily convex as is shown in Figure 4.19. However, solving the optimization problem in (4.34) by grid search over 10^3 generated Pareto optimal points from Theorem 2 gives a single solution which we plot in Figure 4.19. The two Pareto optimal points $(\phi_1^{\text{UP}}, \phi_2^{\text{NE}})$ and $(\phi_2^{\text{NE}}, \phi_1^{\text{UP}})$ are the bounds to the core and are marked with

circles on the Pareto boundary in Figure 4.19. These bounds, as discussed in Section 4.1.1, can be calculated in the Edgeworth box as the intersection of the contract curve and the indifference curves corresponding to the Nash equilibrium. The KS solution which solves the problem in (4.36) using the core bounds is then found by grid search over the generated Pareto optimal points from Theorem 2.

4.3. Proofs

4.3.1. Proof of Lemma 1

The direct and interference power gains, $|\mathbf{h}_{kk}^H \mathbf{w}_k(\lambda_k)|^2$ and $|\mathbf{h}_{k\ell}^H \mathbf{w}_k(\lambda_k)|^2, k \neq \ell$, are calculated as functions of the parameters λ_k by using the expression for the beamforming vectors in (2.9). The direct power gain is calculated as:

$$\begin{aligned} |\mathbf{h}_{kk}^H \mathbf{w}_k(\lambda_k)|^2 &= \left(\sqrt{\lambda_k} \frac{\mathbf{h}_{kk}^H \mathbf{\Pi}_{\mathbf{h}_{k\ell}} \mathbf{h}_{kk}}{\|\mathbf{\Pi}_{\mathbf{h}_{k\ell}} \mathbf{h}_{kk}\|} + \sqrt{1 - \lambda_k} \frac{\mathbf{h}_{kk}^H \mathbf{\Pi}_{\mathbf{h}_{k\ell}}^\perp \mathbf{h}_{kk}}{\|\mathbf{\Pi}_{\mathbf{h}_{k\ell}}^\perp \mathbf{h}_{kk}\|} \right)^2 \\ &= \left(\sqrt{\lambda_k} \|\mathbf{\Pi}_{\mathbf{h}_{k\ell}} \mathbf{h}_{kk}\| + \sqrt{1 - \lambda_k} \|\mathbf{\Pi}_{\mathbf{h}_{k\ell}}^\perp \mathbf{h}_{kk}\| \right)^2. \end{aligned} \quad (4.39)$$

The interference power is:

$$\begin{aligned} |\mathbf{h}_{k\ell}^H \mathbf{w}_k(\lambda_k)|^2 &= \left| \sqrt{\lambda_k} \frac{\mathbf{h}_{k\ell}^H \mathbf{\Pi}_{\mathbf{h}_{k\ell}} \mathbf{h}_{kk}}{\|\mathbf{\Pi}_{\mathbf{h}_{k\ell}} \mathbf{h}_{kk}\|} + \sqrt{1 - \lambda_k} \frac{\mathbf{h}_{k\ell}^H \mathbf{\Pi}_{\mathbf{h}_{k\ell}}^\perp \mathbf{h}_{kk}}{\|\mathbf{\Pi}_{\mathbf{h}_{k\ell}}^\perp \mathbf{h}_{kk}\|} \right|^2 \\ &= \lambda_k \frac{|\mathbf{h}_{k\ell}^H \mathbf{\Pi}_{\mathbf{h}_{k\ell}} \mathbf{h}_{kk}|^2}{\|\mathbf{\Pi}_{\mathbf{h}_{k\ell}} \mathbf{h}_{kk}\|^2} = \lambda_k \|\mathbf{h}_{k\ell}\|^2. \end{aligned} \quad (4.40)$$

These expressions lead to (4.4) and (4.5) in Lemma 1.

4.3.2. Proof of Theorem 1

First, it is easy to see that the SINR expression in (4.6) is continuous. The SINR $\phi_k(x_1^{(k)}, x_2^{(k)})$ is strongly increasing with the goods $x_1^{(k)}$ and $x_2^{(k)}$ if $\phi_k(x_1'^{(k)}, x_2'^{(k)}) > \phi_k(x_1^{(k)}, x_2^{(k)})$ whenever $(x_1'^{(k)}, x_2'^{(k)}) \neq (x_1^{(k)}, x_2^{(k)})$ and $(x_1'^{(k)}, x_2'^{(k)}) \geq (x_1^{(k)}, x_2^{(k)})$ [JR03, Definition A1.17]. Define the directional derivative of ϕ_k at $(x_1^{(k)}, x_2^{(k)})$ in direction \mathbf{z} as

$$\nabla_{\mathbf{z}} \phi_k(x_1^{(k)}, x_2^{(k)}) = \lim_{t \rightarrow 0} \frac{\phi_k\left(\left(x_1^{(k)}, x_2^{(k)}\right) + t\mathbf{z}\right) - \phi_k\left(x_1^{(k)}, x_2^{(k)}\right)}{t}. \quad (4.41)$$

Since $\phi_k(x_1^{(k)}, x_2^{(k)})$ is differentiable, the limit above can be given as [JR03, Chapter A.2]

$$\nabla_{\mathbf{z}} \phi_k(x_1^{(k)}, x_2^{(k)}) = \nabla \phi_k(x_1^{(k)}, x_2^{(k)}) \mathbf{z}, \quad (4.42)$$

where $\nabla \phi_k(x_1^{(k)}, x_2^{(k)})$ is the gradient of ϕ_k at $(x_1^{(k)}, x_2^{(k)})$ written as

$$\nabla \phi_k(x_1^{(k)}, x_2^{(k)}) = \left(\frac{\partial \phi_k(x_1^{(k)}, x_2^{(k)})}{\partial x_k^{(k)}}, \frac{\partial \phi_k(x_1^{(k)}, x_2^{(k)})}{\partial x_\ell^{(k)}} \right), \quad (4.43)$$

with $\ell \neq k$. The directional derivative of $\phi_k(x_1^{(k)}, x_2^{(k)})$ defines the slope of the tangent to $\phi_k(x_1^{(k)}, x_2^{(k)})$ at the point $(x_1^{(k)}, x_2^{(k)})$ in the direction \mathbf{z} . Hence, if the directional derivative is positive for $\mathbf{z} = (z_1, z_2)^T$ with z_1 and z_2 nonnegative and satisfying

$\|\mathbf{z}\| = \sqrt{z_1^2 + z_2^2} = 1$, then the utility function $\phi_k(x_1^{(k)}, x_2^{(k)})$ is strongly increasing. Consequently, the directional derivative in (4.42) is strictly positive if the components of the gradient $\nabla\phi_k(x_1^{(k)}, x_2^{(k)})$ are strictly positive. The first component of $\nabla\phi_k(x_1^{(k)}, x_2^{(k)})$ is

$$\frac{\partial\phi_k(x_1^{(k)}, x_2^{(k)})}{\partial x_k^{(k)}} = \frac{\left(\sqrt{x_k^{(k)}}g_k + \sqrt{(1-x_k^{(k)})\check{g}_k}\right)\left(\sqrt{\frac{g_k}{x_k^{(k)}}} - \sqrt{\frac{\check{g}_k}{1-x_k^{(k)}}}\right)}{\sigma^2 + \lambda_\ell^{\text{MRT}}g_{\ell k} - x_\ell^{(k)}g_{\ell k}}. \quad (4.44)$$

The partial derivative in (4.44) is strictly larger than zero when $x_k^{(k)} < g_k/(\check{g}_k + g_k)$. Substituting \check{g}_k and g_k from Lemma 1 we get

$$x_k^{(k)} < \frac{g_k}{\check{g}_k + g_k} = \frac{\|\mathbf{\Pi}\mathbf{h}_{k\ell}\mathbf{h}_{kk}\|^2}{\|\mathbf{h}_{kk}\|^2} = \lambda_k^{\text{MRT}}. \quad (4.45)$$

Since $x_k^{(k)} \in [0, \lambda_k^{\text{MRT}}]$, the partial derivative in (4.44) is strictly larger than zero except for $x_k^{(k)} = \lambda_k^{\text{MRT}}$. The second component of $\nabla\phi_k(x_1^{(k)}, x_2^{(k)})$ is

$$\frac{\partial\phi_k(x_1^{(k)}, x_2^{(k)})}{\partial x_\ell^{(k)}} = g_{\ell k} \frac{\left(\sqrt{x_k^{(k)}}g_k + \sqrt{(1-x_k^{(k)})\check{g}_k}\right)^2}{\left(\sigma^2 + \lambda_\ell^{\text{MRT}}g_{\ell k} - x_\ell^{(k)}g_{\ell k}\right)^2}, \quad (4.46)$$

with $\ell \neq k$, which is strictly larger than zero for $x_\ell^{(k)} \in [0, \lambda_\ell^{\text{MRT}}]$. Hence, the directional derivative in (4.42) is strictly positive for $(x_1^{(k)}, x_2^{(k)}) \in [0, \lambda_1^{\text{MRT}}] \times [0, \lambda_2^{\text{MRT}}]$ except for the case $x_k^{(k)} = \lambda_k^{\text{MRT}}$ and $\mathbf{z} = (1, 0)$. Since λ_k^{MRT} is the upper bound on $x_k^{(k)}$, the slope of the function $\phi_k(x_1^{(k)}, x_2^{(k)})$ in the direction $x_k^{(k)}$ as is restricted by the condition $\mathbf{z} = (1, 0)$ is not of interest.

Next, we will prove that the SINR function is jointly quasiconcave with the goods by proving that the SINR is strictly pseudoconcave. Consider the SINR expression in (4.6), and define

$$f(x_k^{(k)}) := \left(\sqrt{x_k^{(k)}}g_k + \sqrt{(1-x_k^{(k)})\check{g}_k}\right)^2, \quad (4.47)$$

$$g(x_\ell^{(k)}) := \sigma^2 + \lambda_\ell^{\text{MRT}}g_{\ell k} - x_\ell^{(k)}g_{\ell k}. \quad (4.48)$$

The function $\phi_k(x_1^{(k)}, x_2^{(k)}) = f(x_k^{(k)})/g(x_\ell^{(k)})$ is strictly pseudoconcave if $f(x_k^{(k)})$ is differentiable and strictly concave and $g(x_\ell^{(k)})$ is differentiable and convex [Sch83, Proposition 2]. It is clear that $g(x_\ell^{(k)})$ and $f(x_k^{(k)})$ are differentiable. The function $g(x_\ell^{(k)})$ is convex since it is linear in $x_\ell^{(k)}$. In order to show that $f(x_k^{(k)})$ is strictly concave, we

build the second derivative of $f(x_k^{(k)})$ as follows:

$$\begin{aligned} \frac{d^2 f(x_k^{(k)})}{d^2 x_k^{(k)}} &= \left(\sqrt{g_k/x_k^{(k)}} - \sqrt{\check{g}_k/(1-x_k^{(k)})} \right)^2 \\ &\quad - \left(\sqrt{x_k^{(k)} g_k} + \sqrt{(1-x_k^{(k)}) \check{g}_k} \right) \left(\sqrt{\frac{g_k}{(x_k^{(k)})^3}} + \sqrt{\frac{\check{g}_k}{(1-x_k^{(k)})^3}} \right) \\ &= \frac{g_k}{x_k^{(k)}} + \frac{\check{g}_k}{(1-x_k^{(k)})} - 2 \sqrt{\frac{g_k \check{g}_k}{(1-x_k^{(k)}) (x_k^{(k)})}} - \frac{g_k}{x_k^{(k)}} \end{aligned} \quad (4.49)$$

$$- \frac{\check{g}_k}{(1-x_k^{(k)})} - \sqrt{\frac{(1-x_k^{(k)}) g_k \check{g}_k}{(x_k^{(k)})^3}} - \sqrt{\frac{x_k^{(k)} g_k \check{g}_k}{(1-x_k^{(k)})^3}} \quad (4.50)$$

$$= -2 \sqrt{\frac{g_k \check{g}_k}{(1-x_k^{(k)}) (x_k^{(k)})}} - \sqrt{\frac{(1-x_k^{(k)}) g_k \check{g}_k}{(x_k^{(k)})^3}} - \sqrt{\frac{x_k^{(k)} g_k \check{g}_k}{(1-x_k^{(k)})^3}} < 0.$$

The second derivative of $f(x_k^{(k)})$ is strictly less than zero. Thus, $f(x_k^{(k)})$ is strictly concave. Accordingly, $\phi_k(x_1^{(k)}, x_2^{(k)})$ is strictly pseudoconcave.

4.3.3. Proof of Proposition 3

The indifference curve I_1 (analogously for consumer 2) for a given utility ϕ_1' satisfies

$$\phi_1' = \frac{\left(\sqrt{x_1^{(1)} g_1} + \sqrt{(1-x_1^{(1)}) \check{g}_1} \right)^2}{f(x_2^{(1)})}, \quad (4.51)$$

where $f(x_2^{(1)}) = \sigma^2 + \lambda_2^{\text{MRT}} g_{21} - x_2^{(1)} g_{21}$. We need to solve for $x_1^{(1)}$ in (4.51). Cross multiplying the terms in (4.51) we get

$$\phi_1' f(x_2^{(1)}) = x_1^{(1)} g_1 + (1-x_1^{(1)}) \check{g}_1 + 2 \sqrt{x_1^{(1)} g_1 (1-x_1^{(1)}) \check{g}_1}, \quad (4.52)$$

$$2 \sqrt{x_1^{(1)} g_1 (1-x_1^{(1)}) \check{g}_1} = \phi_1' f(x_2^{(1)}) - x_1^{(1)} g_1 - (1-x_1^{(1)}) \check{g}_1, \quad (4.53)$$

$$4x_1^{(1)} g_1 (1-x_1^{(1)}) \check{g}_1 = \left(\phi_1' f(x_2^{(1)}) - x_1^{(1)} g_1 - (1-x_1^{(1)}) \check{g}_1 \right)^2. \quad (4.54)$$

Collecting the terms $x_1^{(1)}$ and $(x_1^{(1)})^2$ we get the following quadratic equation

$$\underbrace{(x_1^{(1)})^2 (g_1 + \check{g}_1)^2}_{A_1} - 2x_1^{(1)} \underbrace{\left((g_1 - \check{g}_1) (\phi_1' f(x_2^{(1)}) - \check{g}_1) + 2g_1 \check{g}_1 \right)}_{B_1} + \underbrace{\left(\phi_1' f(x_2^{(1)}) - \check{g}_1 \right)^2}_{C_1} = 0. \quad (4.55)$$

The two solutions of the above equation are

$$x_1^{(1)} = \frac{B_1 \pm \sqrt{B_1^2 - A_1 C_1}}{A_1} = \frac{B_1}{A_1} \pm \sqrt{\frac{B_1^2 - A_1 C_1}{A_1^2}}. \quad (4.56)$$

The product of the two solutions in (4.56) is $C_1/A_1 > 0$ which means that both roots have the same sign. Knowing that one root has to be in the set $[0, \lambda_1^{\text{MRT}}]$ from (4.1), then both roots have to be positive. Therefore, the smallest solution from (4.56) is of interest written as

$$x_1^{(1)} = \frac{B_1}{A_1} - \sqrt{\frac{B_1^2 - A_1 C_1}{A_1^2}}. \quad (4.57)$$

Calculating B_1/A_1 we get

$$\frac{B_1}{A_1} = \frac{(g_1 - \check{g}_1)(\phi_1' f(x_2^{(1)}) - \check{g}_1) + 2g_1 \check{g}_1}{(g_1 + \check{g}_1)^2}, \quad (4.58)$$

$$= \frac{g_1 \phi_1' f(x_2^{(1)}) + \check{g}_1 (g_1 + \check{g}_1 - \phi_1' f(x_2^{(1)}))}{(g_1 + \check{g}_1)^2}, \quad (4.59)$$

$$= \frac{g_1 \phi_1' f(x_2^{(1)}) + (g_1 + \check{g}_1 - g_1)(g_1 + \check{g}_1 - \phi_1' f(x_2^{(1)}))}{(g_1 + \check{g}_1)^2}, \quad (4.60)$$

$$= \lambda_1^{\text{MRT}} \frac{\phi_1'}{\phi_1(\lambda_1^{\text{MRT}}, x_2^{(1)})} + (1 - \lambda_1^{\text{MRT}}) \left(1 - \frac{\phi_1'}{\phi_1(\lambda_1^{\text{MRT}}, x_2^{(1)})} \right), \quad (4.61)$$

since $g_1/(g_1 + \check{g}_1) = \lambda_1^{\text{MRT}}$ and

$$\frac{g_1 + \check{g}_1}{f(x_2^{(1)})} = \frac{\|\mathbf{h}_{kk}\|^2}{\sigma^2 + \lambda_2^{\text{MRT}} g_{21} - x_2^{(1)} g_{21}} = \phi_1(\lambda_1^{\text{MRT}}, x_2^{(1)}). \quad (4.62)$$

The discriminant delta $\Delta_1 = B_1 - A_1 C_1$ is calculated as

$$\Delta_1 = \left((g_1 - \check{g}_1)(\phi_1' f(x_2^{(1)}) - \check{g}_1) + 2g_1 \check{g}_1 \right)^2 - (g_1 + \check{g}_1)^2 (\phi_1' f(x_2^{(1)}) - \check{g}_1)^2, \quad (4.63)$$

$$= \left((g_1 - \check{g}_1)(\phi_1' f(x_2^{(1)}) - \check{g}_1) + 2g_1 \check{g}_1 \right) - (g_1 + \check{g}_1)(\phi_1' f(x_2^{(1)}) - \check{g}_1) \times \left((g_1 - \check{g}_1)(\phi_1' f(x_2^{(1)}) - \check{g}_1) + 2g_1 \check{g}_1 \right) + (g_1 + \check{g}_1)(\phi_1' f(x_2^{(1)}) - \check{g}_1), \quad (4.64)$$

$$= \left((\phi_1' f(x_2^{(1)}) - \check{g}_1)(g_1 - \check{g}_1 - g_1 - \check{g}_1) + 2g_1 \check{g}_1 \right) \times \left((\phi_1' f(x_2^{(1)}) - \check{g}_1)(g_1 - \check{g}_1 + g_1 + \check{g}_1) + 2g_1 \check{g}_1 \right), \quad (4.65)$$

$$= 2\check{g}_1 (g_1 + \check{g}_1 - \phi_1' f(x_2^{(1)})) 2g_1 (\phi_1' f(x_2^{(1)})), \quad (4.66)$$

$$= 4\check{g}_1 g_1 (g_1 + \check{g}_1 - \phi_1' f(x_2^{(1)})) (\phi_1' f(x_2^{(1)})). \quad (4.67)$$

Calculating Δ_1/A_1^2 we get

$$\frac{B_1 - A_1 C_1}{A_1^2} = \frac{4\check{g}_1 g_1 (g_1 + \check{g}_1 - \phi'_1 f(x_2^{(1)})) (\phi'_1 f(x_2^{(1)}))}{(g_1 + \check{g}_1)^4}, \quad (4.68)$$

$$= 4 \frac{(g_1 + \check{g}_1 - g_1)}{(g_1 + \check{g}_1)} \frac{g_1}{(g_1 + \check{g}_1)} \frac{(g_1 + \check{g}_1 - \phi'_1 f(x_2^{(1)})) (\phi'_1 f(x_2^{(1)}))}{(g_1 + \check{g}_1) (g_1 + \check{g}_1)}, \quad (4.69)$$

$$= 4(1 - \lambda_1^{\text{MRT}}) \lambda_1^{\text{MRT}} \left(1 - \frac{\phi'_1}{\phi_1(\lambda_1^{\text{MRT}}, x_2^{(1)})} \right) \frac{\phi'_1}{\phi_1(\lambda_1^{\text{MRT}}, x_2^{(1)})}. \quad (4.70)$$

Substituting (4.61) and (4.70) in (4.57) we get

$$x_1^{(1)} = \lambda_1^{\text{MRT}} \frac{\phi'_1}{\phi_1(\lambda_1^{\text{MRT}}, x_2^{(1)})} + (1 - \lambda_1^{\text{MRT}}) \left(1 - \frac{\phi'_1}{\phi_1(\lambda_1^{\text{MRT}}, x_2^{(1)})} \right) - 2 \sqrt{(1 - \lambda_1^{\text{MRT}}) \lambda_1^{\text{MRT}} \left(1 - \frac{\phi'_1}{\phi_1(\lambda_1^{\text{MRT}}, x_2^{(1)})} \right) \frac{\phi'_1}{\phi_1(\lambda_1^{\text{MRT}}, x_2^{(1)})}}, \quad (4.71)$$

$$= \left(\sqrt{\lambda_1^{\text{MRT}} \frac{\phi'_1}{\phi_1(\lambda_1^{\text{MRT}}, x_2^{(1)})}} - \sqrt{(1 - \lambda_1^{\text{MRT}}) \left(1 - \frac{\phi'_1}{\phi_1(\lambda_1^{\text{MRT}}, x_2^{(1)})} \right)} \right)^2, \quad (4.72)$$

which concludes the proof.

4.3.4. Proof of Theorem 2

The partial derivatives of $\phi_1(x_1^{(1)}, x_2^{(1)})$ w.r.t. $x_1^{(1)}$ and $x_2^{(1)}$ are calculated respectively as

$$\frac{\partial \phi_1(x_1^{(1)}, x_2^{(1)})}{\partial x_1^{(1)}} = \frac{\sqrt{x_1^{(1)} g_1} + \sqrt{(1 - x_1^{(1)}) \check{g}_1}}{\sigma^2 + \lambda_2^{\text{MRT}} g_{21} - x_2^{(1)} g_{21}} \times \frac{\sqrt{g_1/x_1^{(1)}} - \sqrt{\check{g}_1/(1 - x_1^{(1)})}}{\sigma^2 + \lambda_2^{\text{MRT}} g_{21} - x_2^{(1)} g_{21}}, \quad (4.73)$$

$$\frac{\partial \phi_1(x_1^{(1)}, x_2^{(1)})}{\partial x_2^{(1)}} = \frac{\left(\sqrt{x_1^{(1)} g_1} + \sqrt{(1 - x_1^{(1)}) \check{g}_1} \right)^2 g_{21}}{\left(\sigma^2 + \lambda_2^{\text{MRT}} g_{21} - x_2^{(1)} g_{21} \right)^2}. \quad (4.74)$$

The partial derivatives of $\phi_2(x_1^{(2)}, x_2^{(2)})$ w.r.t. $x_1^{(2)}$ and $x_2^{(2)}$ are computed analogously. We rewrite condition (4.10) to

$$\frac{\left(\sqrt{\frac{g_1}{x_1^{(1)}}} - \sqrt{\frac{\check{g}_1}{1-x_1^{(1)}}}\right) \left(\frac{\sigma^2}{g_{21}} + \lambda_2^{\text{MRT}} - x_2^{(1)}\right)}{\left(\sqrt{x_1^{(1)} g_1} + \sqrt{(1-x_1^{(1)}) \check{g}_1}\right)} = \frac{\left(\sqrt{x_2^{(2)} g_2} + \sqrt{(1-x_2^{(2)}) \check{g}_2}\right)}{\left(\sqrt{\frac{g_2}{x_2^{(2)}}} - \sqrt{\frac{\check{g}_2}{1-x_2^{(2)}}}\right) \left(\frac{\sigma^2}{g_{12}} + \lambda_1^{\text{MRT}} - x_1^{(2)}\right)}, \quad (4.75)$$

which after rearranging the terms gives

$$\frac{\left(\sqrt{\frac{g_1}{x_1^{(1)}}} - \sqrt{\frac{\check{g}_1}{1-x_1^{(1)}}}\right) \left(\frac{\sigma^2}{g_{12}} + \lambda_1^{\text{MRT}} - x_1^{(2)}\right)}{\left(\sqrt{x_1^{(1)} g_1} + \sqrt{(1-x_1^{(1)}) \check{g}_1}\right)} = \frac{\left(\sqrt{x_2^{(2)} g_2} + \sqrt{(1-x_2^{(2)}) \check{g}_2}\right)}{\underbrace{\left(\sqrt{\frac{g_2}{x_2^{(2)}}} - \sqrt{\frac{\check{g}_2}{1-x_2^{(2)}}}\right) \left(\frac{\sigma^2}{g_{21}} + \lambda_2^{\text{MRT}} - x_2^{(1)}\right)}_C}. \quad (4.76)$$

We define the RHS of (4.76) as C which is a function of $x_2^{(2)}$ since the term $x_2^{(1)} = \lambda_2^{\text{MRT}} - x_2^{(2)}$ from (4.2). Using the definitions in (4.2), we rewrite (4.76) as

$$\left(\sqrt{\frac{g_1}{x_1^{(1)}}} - \sqrt{\frac{\check{g}_1}{(1-x_1^{(1)})}}\right) \left(\frac{\sigma^2}{g_{12}} + x_1^{(1)}\right) = C \left(\sqrt{x_1^{(1)} g_1} + \sqrt{(1-x_1^{(1)}) \check{g}_1}\right). \quad (4.77)$$

Multiplying both sides of (4.77) with $x_1^{(1)}(1-x_1^{(1)})$ we get

$$\left(\sqrt{(1-x_1^{(1)}) g_1} - \sqrt{x_1^{(1)} \check{g}_1}\right) \left(\sigma^2/g_{12} + x_1^{(1)}\right) = C \left(x_1^{(1)} \sqrt{(1-x_1^{(1)}) g_1} + (1-x_1^{(1)}) \sqrt{x_1^{(1)} \check{g}_1}\right). \quad (4.78)$$

Collecting the terms under the square root we get

$$\sqrt{(1-x_1^{(1)}) g_1} \underbrace{\left(\frac{\sigma^2}{g_{12}} + x_1^{(1)} - C x_1^{(1)}\right)}_A = \sqrt{x_1^{(1)} \check{g}_1} \underbrace{\left(\frac{\sigma^2}{g_{12}} + x_1^{(1)} + C(1-x_1^{(1)})\right)}_B. \quad (4.79)$$

Square both sides of the equation, on the condition that both sides have the same sign

$$(1-x_1^{(1)}) g_1 \left(\frac{\sigma^2}{g_{12}} + x_1^{(1)} - C x_1^{(1)}\right)^2 = x_1^{(1)} \check{g}_1 \left(\frac{\sigma^2}{g_{12}} + x_1^{(1)} + C(1-x_1^{(1)})\right)^2. \quad (4.80)$$

Collecting $x_1^{(1)}$ we get the cubic equation in (4.11) with the coefficients in (4.12)-(4.14).

4.3.5. Proof of Theorem 3

Since the function $\phi_k(x_1^{(k)}, x_2^{(k)})$ is strictly quasiconcave from Theorem 1, then this function has a unique maximum. Considering consumer 1 (analogously consumer 2), the Lagrangian function to the constrained optimization problem in (4.23) is

$$\mathcal{L}(x_1^{(1)}, x_2^{(1)}, \mu) = \phi_1(x_1^{(1)}, x_2^{(1)}) + \mu(\lambda_1^{\text{MRT}} p_1 - x_1^{(1)} p_1 - x_2^{(1)} p_2), \quad (4.81)$$

where μ is a Lagrange multiplier. The Karush–Kuhn–Tucker (KKT) conditions for optimality are given as:

$$\frac{\partial \mathcal{L}(x_1^{(1)}, x_2^{(1)}, \mu)}{\partial x_1^{(1)}} = \frac{\partial \phi_1(x_1^{(1)}, x_2^{(1)})}{\partial x_1^{(1)}} - \mu p_1 = 0 \quad (4.82)$$

$$\frac{\partial \mathcal{L}(x_1^{(1)}, x_2^{(1)}, \mu)}{\partial x_2^{(1)}} = \frac{\partial \phi_1(x_1^{(1)}, x_2^{(1)})}{\partial x_2^{(1)}} + \mu p_2 = 0 \quad (4.83)$$

$$\frac{\partial \mathcal{L}(x_1^{(1)}, x_2^{(1)}, \mu)}{\partial \mu} = \lambda_1^{\text{MRT}} p_1 - x_1^{(1)} p_1 - x_2^{(1)} p_2 = 0 \quad (4.84)$$

In Section 4.3.2, we proved that the SINR function is strictly pseudoconcave with the goods. Thus, the KKT conditions for the problem in (4.23) are also sufficient for optimality [Sch83, Proposition 3]. According to conditions (4.82) and (4.83), we get

$$\frac{\partial \phi_1(x_1^{(1)}, x_2^{(1)})}{\partial x_1^{(1)}} \frac{1}{p_1} = - \frac{\partial \phi_1(x_1^{(1)}, x_2^{(1)})}{\partial x_2^{(1)}} \frac{1}{p_2} \quad (4.85)$$

$$\begin{aligned} & \Rightarrow \frac{\left(\sqrt{x_1^{(1)} g_1} + \sqrt{(1-x_1^{(1)}) \check{g}_1} \right) \left(\frac{\sqrt{g_1}}{\sqrt{x_1^{(1)}}} - \frac{\sqrt{\check{g}_1}}{\sqrt{1-x_1^{(1)}}} \right)}{\sigma^2 + \lambda_2^{\text{MRT}} g_{21} - x_2^{(1)} g_{21}} \\ & = \frac{\left(\sqrt{x_1^{(1)} g_1} + \sqrt{(1-x_1^{(1)}) \check{g}_1} \right)^2 g_{21} p_1}{\left(\sigma^2 + \lambda_2^{\text{MRT}} g_{21} - x_2^{(1)} g_{21} \right)^2 p_2} \end{aligned} \quad (4.86)$$

$$\Rightarrow \frac{\sqrt{g_1}}{\sqrt{x_1^{(1)}}} - \frac{\sqrt{\check{g}_1}}{\sqrt{1-x_1^{(1)}}} = \frac{\left(\sqrt{x_1^{(1)} g_1} + \sqrt{(1-x_1^{(1)}) \check{g}_1} \right) g_{21} p_1}{\left(\sigma^2 + \lambda_2^{\text{MRT}} g_{21} - x_2^{(1)} g_{21} \right) p_2}. \quad (4.87)$$

Substituting $x_2^{(1)}$ from (4.84) we get

$$\sqrt{(1-x_1^{(1)}) g_1} - \sqrt{x_1^{(1)} \check{g}_1} = \frac{\left(x_1^{(1)} \sqrt{(1-x_1^{(1)}) g_1} + (1-x_1^{(1)}) \sqrt{x_1^{(1)} \check{g}_1} \right) \frac{p_1}{p_2}}{\underbrace{\left(\frac{\sigma^2}{g_{21}} + \lambda_2^{\text{MRT}} - \lambda_1^{\text{MRT}} \frac{p_1}{p_2} + x_1^{(1)} \frac{p_1}{p_2} \right)}_B}, \quad (4.88)$$

which leads to

$$\sqrt{(1 - x_1^{(1)})g_1 B} - \sqrt{x_1^{(1)}\check{g}_1 B} - x_1^{(1)}\frac{p_1}{p_2}\sqrt{x_1^{(1)}\check{g}_1} = (1 - x_1^{(1)})\sqrt{x_1^{(1)}\check{g}_1}\frac{p_1}{p_2} \quad (4.89)$$

$$\sqrt{x_1^{(1)}\check{g}_1}\left(B + \frac{p_1}{p_2}\right) = \sqrt{(1 - x_1^{(1)})g_1 B}. \quad (4.90)$$

Squaring both sides on the condition that $B \geq 0$ we can write

$$x_1^{(1)}\check{g}_1\left(B + \frac{p_1}{p_2}\right)^2 = (1 - x_1^{(1)})g_1 B^2. \quad (4.91)$$

We solve for $x_1^{(1)}$ to get

$$x_1^{(1)} = \left(1 + \frac{\check{g}_1}{g_1}\left(1 + \frac{p_1}{p_2 B}\right)^2\right)^{-1}. \quad (4.92)$$

Substituting B from (4.88) we get the expression in (4.25). $x_2^{(1)}$ is calculated according to (4.84).

Chapter 5.

Conclusions

We consider the MISO IFC in which multiple links operate concurrently in the same spectral band. We assume single-user decoding capabilities at the receivers, i.e., the receivers treat interference as noise. Moreover, each transmitter has perfect local CSI such that each transmitter knows the channels between itself and all receivers perfectly. This setting is strictly competitive and can be suitably analyzed using tools from game theory and microeconomic theory.

Our interest in this thesis has been in the joint beamforming design at the transmitters such that Pareto optimal solutions are attained. At a Pareto optimal point, a change in the beamforming vectors of the transmitters leads to a degradation in performance to at least one link. With this respect, Pareto optimality ensures efficient exploitation of the available resources.

Noncooperative games in the MISO IFC are modeled by games in strategic form. The Nash equilibrium of a strategic game determines the noncooperative choice of strategies of the players (links). A link in the MISO IFC is noncooperative if its transmission does not take into account the interference it generates at other links. We reveal that noncooperative operation of the links corresponding to joint MRT is generally not efficient. This fact drives us to design coordination and cooperation mechanisms to improve the joint performance of the links from the Nash equilibrium. We prove that for a specific design of constraints at the transmitters, the Nash equilibrium can be improved. Specifically, we characterize the necessary null-shaping constraints on the strategy space of each transmitter such that the Nash equilibrium outcome is Pareto optimal. The null shaping constraints are to be set by an arbitrator which is an existing authority that coordinates the strategies of the transmitters.

In contrast to strategic games, coalitional games in game theory provide cooperative solutions between the players. We study cooperation between the links via coalitional games without transferable utility. In coalitional games, a player has an incentive to

cooperate with other players if this improves his payoff. We model the setting as a game in coalitional form without transferable utility. The players in a coalition either perform ZF transmission or WF precoding to each other. Necessary and sufficient conditions, in terms of a lower SNR threshold, are provided under which all players have the incentive to cooperate and form a grand coalition with ZF transmission. In addition, we provide sufficient conditions under which all players have no incentive to cooperate. In this case, the SNR has to be below a specified SNR threshold. Hence, there exists an SNR range in which the links would profit in forming subcoalitions. Therefore, we turn our attention to coalition formation games between the links. We utilize a coalition formation algorithm, called merge-and-split, to determine stable user grouping. Numerical results show that while in the low SNR regime noncooperation is efficient with single-player coalitions, in the high SNR regime all users benefit in forming a grand coalition. Coalition formation shows its significance in the mid SNR regime where subset user cooperation provides joint performance gains.

The conflict between two links in the MISO IFC can be related to models from microeconomic theory. In such models, general equilibrium theory is used to determine equilibrium measures that are Pareto optimal. First, we consider the links to be consumers that can trade goods within themselves. The goods in our setting correspond to the parameters of the beamforming vectors necessary to achieve all Pareto optimal points in the SINR region. We utilize the Edgeworth box to illustrate the allocation of the goods between the consumers. Pareto optimal allocations in the Edgeworth box correspond to the contract curve which we characterize in closed-form. The exchange equilibria are a subset of the points on the Pareto boundary at which both consumers achieve larger utility than at the Nash equilibrium. The set of exchange equilibria is related to the core concept in coalitional games. Thus, the exchange equilibria are acceptable cooperative outcomes for a bargaining process between the two consumers. We propose a decentralized bargaining process between the consumers which starts at the Nash equilibrium and ends at an outcome arbitrarily close to an exchange equilibrium. This process requires four-bit signaling between the transmitters at each bargaining-step. The design of the bargaining process relies on a systematic study of the allocations in the Edgeworth box. In comparison to existing bargaining approaches, our bargaining outcome is arbitrarily close to the Pareto boundary of the SINR region.

We model the situation between the links as a competitive market which extends the exchange model to define prices for the goods. The equilibrium in this economy is called Walrasian and corresponds to the prices that equate the demand to the supply of goods. We characterize the unique Walrasian equilibrium and propose a coordina-

tion process that is realized by the arbitrator to distribute the Walrasian prices to the consumers. The consumers then calculate in a decentralized manner their optimal demand corresponding to beamforming vectors to achieve the Walrasian equilibrium. This outcome is Pareto optimal and lies in the set of exchange equilibria. Accordingly, the Walrasian equilibrium shares similar properties with the Nash bargaining solution and the Kalai-Smorodinsky solution from axiomatic bargaining theory.

Game theoretic models as well as models from microeconomic theory are successfully applied to the beamforming problem in the MISO IFC. Performance improvement from the Nash equilibrium can be achieved whenever cooperation between the links or coordination from an arbitrator is possible. While the game theoretic results are applicable for the K -user MISO IFC, the models from microeconomic theory have been applied only for the two-user case. Next, we discuss open problems and extensions of our results.

5.1. Open Problems

While the tools in microeconomic theory can be applied to general K consumer and n goods economy as can be found in [JR03, MCWG95], the application to the beamforming problem in the MISO IFC can currently be done only for the two-user case. This is mainly because of the structure of the parametrization available for the efficient beamforming vectors in the general case.

Using the parametrization in (2.9) for two-users, we have chosen the amount of good for consumer 1 in Section 4.1.1 as $x_1^{(1)} = \lambda_1$ and the amount of good for consumer 2 from good 1 as $x_1^{(2)} = \lambda_1^{\text{MRT}} - \lambda_1$. With this relation between the parameters and the goods and due to the structure of the expression in (4.1), the SINR in (4.6) for link 1 depends only on $x_1^{(1)}$ and $x_2^{(1)}$ which are the amounts from good 1 and good 2 for consumer 1. This method of defining the goods in terms of the parameters does not carry on for the K -user MISO IFC case. We illustrate this drawback based on an example in the 3-user case. The parametrization for the beamforming vectors from (2.12) are

$$\begin{aligned} \mathbf{w}_1(\xi_{11}, \xi_{12}, \xi_{13}) &= \mathbf{v}_{max} \left(\xi_{11} \mathbf{h}_{11} \mathbf{h}_{11}^H - \xi_{12} \xi_{12} \mathbf{h}_{12} \mathbf{h}_{12}^H - \xi_{13} \mathbf{h}_{13} \mathbf{h}_{13}^H \right) \\ \mathbf{w}_2(\xi_{21}, \xi_{22}, \xi_{23}) &= \mathbf{v}_{max} \left(-\xi_{21} \mathbf{h}_{21} \mathbf{h}_{21}^H + \xi_{22} \xi_{22} \mathbf{h}_{22} \mathbf{h}_{22}^H - \xi_{23} \mathbf{h}_{23} \mathbf{h}_{23}^H \right) \\ \mathbf{w}_3(\xi_{31}, \xi_{32}, \xi_{33}) &= \mathbf{v}_{max} \left(-\xi_{31} \mathbf{h}_{31} \mathbf{h}_{31}^H - \xi_{32} \xi_{32} \mathbf{h}_{32} \mathbf{h}_{32}^H + \xi_{33} \mathbf{h}_{33} \mathbf{h}_{33}^H \right) \end{aligned} \quad (5.1)$$

where $\xi_{k1} + \xi_{k2} + \xi_{k3} = 1, k \in \{1, 2, 3\}$. Note that different real-valued parameterizations are also provided in [SCP11, ZC10, BBO12] which also lead to the same conclusion in terms of the application of the exchange economy model. We use the parametrization in (5.1) in order to highlight the usage of the different parameters. In (5.1), three goods

can be directly distinguished each corresponding to the parameters of each transmitter. We can choose the amount of good 1 (analogously for goods 2 and 3) to be divided between the three links as $x_1^{(1)} = \xi_{11}$ for link 1, $x_1^{(2)} = \xi_{12}$ for link 2, and $x_1^{(3)} = \xi_{13}$ for link 3. In order to model this setting as an exchange economy, the utility (SINR) of link k should only depend on the amounts of goods $x_1^{(k)}, x_2^{(k)}, x_3^{(k)}$. However, with the parametrization in (5.1), the SINR expression of a link k would depend on all parameters. Hence, in formulating the demand of consumer k as is done in the two-user case in (4.23), the solution depends also on the demands of the other consumers. In this case, each consumer cannot find his optimal demand of goods independently without knowing what the other consumers demand. Due to this fact, it is currently not possible to find the Walrasian equilibrium in the general K -user MISO IFC case. A new parametrization of the beamforming vectors should be devised that is suitable for modeling the parameters of the efficient beamforming vectors as goods.

The extension of our results to the MIMO IFC requires a characterization of the efficient beamforming vector for this case. Currently there exists no parametrization for the necessary beamforming vectors to achieve all points on the Pareto boundary of the MIMO IFC rate region. As most of our results in the MISO IFC rely on the parametrization of the efficient beamforming vectors, providing a parametrization in the MIMO IFC is important. Currently, the only work which exists that deals with this problem is [CJS12]. In [CJS12], the Pareto boundary of the two-user MIMO IFC rate region with single stream beamforming is characterized by an approach of maximizing the rate of a single link while fixing the rate of the other link. Due to the coupling in the optimizations of the transmitters, an iterative alternating algorithm is used which solves at each instant a quadratically constrained quadratic program (QCQP) at each transmitter.

In this thesis, we have assumed perfect CSI at the transmitters. Extensions towards more practical assumptions such as partial or imperfect CSI at the transmitters is essential. Another extension of our results is to consider multi-user decoding (MUD) capabilities at the receivers. An investigation would be interesting whether the microeconomic models used in Chapter 4 are applicable for the parametrization in [HGJM11] in order to derive Pareto optimal coordination or cooperation mechanisms.

Appendix A.

Further Contributions

During the period of my Ph.D. studies, I have been involved in further publications which have not been included in this theses. The reason for not including the corresponding contributions is to restrict our analysis to a unified system model of the MISO IFC on which models from game theory and microeconomic theory are applied. Here, we list the further contributions.

In [DMSG11] and [DSMG09] results from my Diploma thesis under the supervision of Dr. Walteneus Dargie have been published. My Diploma thesis has been concerned with the development of an energy-efficient topology control protocol for wireless sensor networks.

[DMSG11] W. Dargie, R. Mochaourab, A. Schill, and L. Guan, “A topology control protocol based on eligibility and efficiency metrics,” *Journal of Systems and Software*, vol. 84, no. 1, pp. 2–11, 2011.

[DSMG09] W. Dargie, A. Schill, R. Mochaourab, and L. Guan, “A topology control protocol for 2D Poisson distributed wireless sensor networks,” in *Proc. IEEE AINA Workshops*, May 2009, pp. 582–587.

In [JMM09] and the journal version [JMM10], the maximization of the effective capacity in a single-user MIMO system is conducted with partial CSI at the transmitter. The effective capacity is a performance measure which takes into account the communication delay.

[JMM09] E. A. Jorswieck, R. Mochaourab, and M. Mittelbach, “Effective capacity maximization in multi-antenna channels with covariance feedback,” in *Proc. IEEE ICC*, Jun. 2009, pp. 1–5.

[JMM10] E. A. Jorswieck, R. Mochaourab, and M. Mittelbach, “Effective capacity maximization in multi-antenna channels with covariance feedback,” *IEEE Trans. Wireless Commun.*, vol. 9, no. 10, pp. 2988–2993, 2010.

Appendix A. Further Contributions

In [LJLM09], noncooperative and cooperative game theoretic models are presented for conflict analysis and resource allocation in the interference channel. This work has been a motivation for me to utilize game theoretic tools in the MISO IFC.

- [LJLM09] E. G. Larsson, E. A. Jorswieck, J. Lindblom, and R. Mochaourab, “Game theory and the flat-fading Gaussian interference channel,” *IEEE Signal Process. Mag.*, vol. 26, no. 5, pp. 18–27, Sep. 2009.

In [JM09b], a strategic game is studied in the two-user MISO IFC with eavesdropping possibilities at the receivers. The achievable secrecy rate region is characterized. It is shown that the Nash equilibrium in this setting is more efficient than in the case without considering secrecy.

- [JM09b] E. A. Jorswieck and R. Mochaourab, “Secrecy rate region of MISO interference channel: Pareto boundary and non-cooperative games,” in *Proc. 13th International ITG Workshop on Smart Antennas (WSA)*, Feb. 2009.

In [JM09a] and [MJ09], a setting is considered in which two cells operate on protected and shared bands. Each cell can use two frequency bands. One band is for exclusive use and the other band is shared with the other cell. In each cell, a single user is selected for transmission based on its channel conditions. In [JM09a], the problem of the manipulability of the Nash equilibrium by user cheating is studied. Results from mechanism design are applied to force truthful feedback from the users. In [MJ09], the Nash equilibrium in this setting is analyzed regarding uniqueness, global stability and efficiency. Properties from supermodular games are exploited for this purpose.

- [JM09a] E. A. Jorswieck and R. Mochaourab, “Power control game in protected and shared bands: Manipulability of Nash equilibrium,” in *Proc. 1st International Conference on Game Theory for Networks (GameNets)*, May. 2009, pp. 428–437, invited.
- [MJ09] R. Mochaourab and E. A. Jorswieck, “Resource allocation in protected and shared bands: Uniqueness and efficiency of Nash equilibria,” in *Proc. 3rd ICST/ACM International Workshop on Game Theory in Communication Networks (Gamecomm)*, Oct. 2009, pp. 1–10.

In [MCJ10] and the journal version [CMJ10], noncooperative games in the two-user SISO IFC are studied. Energy-efficiency is achieved when each system pays a price proportional to its allocated transmit power. An arbitrator is introduced to the system who

determines the prices to satisfy minimum QoS requirements as well as minimum total power consumption. The Nash equilibrium with pricing is studied regarding uniqueness and global stability.

- [CMJ10] Z. Chong, R. Mochaourab, and E. A. Jorswieck, "Pricing in noncooperative interference channels for improved energy efficiency," *EURASIP J. Wirel. Commun. Netw.*, vol. 2010, p. 12, 2010.
- [MCJ10] R. Mochaourab, Z. Chong, and E. A. Jorswieck, "Pricing in noncooperative interference channels for improved energy-efficiency," in *Proc. CROWNCOM*, Jun. 2010, pp. 1–5.

In [HGJM10] and the journal version [HGJM11], the two-user MISO IFC is studied with MUD capabilities at the receivers. The necessary beamforming vectors to achieve the Pareto boundary of the achievable Rate region are characterized.

- [HGJM10] K. M. Z. Ho, D. Gesbert, E. A. Jorswieck, and R. Mochaourab, "Beamforming on the MISO interference channel with multi-user decoding capability," in *Proc. ACSSC*, Nov. 2010, pp. 1196–1201.
- [HGJM11] K. M. Z. Ho, D. Gesbert, E. A. Jorswieck, and R. Mochaourab, "Beamforming on the MISO interference channel with multi-user decoding capability," *IEEE Trans. Inf. Theory*, 2011, submitted. Available online at <http://arxiv.org/abs/1107.0416>.

In [MJ11b], the journal version of [Jor10], the beamforming vectors for a general MISO setting depending on the monotonicity properties of the power gains at the receivers in the network are characterized. The characterization is made utilizing the concept of power gain region which is associated with a single transmitter. The number of parameters needed to characterize the efficient beamforming vectors is $T(K-1)$ where T is the number of transmitters and K the number of receivers in the network. In [JM10a] and [JM10b], the framework in [MJ11b] is used to characterize the Pareto boundary of the rate region of the MISO IFC in cognitive radio settings. In [JM10b], the secondary transmitters are to operate under the constraints of producing restricted amount of interference at the primary users. We consider two settings. In the first setting, the primary systems are assumed to tolerate an amount of interference originating from secondary systems. This amount of interference is controlled by a pricing mechanism that penalizes the secondary systems in proportion to the interference they produce on the primary users. In the second setting, null-shaping constraints are imposed on the secondary transmitters. We characterize for both settings transmission strategies that

correspond to Pareto optimal operation points for the secondary systems. In [JM10a], motivated by the surprising result that all Pareto efficient points can be achieved as a Nash equilibrium by imposing certain virtual null-shaping constraints, we consider the problem of selecting a subset of the noncooperative secondary users for operation under the objective of maximizing their achievable sum rate. A low complexity suboptimal greedy secondary user selection algorithm is proposed.

- [MJ11b] R. Mochaourab and E. A. Jorswieck, “Optimal beamforming in interference networks with perfect local channel information,” *IEEE Trans. Signal Process.*, vol. 59, no. 3, pp. 1128–1141, Mar. 2011.
- [JM10a] E. A. Jorswieck and R. Mochaourab, “Beamforming in underlay cognitive radio: Null-shaping constraints and greedy user selection,” in *Proc. CROWNCOM*, Jun. 2010, pp. 1–5, invited.
- [JM10b] E. A. Jorswieck and R. Mochaourab, “Beamforming in underlay cognitive radio: Null-shaping design for efficient Nash equilibrium,” in *Proc. 2nd International Workshop on Cognitive Information Processing (CIP)*, Jun. 2010, pp. 476–481, invited.

In [MJ11a], the MISO IFC is considered where each transmitter is equipped with a uniform linear array. By controlling the geometry of the array, i.e. adapting the antenna spacing, the rotation of the array, and the number of antenna elements, we investigate whether the capacity of the channel can be achieved with single-user decoding capabilities at the receivers. This objective is reached when it is possible for each transmitter to perform MRT to its intended receiver while simultaneously nulling the interference at all unintended receivers. We provide for the two and three user case the necessary antenna spacing and rotation angle of the array in closed-form. For the four user case, an integer programming problem is formulated which additionally determines the required number of antennas.

- [MJ11a] R. Mochaourab and E. A. Jorswieck, “Beamforming in interference networks for uniform linear arrays,” in *Proc. 5th European Conference on Antennas and Propagation (EuCAP)*, Apr. 2011, pp. 2445–2449.

In [MJ11c] and the journal version [MJ12b], the MISO IFC with imperfect CSI at the transmitters is considered. The beamforming vectors that achieve the Pareto boundary of the two-user robust rate region are characterized in [MJ11c]. The extension to the K -user case is done in [MJ12b]. The beamforming vectors that are necessary to achieve all Pareto optimal points in the robust rate region are parameterized by $K(K - 1)$ real-valued parameters. We analyze the system’s spectral efficiency at high and low SNR. ZF

transmission achieves full multiplexing gain at high SNR only if the estimation errors scale linearly with inverse SNR. If the errors are SNR independent, then single-user transmission is optimal at high SNR. At low SNR, robust MRT optimizes the minimum energy per bit for reliable communication.

- [MJ11c] R. Mochaourab and E. A. Jorswieck, “Robust Pareto optimal beamforming in two-user multiple-input single-output interference channel,” in *Proc. 19th European Signal Processing Conference (EUSIPCO)*, Aug. 2011, invited.
- [MJ12b] R. Mochaourab and E. A. Jorswieck, “Robust beamforming in interference channels with imperfect transmitter channel information,” *Signal Processing*, vol. 92, no. 10, pp. 2509–2518, 2012.

Bibliography

- [AA03] E. Altman and Z. Altman, “S-modular games and power control in wireless networks,” *IEEE Trans. Autom. Control*, vol. 48, no. 5, pp. 839–842, May 2003.
- [ABH59] K. J. Arrow, H. D. Block, and L. Hurwicz, “On the stability of the competitive equilibrium, ii,” *Econometrica*, vol. 27, no. 1, pp. 82–109, 1959.
- [ACH07] J. G. Andrews, W. Choi, and R. W. Heath, “Overcoming interference in spatial multiplexing MIMO cellular networks,” *IEEE Wireless Commun.*, vol. 14, no. 6, pp. 95–104, Dec. 2007.
- [AD74] R. J. Aumann and J. H. Dreze, “Cooperative games with coalition structures,” *International Journal of Game Theory*, vol. 3, no. 4, pp. 217–237, 1974.
- [AKG11] A. Attar, V. Krishnamurthy, and O. N. Gharehshiran, “Interference management using cognitive base-stations for UMTS LTE,” *IEEE Commun. Mag.*, vol. 49, no. 8, pp. 152–159, Aug. 2011.
- [Aum67] R. J. Aumann, “A survey of cooperative games without side payments,” in *Essays in Mathematical Economics*, M. Shubik, Ed. Princeton, N.J.: Princeton University Press, 1967, pp. 3–27.
- [AW09] K. R. Apt and A. Witzel, “A generic approach to coalition formation,” *International Game Theory Review*, vol. 11, no. 3, pp. 347–367, 2009.
- [BBO12] E. Björnson, M. Bengtsson, and B. Ottersten, “Pareto characterization of the multicell MIMO performance region with simple receivers,” *IEEE Trans. Signal Process.*, 2012, to appear.
- [BJBO11] E. Björnson, N. Jalden, M. Bengtsson, and B. Ottersten, “Optimality properties, distributed strategies, and measurement-based evaluation of coordinated multicell OFDMA transmission,” *IEEE Trans. Signal Process.*, vol. 59, no. 12, pp. 6086–6101, Dec. 2011.

Bibliography

- [BN10] H. H. Brunner and J. A. Nossek, “Mitigation of intercell interference without base station cooperation,” in *Proc. 14th International ITG Workshop on Smart Antennas (WSA)*, Feb. 2010, pp. 1–7.
- [BO98] T. Basar and G. J. Olsder, *Dynamic Noncooperative Game Theory (Classics in Applied Mathematics, 23)*. Soc for Industrial & Applied Math, December 1998.
- [BO01] M. Bengtsson and B. Ottersten, “Optimum and suboptimum transmit beamforming,” in *Handbook of Antennas in Wireless Communications*, L. C. Godara, Ed. CRC Press, 2001.
- [BPG⁺09] G. Boudreau, J. Panicker, N. Guo, R. Chang, N. Wang, and S. Vrzic, “Interference coordination and cancellation for 4G networks,” *IEEE Commun. Mag.*, vol. 47, no. 4, pp. 74–81, Apr. 2009.
- [Bra68] D. Braess, “Über ein Paradoxon aus der Verkehrsplanung,” *Unternehmensforschung*, vol. 12, pp. 258–268, 1968.
- [BV04] S. Boyd and L. Vandenberghe, *Convex Optimization*. Cambridge University Press, Mar. 2004.
- [BZBO12] E. Björnson, G. Zheng, M. Bengtsson, and B. Ottersten, “Robust monotonic optimization framework for multicell MISO systems,” *IEEE Trans. Signal Process.*, vol. 60, no. 5, pp. 2508–2523, May. 2012.
- [BZGO10] E. Björnson, R. Zakhour, D. Gesbert, and B. Ottersten, “Cooperative multicell precoding: Rate region characterization and distributed strategies with instantaneous and statistical CSI,” *IEEE Trans. Signal Process.*, vol. 58, no. 8, pp. 4298–4310, Aug. 2010.
- [Car78] A. Carleial, “Interference channels,” *IEEE Trans. Inf. Theory*, vol. 24, no. 1, pp. 60–70, Jan. 1978.
- [CJS12] P. Cao, E. A. Jorswieck, and S. Shi, “On the Pareto boundary for the two-user single-beam MIMO interference channel,” *IEEE Trans. Signal Process.*, 2012, submitted. Available online at <http://arxiv.org/abs/1202.5474>.
- [Cos85] M. H. M. Costa, “On the Gaussian interference channel,” *IEEE Trans. Inf. Theory*, vol. 31, no. 5, pp. 607–615, Sep. 1985.

- [CT91] T. M. Cover and J. A. Thomas, *Elements of information theory*. New York, NY, USA: Wiley-Interscience, 1991.
- [DG80] J. H. Drèze and J. Greenberg, “Hedonic coalitions: Optimality and stability,” *Econometrica*, vol. 48, no. 4, pp. pp. 987–1003, 1980.
- [DMC⁺12] A. Damnjanovic, J. Montojo, J. Cho, H. Ji, J. Yang, and P. Zong, “UE’s role in LTE advanced heterogeneous networks,” *IEEE Commun. Mag.*, vol. 50, no. 2, pp. 164–176, Feb. 2012.
- [DUD11] A. Dotzler, W. Utschick, and G. Dietl, “Efficient zero-forcing based interference coordination for MISO networks,” in *Proc. IEEE VTC*, May 2011, pp. 1–5.
- [DY10] H. Dahrouj and W. Yu, “Coordinated beamforming for the multicell multi-antenna wireless system,” *IEEE Trans. Wireless Commun.*, vol. 9, no. 5, pp. 1748–1759, May 2010.
- [Edg81] F. Y. Edgeworth, *Mathematical Psychics: An Essay on the Application of Mathematics to the Moral Sciences*. London, U.K.: C. K. Paul, 1881.
- [EPT07] R. H. Etkin, A. Parekh, and D. Tse, “Spectrum sharing for unlicensed bands,” *IEEE J. Sel. Areas Commun.*, vol. 25, no. 3, pp. 517–528, Apr. 2007.
- [ETW08] R. H. Etkin, D. Tse, and H. Wang, “Gaussian interference channel capacity to within one bit,” *IEEE Trans. Inf. Theory*, vol. 54, no. 12, pp. 5534–5562, Dec. 2008.
- [GHH⁺10] D. Gesbert, S. Hanly, H. Huang, S. Shamai Shitz, O. Simeone, and W. Yu, “Multi-cell MIMO cooperative networks: A new look at interference,” *IEEE J. Sel. Areas Commun.*, vol. 28, no. 9, pp. 1380–1408, Dec. 2010.
- [GJMS09] A. Goldsmith, S. A. Jafar, I. Maric, and S. Srinivasa, “Breaking spectrum gridlock with cognitive radios: An information theoretic perspective,” *Proc. IEEE*, vol. 97, no. 5, pp. 894–914, May 2009.
- [Gre94] J. Greenberg, “Coalition structures,” in *Handbook of Game Theory with Economic Applications*, ser. Handbook of Game Theory with Economic Applications, R. Aumann and S. Hart, Eds. Elsevier, 00 1994, vol. 2, ch. 37, pp. 1305–1337.

Bibliography

- [GSS⁺10] A. B. Gershman, N. D. Sidiropoulos, S. Shahbazpanahi, M. Bengtsson, and B. Ottersten, “Convex optimization-based beamforming,” *IEEE Signal Process. Mag.*, vol. 27, no. 3, pp. 62–75, May 2010.
- [Hay96] S. Haykin, *Adaptive Filter Theory*, 3rd ed. Prentice-Hall, 1996.
- [Hay05] —, “Cognitive radio: brain-empowered wireless communications,” *IEEE J. Sel. Areas Commun.*, vol. 23, no. 2, pp. 201–220, Feb. 2005.
- [HBH06] J. Huang, R. A. Berry, and M. L. Honig, “Distributed interference compensation for wireless networks,” *IEEE J. Sel. Areas Commun.*, vol. 24, no. 5, pp. 1074–1084, May 2006.
- [HG08] Z. K. M. Ho and D. Gesbert, “Spectrum sharing in multiple-antenna channels: A distributed cooperative game theoretic approach,” in *Proc. IEEE PIMRC*, Sep. 2008, pp. 1–5.
- [HG10] —, “Balancing egoism and altruism on the interference channel: The MIMO case,” in *Proc. IEEE ICC*, May 2010, pp. 1–5.
- [HGJM11] K. M. Z. Ho, D. Gesbert, E. A. Jorswieck, and R. Mochaourab, “Beamforming on the MISO interference channel with multi-user decoding capability,” *IEEE Trans. Inf. Theory*, 2011, submitted. Available online at <http://arxiv.org/abs/1107.0416>.
- [HJ85] R. A. Horn and C. R. Johnson, *Matrix Analysis*. Cambridge: Cambridge Univ. Press, 1985.
- [HK81] T. Han and K. Kobayashi, “A new achievable rate region for the interference channel,” *IEEE Trans. Inf. Theory*, vol. 27, no. 1, pp. 49–60, Jan. 1981.
- [HK83] S. Hart and M. Kurz, “Endogenous formation of coalitions,” *Econometrica*, vol. 51, no. 4, pp. 1047–1064, 1983.
- [HL08] Z. Han and K. J. R. Liu, *Resource Allocation for Wireless Networks: Basics, Techniques, and Applications*. New York, NY, USA: Cambridge University Press, 2008.
- [HSHS08] N. Hassanpour, J. E. Smee, J. Hou, and J. B. Soriaga, “Distributed beamforming based on signal-to caused-interference ratio,” in *Proc. IEEE ISSSTA*, Aug. 2008, pp. 405–410.

- [JB04] E. A. Jorswieck and H. Boche, "Performance analysis of capacity of MIMO systems under multiuser interference based on worst case noise behavior," *EURASIP J. Wirel. Commun. Netw.*, vol. 2, pp. 273–285, 2004.
- [JBN10] E. A. Jorswieck, H. Boche, and S. Naik, "Energy-aware utility regions: Multiple access Pareto boundary," *IEEE Trans. Wireless Commun.*, vol. 9, no. 7, pp. 2216–2226, Jul. 2010.
- [JL10] E. A. Jorswieck and E. G. Larsson, "Monotonic optimization framework for the two-user MISO interference channel," *IEEE Trans. Commun.*, vol. 58, pp. 2159–2168, Jul. 2010.
- [JLD08] E. A. Jorswieck, E. G. Larsson, and D. Danev, "Complete characterization of the Pareto boundary for the MISO interference channel," *IEEE Trans. Signal Process.*, vol. 56, no. 10, pp. 5292–5296, Oct. 2008.
- [Jor10] E. A. Jorswieck, "Beamforming in interference networks: Multicast, MISO IFC and secrecy capacity," in *Proc. IZS*, 2010, invited.
- [JR03] G. A. Jehle and P. J. Reny, *Advanced Microeconomic Theory*, 2nd ed., ser. Addison-Wesley. Pearson Education, 2003.
- [JUN05] M. Joham, W. Utschick, and J. A. Nossek, "Linear transmit processing in MIMO communications systems," *IEEE Trans. Signal Process.*, vol. 53, no. 8, pp. 2700–2712, Aug. 2005.
- [KFV06] M. K. Karakayali, G. J. Foschini, and R. A. Valenzuela, "Network coordination for spectrally efficient communications in cellular systems," *IEEE Wireless Commun.*, vol. 13, no. 4, pp. 56–61, Aug. 2006.
- [KGLL09] E. Karipidis, A. Grundinger, J. Lindblom, and E. G. Larsson, "Pareto-optimal beamforming for the MISO interference channel with partial CSI," in *Proc. IEEE CAMSAP*, Dec. 2009, pp. 5–8.
- [KL10] E. Karipidis and E. G. Larsson, "Efficient computation of the Pareto boundary for the MISO interference channel with perfect CSI," in *Proc. WIOPT*, Jun. 2010, pp. 573–577.
- [KP99] E. Koutsoupias and C. Papadimitriou, "Worst-case equilibria," in *Proc. 16th Annual Conference on Theoretical Aspects of Computer Science (STACS)*, 1999, pp. 404–413.

Bibliography

- [KS75] E. Kalai and M. Smorodinsky, “Other solutions to Nash’s bargaining problem,” *Econometrica*, vol. 43, no. 3, pp. 513–518, 1975.
- [LDJ08] E. G. Larsson, D. Danev, and E. A. Jorswieck, “Asymptotically optimal transmit strategies for the multiple antenna interference channel,” in *Proc. 46th Annual Allerton Conference on Communication, Control, and Computing (Allerton)*, Sep. 2008, pp. 708–714.
- [LDL11] Y.-F. Liu, Y.-H. Dai, and Z.-Q. Luo, “Coordinated beamforming for MISO interference channel: Complexity analysis and efficient algorithms,” *IEEE Trans. Signal Process.*, vol. 59, no. 3, pp. 1142–1157, Mar. 2011.
- [LE11] X. Liu and E. Erkip, “A game-theoretic view of the interference channel: Impact of coordination and bargaining,” *IEEE Trans. Inf. Theory*, vol. 57, no. 5, pp. 2805–2820, May 2011.
- [LEG08] L. Lai and H. El Gamal, “The water-filling game in fading multiple-access channels,” *IEEE Trans. Inf. Theory*, vol. 54, no. 5, pp. 2110–2122, May 2008.
- [Leo95] R. J. Leonard, “From parlor games to social science: Von Neumann, Morgenstern, and the creation of game theory, 1928–1994,” *Journal of Economic Literature*, vol. 33, no. 2, pp. 730–761, Jun. 1995.
- [LJ08] E. G. Larsson and E. A. Jorswieck, “Competition versus cooperation on the MISO interference channel,” *IEEE J. Sel. Areas Commun.*, vol. 26, no. 7, pp. 1059–1069, Sep. 2008.
- [LJ11] ———, “Game theory,” in *Mathematical Foundations for Signal Processing, Communications and Networking*, D. R. T. Chen and E. Servedin, Eds. CRC Press, 2011, pp. 691–732.
- [LJLM09] E. G. Larsson, E. A. Jorswieck, J. Lindblom, and R. Mochaourab, “Game theory and the flat-fading Gaussian interference channel,” *IEEE Signal Process. Mag.*, vol. 26, no. 5, pp. 18–27, Sep. 2009.
- [LK10] J. Lindblom and E. Karipidis, “Cooperative beamforming for the MISO interference channel,” in *Proc. 16th European Wireless Conference (EW)*, Apr. 2010, pp. 631–638.

- [LKL09] J. Lindblom, E. Karipidis, and E. G. Larsson, “Selfishness and altruism on the MISO interference channel: The case of partial transmitter CSI,” *IEEE Commun. Lett.*, vol. 13, no. 9, pp. 667–669, Sep. 2009.
- [LKL11a] ———, “Closed-form parameterization of the Pareto boundary for the two-user MISO interference channel,” in *Proc. IEEE ICASSP*, May 2011, pp. 3372–3375.
- [LKL11b] ———, “Efficient computation of the Pareto boundary for the two-user MISO interference channel with multi-user decoding capable receivers,” in *Proc. IEEE CAMSAP*, Dec. 2011, pp. 241–244.
- [LLJ10] J. Lindblom, E. G. Larsson, and E. A. Jorswieck, “Parameterization of the MISO IFC rate region: the case of partial channel state information,” *IEEE Trans. Commun.*, vol. 9, no. 2, pp. 500–504, Feb. 2010.
- [LLL⁺10] Q. Li, G. Li, W. Lee, M. Lee, D. Mazzaresse, B. Clerckx, and Z. Li, “MIMO techniques in WiMAX and LTE: A feature overview,” *IEEE Commun. Mag.*, vol. 48, no. 5, pp. 86–92, May 2010.
- [LMF⁺11] Y. Li, A. Maeder, L. Fan, A. Nigam, and J. Chou, “Overview of femtocell support in advanced WiMAX systems,” *IEEE Commun. Mag.*, vol. 49, no. 7, pp. 122–130, Jul. 2011.
- [LNR⁺09] Y. Lebrun, J. Nsenga, V. Ramon, A. Bourdoux, F. Horlin, and R. Lauwereins, “Maximum SINR-based beamforming for the MISO interference channel,” in *Proc. 17th European Signal Processing Conference (EUSIPCO)*, Aug. 2009.
- [LPNV10] M. A. Lagunas, A. I. Perez-Neira, and M. A. Vazquez, “Joint temporal-spatial reference beamforming: EIG beamforming,” in *Proc. 10th WSEAS International Conference on Communications*, Jul. 2010, pp. 91–97.
- [LR57] R. D. Luce and H. Raiffa, *Games and decisions: introduction and critical survey*. Wiley, New York, 1957.
- [LRB⁺10] Y. Lebrun, V. Ramon, A. Bourdoux, S. Pollin, F. Horlin, and R. Lauwereins, “Maximum SINR-based beamforming for the MISO OFDM interference channel,” in *Proc. IEEE ICC*, May 2010, pp. 1–5.

Bibliography

- [LTY09] M.-H. Lin, J.-F. Tsai, and Y. Ye, “Budget allocation in a competitive communication spectrum economy,” *EURASIP J. Adv. Signal Process.*, vol. 2009, pp. 1–13, 2009.
- [LZ08] A. Leshem and E. Zehavi, “Cooperative game theory and the Gaussian interference channel,” *IEEE J. Sel. Areas Commun.*, vol. 26, no. 7, pp. 1078–1088, Sep. 2008.
- [LZC12] L. Liu, R. Zhang, and K.-C. Chua, “Achieving global optimality for weighted sum-rate maximization in the K-user Gaussian interference channel with multiple antennas,” *IEEE Trans. Wireless Commun.*, vol. 11, no. 5, pp. 1933–1945, 2012.
- [Mar07] M. Marini, “An overview of coalition & network formation models for economic applications,” University of Urbino Carlo Bo, Department of Economics, Society & Politics, Working Papers 0712, Apr. 2007.
- [MCWG95] A. Mas-Colell, M. D. Whinston, and J. R. Green, *Microeconomic Theory*. Oxford, U.K.: Oxford Univ. Press, 1995.
- [MJ11] R. Mochaourab and E. A. Jorswieck, “Optimal beamforming in interference networks with perfect local channel information,” *IEEE Trans. Signal Process.*, vol. 59, no. 3, pp. 1128–1141, Mar. 2011.
- [MNS53] J. P. Mayberry, J. F. Nash, and M. Shubik, “A comparison of treatments of a duopoly situation,” *Econometrica*, vol. 21, no. 1, pp. 141–154, 1953.
- [MPS07] F. Meshkati, H. V. Poor, and S. Schwartz, “Energy-efficient resource allocation in wireless networks,” *IEEE Signal Process. Mag.*, vol. 24, no. 3, pp. 58–68, May 2007.
- [MSM08] S. Mathur, L. Sankar, and N. B. Mandayam, “Coalitions in cooperative wireless networks,” *IEEE J. Sel. Areas Commun.*, vol. 26, no. 7, pp. 1104–1115, Sep. 2008.
- [Mye83] R. B. Myerson, “Bayesian equilibrium and incentive-compatibility: An introduction,” Northwestern University, Center for Mathematical Studies in Economics and Management Science, Discussion Papers 548, Feb. 1983.
- [Mye84] ———, “An introduction to game theory,” Northwestern University, Center for Mathematical Studies in Economics and Management Science, Discussion Papers 623, Sep. 1984.

- [Mye99] —, “Nash equilibrium and the history of economic theory,” *Journal of Economic Literature*, vol. 37, no. 3, pp. 1067–1082, Sep. 1999.
- [Mye08] —, “Perspectives on mechanism design in economic theory,” *American Economic Review*, vol. 98, no. 3, pp. 586–603, Jun. 2008.
- [Nas50a] J. F. Nash, “The bargaining problem,” *Econometrica*, vol. 18, no. 2, pp. 155–162, 1950.
- [Nas50b] —, “Equilibrium points in n-person games,” *Proc. of National Academy of Sciences*, vol. 36, no. 1, pp. 48–49, 1950.
- [NH08] D. Niyato and E. Hossain, “Market-equilibrium, competitive, and cooperative pricing for spectrum sharing in cognitive radio networks: Analysis and comparison,” *IEEE Trans. Wireless Commun.*, vol. 7, no. 11, pp. 4273–4283, Nov. 2008.
- [NH10] —, “A microeconomic model for hierarchical bandwidth sharing in dynamic spectrum access networks,” *IEEE Trans. Comput.*, vol. 59, no. 7, pp. 865–877, Jul. 2010.
- [NS09] M. Nokleby and A. L. Swindlehurst, “Bargaining and the MISO interference channel,” *EURASIP J. Adv. Signal Process.*, vol. 2009, pp. 1–13, Jan. 2009.
- [OR94] M. J. Osborne and A. Rubinstein, *A Course in Game Theory*. The MIT Press, 1994.
- [Pap01] C. Papadimitriou, “Algorithms, games, and the internet,” in *Proc. 33rd Annual ACM Symposium on Theory of Computing (STOC)*, 2001, pp. 749–753.
- [Par94] V. Pareto, “Il massimo di utilità dato dalla libera concorrenza. the maximum of utility given by free competition,” *Giornale degli Economisti*, vol. 9, no. 2, pp. 48–66, Jul. 1894.
- [PCL03] D. P. Palomar, J. M. Cioffi, and M. A. Lagunas, “Uniform power allocation in MIMO channels: a game-theoretic approach,” *IEEE Trans. Inf. Theory*, vol. 49, no. 7, pp. 1707–1727, Jul. 2003.
- [Pet92] H. J. M. Peters, *Axiomatic Bargaining Game Theory*, ser. Game Theory, Mathematical Programming and Operations Research, W. Leinfellner and G. Eberlein, Eds. Kluwer Academic Publishers, 1992, vol. 9.

Bibliography

- [PNLV11] A. I. Perez-Neira, M. A. Lagunas, and M. A. Vazquez, “Autonomous design for the MISO interference channel with mask constraints at reception,” in *Proc. IEEE AEMC*, Dec. 2011, pp. 18–22.
- [PPL10] S.-H. Park, H. Park, and I. Lee, “Distributed beamforming techniques for weighted sum-rate maximization in MISO interference channels,” *IEEE Commun. Lett.*, vol. 14, no. 12, pp. 1131–1133, Dec. 2010.
- [PPL11] —, “Beamforming design based on virtual SINR maximization for interference networks,” in *Proc. IEEE ICC*, Jun. 2011, pp. 1–5.
- [QZLC11] J. Qiu, R. Zhang, Z.-Q. Luo, and S. Cui, “Optimal distributed beamforming for MISO interference channels,” *IEEE Trans. Signal Process.*, vol. 59, no. 11, pp. 5638–5643, Nov. 2011.
- [Raz11] H. Raza, “A brief survey of radio access network backhaul evolution: Part I,” *IEEE Commun. Mag.*, vol. 49, no. 6, pp. 164–171, Jun. 2011.
- [RFLT98] F. Rashid-Farrokhi, K. J. R. Liu, and L. Tassiulas, “Transmit beamforming and power control for cellular wireless systems,” *IEEE J. Sel. Areas Commun.*, vol. 16, no. 8, pp. 1437–1450, Oct. 1998.
- [Ros65] J. B. Rosen, “Existence and uniqueness of equilibrium points for concave n -person games,” *Econometrica*, vol. 33, no. 3, pp. 520–534, 1965.
- [RTSH11] M. Rossi, A. M. Tulino, O. Simeone, and A. M. Haimovich, “Non-convex utility maximization in Gaussian MISO broadcast and interference channels,” in *Proc. IEEE ICASSP*, May 2011, pp. 2960–2963.
- [Rub82] A. Rubinstein, “Perfect equilibrium in a bargaining model,” *Econometrica*, vol. 50, no. 1, pp. 97–109, 1982.
- [Sat81] H. Sato, “The capacity of the Gaussian interference channel under strong interference,” *IEEE Trans. Inf. Theory*, vol. 27, no. 6, pp. 786–788, Nov. 1981.
- [Sch83] S. Schaible, “Fractional programming,” *Mathematical Methods of Operations Research*, vol. 27, pp. 39–54, 1983.
- [SCP11] X. Shang, B. Chen, and H. V. Poor, “Multiuser MISO interference channels with single-user detection: Optimality of beamforming and the achievable

- rate region,” *IEEE Trans. Inf. Theory*, vol. 57, no. 7, pp. 4255–4273, Jul. 2011.
- [SHD⁺09] W. Saad, Z. Han, M. Debbah, A. Hjørungnes, and T. Basar, “Coalitional game theory for communication networks: A tutorial,” *IEEE Signal Process. Mag.*, vol. 26, no. 5, pp. 77–97, Sep. 2009.
- [SHDH09] W. Saad, Z. Han, M. Debbah, and A. Hjørungnes, “A distributed coalition formation framework for fair user cooperation in wireless networks,” *IEEE Trans. Wireless Commun.*, vol. 8, no. 9, pp. 4580–4593, Sep. 2009.
- [Shu59] M. J. Shubik, “Edgeworth market games,” in *Contributions to the Theory of Games IV. Strategy and Market Structure*, Luce and Tucker, Eds. Princeton University Press, 1959, pp. 267–278.
- [Shu61] ———, “Extended Edgeworth bargaining games and competitive equilibrium,” Cowles Foundation, Yale University, Cowles Foundation Discussion Papers 107, 1961.
- [SMG01] C. U. Saraydar, N. B. Mandayam, and D. J. Goodman, “Pricing and power control in a multicell wireless data network,” *IEEE J. Sel. Areas Commun.*, vol. 19, no. 10, pp. 1883–1892, Oct. 2001.
- [SMG02] ———, “Efficient power control via pricing in wireless data networks,” *IEEE Trans. Commun.*, vol. 50, no. 2, pp. 291–303, Feb. 2002.
- [SPB08] G. Scutari, D. Palomar, and S. Barbarossa, “Asynchronous iterative waterfilling for Gaussian frequency-selective interference channels,” *IEEE Trans. Inf. Theory*, vol. 54, no. 7, pp. 2868–2878, Jul. 2008.
- [SPB09] ———, “The MIMO iterative waterfilling algorithm,” *IEEE Trans. Signal Process.*, vol. 57, no. 5, pp. 1917–1935, May 2009.
- [SPPF09] G. Scutari, D. Palomar, J.-S. Pang, and F. Facchinei, “Flexible design of cognitive radio wireless systems,” *IEEE Signal Process. Mag.*, vol. 26, no. 5, pp. 107–123, Sep. 2009.
- [SSB⁺09] D. Schmidt, C. Shi, R. A. Berry, M. L. Honig, and W. Utschick, “Distributed resource allocation schemes,” *IEEE Signal Process. Mag.*, vol. 26, no. 5, pp. 53–63, Sep. 2009.

Bibliography

- [SZ95] E. Screpanti and S. Zamagni, *An Outline of the History of Economic Thought*. Oxford University Press, Sep. 1995.
- [TGC10] M. Tiwari, T. Groves, and P. C. Cosman, “Competitive equilibrium bitrate allocation for multiple video streams,” *IEEE Trans. Image Process.*, vol. 19, no. 4, pp. 1009–1021, Apr. 2010.
- [Top98] D. M. Topkis, *Supermodularity and Complementarity*. Princeton University Press, 1998.
- [Tuy00] H. Tuy, “Monotonic optimization: Problems and solution approaches,” *SIAM Journal on Optimization*, vol. 11, no. 2, pp. 464–494, 2000.
- [UB12] W. Utschick and J. Brehmer, “Monotonic optimization framework for coordinated beamforming in multicell networks,” *IEEE Trans. Signal Process.*, vol. 60, no. 4, pp. 1899–1909, Apr. 2012.
- [VJ04] S. Vishwanath and S. A. Jafar, “On the capacity of vector Gaussian interference channels,” in *Proc. IEEE ITW*, Oct. 2004, pp. 365–369.
- [vNM44] J. von Neumann and O. Morgenstern, *Theory of Games and Economic Behavior*. Princeton University Press, 1944.
- [VPNL11] M. A. Vazquez, A. I. Perez-Neira, and M. A. Lagunas, “Space-time ML receiver and its reciprocal transmitter design for interference networks,” in *Proc. 15th International ITG Workshop on Smart Antennas (WSA)*, Feb. 2011, pp. 1–8.
- [Wal74] L. Walras, *Elements d’économie politique pure: ou, Théorie de la richesse sociale. Elements of Pure Economics; Or the Theory of Social Wealth*. Paris: R. Pichon et R. Durand-Auzias; Lausanne: F. Rouge, Libraire-Éditeur, 1874.
- [XAY10] Y. Xie, B. Armbruster, and Y. Ye, “Dynamic spectrum management with the competitive market model,” *IEEE Trans. Signal Process.*, vol. 58, no. 4, pp. 2442–2446, Apr. 2010.
- [Ye07] Y. Ye, “Competitive communication spectrum economy and equilibrium,” 2007, working Paper, Stanford.
- [Yi03] S.-S. Yi, “Endogenous formation of economic coalitions: A survey on the partition function approach,” *The Endogenous Formation of Economic Coalitions*, Carlo Carraro, ed., Edward Elgar: London, 2003.

- [ZC10] R. Zhang and S. Cui, “Cooperative interference management with MISO beamforming,” *IEEE Trans. Signal Process.*, vol. 58, no. 10, pp. 5454–5462, Oct. 2010.
- [ZG09] R. Zakhour and D. Gesbert, “Coordination on the MISO interference channel using the virtual SINR framework,” in *Proc. 13th International ITG Workshop on Smart Antennas (WSA)*, Feb. 2009.
- [ZG10] —, “Distributed multicell-MISO precoding using the layered virtual SINR framework,” *IEEE Trans. Wireless Commun.*, vol. 9, no. 8, pp. 2444–2448, Aug. 2010.
- [ZHG09] R. Zakhour, K. M. Z. Ho, and D. Gesbert, “Distributed beamforming coordination in multicell MIMO channels,” in *Proc. IEEE VTC*, Apr. 2009, pp. 1–5.